

UNDERSTANDING EMERGING ZOOONOTIC RESPIRATORY VIRUSES

ANIMAL MODELS FOR HUMAN INFLUENZA AND
CORONAVIRUS INFECTIONS

Lidewij Wiersma

Understanding emerging zoonotic respiratory viruses: Animal models for human influenza and coronavirus infections

Thesis, Erasmus University, Rotterdam (The Netherlands) with summary in Dutch.

ISBN: 978-94-6295-335-2

Cover: Layout Caterina Benincasa. Photo front Rienke Wiersma, photo back Lidewij Wiersma both taken in Jordan in 2014.

Print: BOXPress | Proefschriftenmaken.nl

© Lidewij Wiersma, 2016

All rights reserved. Save exceptions stated by law, no part of this publication may be produced or transmitted in any form or by any means, electronic or mechanical, without prior written permission of the author, or where appropriate, the publisher of the articles.

Understanding Emerging Zoonotic Respiratory Viruses: Animal models for human influenza and coronavirus infections

Opkomende zoonotische respiratoire ziekten begrijpen: Diermodellen voor het
bestuderen van influenza en coronavirus infecties bij de mens.

Thesis

to obtain the degree of Doctor

from Erasmus University Rotterdam

by command of the rector magnificus

Prof.dr. H.A.P. Pols

and in accordance with the decision of the Doctorate Board.

The public defense shall be held on

Tuesday 29 March 2016 at 15.30 hours

by

Lidewij Cornelia Maria Wiersma

born in Gouda

Doctoral committee

Supervisors:	Prof.dr. G.F. Rimmelzwaan
	Prof.dr. A.D.M.E. Osterhaus
Other members:	Prof.dr. T. Kuiken
	Prof.dr. R.W. Hendriks
	Prof.dr. M.D. de Jong
Co-supervisor:	Dr. B.L. Haagmans

The research described in this thesis was conducted at the Department of Viroscience, Erasmus Medical Centre, Rotterdam, with the financial support of EU FP7 projects FLUPIG and FLUPLAN.

Voor mijn allerliefste Papa



Als hij had opgelet toen ik hem over mijn werk vertelde, had mij misschien deze Balinese vleurhond niet zo vrolijk uit zijn hand had laten eten!

TABLE OF CONTENTS

CHAPTER 1	9
INTRODUCTION	
CHAPTER 2	29
PATHOGENESIS OF INFECTION WITH 2009 PANDEMIC H1N1 INFLUENZA VIRUS IN ISOGENIC GUINEA PIGS AFTER INTRANASAL OR INTRATRACHEAL INOCULATION	
CHAPTER 3	45
VIRUS REPLICATION KINETICS AND PATHOGENESIS OF INFECTION WITH H7N9 INFLUENZA VIRUS IN ISOGENIC GUINEA PIGS UPON INTRATRACHEAL INOCULATION	
CHAPTER 4	57
HETEROSUBTYPIC IMMUNITY TO H7N9 INFLUENZA VIRUS IN ISOGENIC GUINEA PIGS AFTER INFECTION WITH PANDEMIC H1N1 VIRUS	
CHAPTER 5	71
A SINGLE IMMUNIZATION WITH MODIFIED VACCINIA VIRUS ANKARA-BASED INFLUENZA VIRUS H7 VACCINE AFFORDS PROTECTION IN THE INFLUENZA A(H7N9) PNEUMONIA FERRET MODEL	
CHAPTER 6	87
CONFINED DPP4 EXPRESSION AND INTERFERON SIGNALING IN THE RESPIRATORY TRACT OF NON-HUMAN PRIMATES ARE ASSOCIATED WITH RESTRICTED MERS CORONAVIRUS REPLICATION	
CHAPTER 7	105
SUMMARIZING DISCUSSION	
COMMON ABBREVIATIONS	114
REFERENCES	115
NEDERLANDSE SAMENVATTING	129
ABOUT THE AUTHOR	135
ACKNOWLEDGEMENTS	140

CHAPTER 1

INTRODUCTION

PARTIALLY BASED ON DEVELOPING UNIVERSAL INFLUENZA VACCINES:
HITTING THE NAIL, NOT JUST ON THE HEAD

Wiersma LC, Rimmelzwaan GF, de Vries RD

Vaccines, 2015 Mar 26;3(2):239-62

During the three years in which this thesis was conceived, two major zoonotic respiratory viruses emerged: Middle East Respiratory Syndrome (MERS) coronavirus (CoV), which originated in dromedary camels, and Influenza A/H7N9 virus, which originated in poultry. This gives some indication of the high rate of emergence of novel viruses the world is currently facing, at least in part, due to changes in the structure and demographics of human populations and our behaviour [1, 2]. A particularly important aspect in the case of these two zoonotic viruses is the intensification of livestock production [3]. Camel populations in Saudi Arabia alone were estimated at almost 300,000, on a population of only 30 million (FAOSTAT 2013). Even more mind-boggling are the statistics on poultry in China, with an estimated 5 billion live chickens for 1.35 billion inhabitants (FAOSTAT 2013), i.e. there are approximately 3.7 times more chickens than people in China. Close interaction with these livestock species, in for example backyard flocks, live poultry markets or camel slaughterhouses, camel sporting events, and even camel beauty pageants, provide ample opportunity for viruses to cross the species barrier. The high human population densities and the frequency of travel in turn provide fertile ground for a pandemic if these pathogens acquire the ability to efficiently spread from human to human, as happened in 2009 for Influenza A/H1N1 virus. Fortunately so far, neither A/H7N9 virus nor MERS-CoV is capable of wreaking such havoc, but it is not clear whether we will remain so lucky. It is therefore essential that we elucidate host/pathogen interactions with the ultimate goal of creating effective prevention and intervention strategies. For elucidating host/pathogen interactions as well as testing candidate vaccines, animal models that mimic human disease as closely as possible are indispensable. In this introduction, an overview will be given of the general characteristics, the existing animal models and the current advances in vaccine development for both human influenza A and coronaviruses.

BACKGROUND

INFLUENZA VIRUSES

Influenza viruses are enveloped, single-stranded, negative-sense RNA viruses that belong to the family of *Orthomyxoviridae* and are divided into three types: A, B and C. Influenza C viruses are rarely isolated and disease caused by these viruses is usually limited to mild symptoms in children [4, 5]. Influenza B viruses have no animal reservoir, unlike influenza A viruses, and predominantly infect humans. Influenza B can be divided into two

phylogenetic lineages: Yamagata 16/88-like and Victoria 2/87-like [6]. These viruses have lower mutation rates [7], but also contribute to seasonal influenza activity considerably (van de Sandt et al 2015, *Future Microbiology*, in press). This thesis, however, will focus on Influenza A viruses which can infect many different species and are responsible for substantial morbidity and mortality during seasonal epidemics. Furthermore, a zoonotic spillover event of influenza A could potentially be the cause of a novel pandemic. The influenza A genome consists of 8 segments encoding 11 major proteins: Polymerase basic (PB)2 protein, PB1 and PB1-F2 proteins, Polymerase Acidic (PA) protein, Haemagglutinin (HA), Nucleoprotein (NP), Neuraminidase (NA), Matrix (M)1 and M2 proteins, non-structural (NS)1 and nuclear export (NE) proteins and these viruses are further divided into subtypes based on the surface glycoproteins HA and NA. According to the HA designation, viruses are classified into two groups. H1, H2, H5, H6, H8, H9, H11, H12, H13, H16, H17 and H18 are considered group 1 HAs and H3, H4, H7, H10, H14 and H15 belong to group 2 HAs.

Both seasonal and pandemic influenza viruses can have huge public health consequences. In 2003 in the United States alone the total annual economic burden of seasonal influenza was estimated to be \$87.1 billion [8]. Introduction of novel subtypes of influenza A virus into the human population may lead to pandemic outbreaks, as has happened three times in the previous century: in 1918 (Spanish flu, caused by A(H1N1) viruses), in 1957 (Asian flu, caused by A(H2N2) viruses) and in 1968 (Hong Kong flu, caused by A(H3N2) viruses). The most recent influenza pandemic in 2009 was caused by an H1N1 influenza A virus of swine origin [9]. Each of these pandemic outbreaks of influenza was associated with excess morbidity and mortality. On several occasions, zoonotic transmission of avian influenza A viruses from birds to humans of subtypes H5N1 [10, 11] H7N9 [12], H9N2 [13], H6N1 [14], H7N3 [15, 16] and H10N8 [17] has occurred, sometimes leading to fatal disease. Although thus far human-to-human transmission remains limited for these subtypes, infections with H5N1 and H7N9 viruses in particular constitute a pandemic threat [18]. It has been demonstrated recently that only a limited number of mutations in the HA and the viral polymerases are required to make airborne transmission of highly pathogenic avian influenza A viruses of the H5N1 subtype possible [19-21]. Indeed, some of these adaptive mutations were already found in circulating H5N1 viruses [22]. Influenza viruses can acquire additional genetic changes rapidly, either by mutation or by reassortment with viruses adapted to replicate in mammalian hosts [23].

CORONAVIRUSES

Coronaviruses are enveloped, single stranded, positive-sense RNA viruses with the largest genome of all RNA viruses: 26-32 kb. They belong to the family *Coronaviridae* and comprise four genera: α , β , γ and δ coronaviruses. A wide range of birds and mammals are susceptible to these viruses, and they are known to cause predominantly gastrointestinal and/or respiratory disease. However in humans they appear to be exclusively respiratory pathogens, with only few reports of associated gastrointestinal disease [24].

Coronaviruses attach to cells via the spike (S) protein, a characteristically shaped transmembrane peplomer that gives the viral surface the crown-like morphology to which the virus lends its name and which largely determines the viral host range. The S protein plays a key role in inducing both cellular and humoral immunity and consists of two subunits: the S1 subunit contains a receptor-binding domain (RBD) that engages the host receptor and the S2 subunit that mediates fusion between the viral and host cell membrane [25]. Once the virus has entered the cytoplasm, RNA dependent RNA polymerase is produced. This polymerase subsequently transcribes negative sense RNA that is used as a template to produce either progeny genomes or subgenomic RNA encoding the various viral proteins. Coronavirus genomes consist of six to ten open reading frames (ORFs) that encode the structural proteins (Spike (S), Envelope (E), Membrane (M), Nucleocapsid (N) and, depending on the virus, hemagglutinin esterase (HE)) the replicase proteins, and variable numbers of accessory proteins. When transcription and translation of viral elements is complete, the genome is packaged into a helix with the N protein and enveloped by a host-derived membrane containing M, E, S and sometimes HE viral proteins [26].

To date, there are six coronaviruses that are known to infect humans (HCoVs). Two are alphacoronaviruses (NL63 [27] and 229E [28] viruses) and the remainder are betacoronaviruses (HKU1 [29], OC43 [30], Severe Acute Respiratory Syndrome (SARS) [31] and Middle Eastern Respiratory Syndrome (MERS) [32] coronaviruses). All human coronaviruses except SARS-CoV and MERS-CoV are known to cause seasonally recurring infections of predominantly the upper respiratory tract, rarely progressing to more severe disease in the form of pneumonia. SARS-CoV emerged in 2002 and caused an outbreak that was relatively quickly contained and affected a limited number of people (8,000 confirmed cases, approximately 770 fatal [33]) but that nonetheless had an enormous economic impact, with global economic losses estimated at close to \$40 billion in 2003 [34]. MERS-CoV continues to circulate at the time of writing and has been shown to infect 1638 people, claiming 587 lives (WHO).

Both SARS-CoV and MERS-CoV are zoonotic and appear to have originated in bats, as they are closely related to bat coronaviruses HKU4-CoV and HKU5-CoV [35]. However humans were not found to be infected with SARS-CoV directly through bats, but rather via an intermediate animal reservoir, the palm civet [36]. Much effort concentrated on finding the animal reservoir for MERS-CoV has led to the dromedary camel as the most likely culprit [37, 38]. Like MERS-CoV and SARS-CoV, there is some evidence that NL63 also originally emerged from a bat reservoir [39] but it is now effectively transmitted and maintained within the human population without an intermediate host.

Overall, coronaviruses mutate more slowly than influenza viruses due to numerous RNA enzymes that improve the fidelity of the RNA dependent RNA polymerase [40]. However, in addition to point mutations, like influenza viruses, they are able to recombine, especially in the context of a co-infection [41, 42]. Both of these mechanisms, especially when considering genetic changes in the receptor binding domain (RBD) of the S protein, may explain how new coronaviruses are able to emerge from animal reservoirs [40].

ANIMAL MODELS

Animal models, despite their limitations, are still the mainstay of research into pathogenesis and replication kinetics of many viral diseases, as well as providing the only way of pre-clinically testing prevention/intervention methods. Ideally, a model should reproduce all the hallmarks of the human disease as faithfully as possible in an immunocompetent animal that has been administered a realistic quantity of unadapted virus via an appropriate inoculatory route. However, the extent to which an animal model represents its human counterpart is often difficult to ascertain in the absence of accurate descriptions of human disease. This has especially proved an issue for MERS-CoV, as its geographical origin (i.e. the Middle East) precludes autopsies on deceased patients for cultural reasons. Lack of an appropriate animal model is a substantial obstacle in the development of intervention strategies, as will be discussed subsequently under the heading vaccine development.

INFLUENZA VIRUSES

Animal models for influenza have been repeatedly and extensively reviewed [43-46]. A wide range of species has been assessed for suitability but only few species are routinely used and these are discussed below.

Ferrets

Ferrets are considered the gold standard animal model for influenza as the hallmarks of human disease are most closely mimicked in this species. They are susceptible to many unadapted human influenza viruses (both A and B) as well as some avian and swine influenza A viruses. The distribution of the α 2,3-linked (avian) and α 2,6-linked (mammalian) sialic acid (SA) influenza virus receptors closely resembles that of humans; i.e. α 2,6 is more abundant in the upper respiratory tract and α 2,3 is more abundant in the lower respiratory tract [47]. The pathology induced by the different influenza subtypes mirrors this receptor distribution; as for humans, fully mammalian adapted subtypes cause predominantly transient upper respiratory tract infections and avian viruses such as H5N1 cause more severe, lower respiratory tract pathology [23]. Clinical signs in ferrets roughly resemble human "flu-like symptoms" and include fever, malaise, anorexia, yawning, sneezing and nasal discharge and congestion. A salient difference is that ferrets appear to develop neurological symptoms/invasion of the central nervous system more frequently than humans, although this effect does appear to be subtype and dose dependent. Ferrets develop neutralizing antibodies in response to infection but unfortunately detailed studies of cellular correlates of protection in this species are largely lacking because both inbred animals and reagents are not available. However, depletion of alveolar macrophages was shown to cause higher viral loads and more prominent inflammatory infiltrates [48] and heterosubtypic immunity following natural infection has also been demonstrated [49, 50]. Ferrets are also known to efficiently transmit influenza virus, both directly (contact transmission) and indirectly (airborne transmission) [51].

Mice

Although ferrets may be the gold standard, mice clearly afford some practical advantages including cost, ease of handling and husbandry, availability of reagents and a wide range of genetic backgrounds. However, mice are generally not susceptible to unadapted human influenza viruses and develop lower respiratory tract disease that is rather dissimilar to that caused by the homologous virus in humans. SA receptor distribution of the mouse has rarely been reported and existing reports are incongruent, possibly

indicating that different mouse strains express SA's differently [52, 53]. Clinical signs in mice are generally more severe than in humans and lack the febrile nature. They include marked anorexia, lethargy, hunching, labored breathing, fur ruffling, huddling, hypothermia and dehydration. Although clearly this model is not a faithful reproduction of the disease in humans, one big advantage, apart from cost and ease of handling, is that it allows for more detailed study of cellular immunity to influenza virus infection. A vast amount of information has accumulated on this topic, and summarized in numerous reviews, including [54]. Another potential issue of the mouse is that transmission of influenza viruses is, at best, inefficient in this model [55]. Considering the obvious limitations, one may ask; if murine disease appears to be so dissimilar from humans, to what extent is information gained from this model useful? This has been further discussed in more detail in [56].

Guinea pigs

Guinea pigs are highly susceptible to unadapted human influenza viruses, as well as avian and swine viruses [55], and they have therefore frequently been used as an animal model for influenza virus infection. Guinea pigs were shown to express $\alpha 2,3$ - and $\alpha 2,6$ -SA receptors in the nasal cavity and the trachea, whereas in the lungs, the $\alpha 2,3$ -SA receptor is most widely present [57]. The pathogenesis of influenza in guinea pigs depends on the inoculatory route, as will be discussed further in Chapter 2 of this thesis. When inoculated intranasally, as is most commonly done, infection appears to be limited to the upper respiratory tract [58]. Clinical signs in this model again are rather unlike to those in humans as they are generally very mild and, in contrast to ferrets and mice, lethal infection is rarely observed. They are however, commonly used as a model for transmission as (like ferrets) they readily transmit influenza viruses, but (in contrast to ferrets) they are smaller, easier to handle and less costly. Although some work has been carried out on the innate immune response of guinea pigs to influenza virus infection, little is known about cellular immunity. In this thesis, the isogenic (strain 2) guinea pig model will be further discussed as a potentially unique way of studying cellular immunity and its effect on (airborne) transmission. The isogenic guinea pig model derives its uniqueness from the fact that it combines the advantages of the ferret (transmission) and the mouse model (isogenicity). This way, the effect of cellular immunity on transmission can be studied for the first time.

CORONAVIRUSES

Unfortunately, finding an appropriate animal model for human coronaviruses has proved to be more troublesome than for influenza. Interest in developing animal models for seasonally circulating human coronaviruses such as OC43-CoV, 229E-CoV, HKU1-CoV and NL63-CoV has been very limited. 229E-CoV has only been studied in (double) transgenic mice [59]. OC43-CoV has also been studied in mice, but not as a representative of human respiratory infection but rather to assess the neural pathology and neuroinvasion [60, 61]. Neither HKU1-CoV nor NL63-CoV have been tested in animal models, although serological investigation on captive rhesus macaques suggests that these animals can be naturally infected with NL63-CoV during their lifespan [62]. We report for the first time on infection of macaques with NL63-CoV in Chapter 6.

Significantly more effort has focused on developing animal models for MERS-CoV and SARS-CoV than for the other human coronaviruses, but the models developed to date are disappointingly far from the 'gold standard' (reviewed in detail in [45] and [63] respectively). The most commonly used species are briefly discussed below, and non-human primate models for coronaviruses are also the subject of Chapter 6.

Non-human primates

Cynomolgous macaques appear to be susceptible to infection with MERS-CoV, SARS-CoV and NL63-CoV, however, disease in young immunocompetent animals is mild and transient (Chapter 6). Similar results have been found by several other groups using rhesus macaques as a model for MERS-CoV, [64, 65]. Receptor distribution for SARS-CoV and NL63-CoV (ACE2) and MERS-CoV (DPP4) in macaques mimics human receptor distribution [66, 67] rather well: ACE2 is present throughout the respiratory tract whereas DPP4 is present only in the lower respiratory tract (Chapter 6). This receptor distribution and the associated tissue tropism explains (at least in part), why MERS-CoV transmits poorly between humans compared to SARS-CoV and NL63-CoV; its predilection for the lower respiratory tract likely decreases virus excretion. For SARS-CoV, the model that most faithfully represents human disease is the aged macaque [68], however use of this model is very limited due to ethical, logistical and financial constraints, which is also why this model has not yet been used for MERS-CoV. However the aged macaque model may prove to reflect disease in humans more accurately than young immunocompetent individuals as MERS-CoV causes severe disease predominantly in middle aged individuals with co-morbidities. In addition to macaques, the common marmoset was identified as a promising and more practical non-human primate model in which severe lethal disease

was reported [69], however these findings were subsequently refuted by another group [70].

Mice and other small animals

Although young immunocompetent mice naturally show only moderate susceptibility to SARS-CoV and no susceptibility to MERS-CoV, various adaptations have been devised to allow their use. Such adaptations are justified by the fact that this model shows obvious ethical, practical and financial advantages over the non-human primates discussed above. Engineering mice so that they express human DPP4 renders them susceptible to infection with MERS-CoV and induces a severe and fatal respiratory disease [71]. To allow for improved infection of SARS-CoV in the murine model, either older animals are used [72], or the virus can be adapted to the murine host by serial passaging [73]. Although questions may be posed regarding the extent to which such adapted models remain representative of disease in humans, considering the relative lack of suitable alternatives, they are presently the most commonly used model to study these viruses. In addition to the mouse model, SARS-CoV has also been studied successfully in ferrets [74-76]. Due to the same differences in DPP4 that preclude infection of non-adapted mice, of the other small animals that were inoculated with MERS-CoV, only the rabbit was productively infected. However, infection of rabbits was asymptomatic and limited to the upper respiratory tract, and as such the pathogenesis appears to resemble the disease in camels rather than humans [77].

VACCINE DEVELOPMENT

Evidently the purpose of developing animal models is not only to understand viral replication kinetics, pathogenesis and immune responses, but ultimately to use this information for the development of effective intervention strategies. Although vaccine approaches for influenza are far more abundant than for coronaviruses, the holy grail of influenza vaccine development, a universal vaccine, remains elusive [78]. Coronavirus vaccine development has been plagued in part by the difficulties in finding appropriate animal models, as discussed above, and in part by the lack of incentive for the pharmaceutical industry to go through the costly development of a vaccine for a disease that affects a relatively low number of people [79].

INFLUENZA VIRUSES

Most existing influenza vaccines are produced using labor intensive and time-consuming production methods that rely on the availability of embryonated chicken eggs. In the face of an outbreak caused by a novel emerging subtype, these methods suffer from logistical problems that preclude an adequate response. The delayed availability of sufficient numbers of vaccine doses may have disastrous consequences for public health. As will be discussed in this review, the limitations of the current vaccines highlight the pressing need for game-changing vaccines that induce long-lasting immunity against a wide range of influenza viruses.

Currently used vaccines to protect against seasonal and pandemic influenza virus infections predominantly aim at the induction of antibodies directed at specific sites on the highly variable head domain of the HA surface glycoprotein and to a lesser extent, the NA glycoprotein [80]. Since the error rate of influenza virus is high due to low fidelity of the RNA polymerase complex, mutations in the viral genome can accumulate quickly, under selective pressure e.g. exerted by virus neutralizing antibodies induced by previous infections or vaccinations. Vaccines that induce HA globular head-specific antibodies will become less effective when mutations in HA accumulate to such an extent that vaccine-induced HA-specific antibodies can no longer recognize their target, a process known as antigenic drift. Currently used vaccines are generally trivalent; they contain components of two influenza A strains (H1N1 and H3N2) and one influenza B strain. The strains used in seasonal vaccines are selected annually approximately eight months before the start of the seasonal vaccination campaign. Selection of vaccine components is based on prediction of strains likely to circulate in the subsequent influenza season. Although some methods, such as mathematical modeling of influenza virus evolution [81], have been developed to aid this prediction, the recommendation of the best possible vaccine strains remains difficult [82]. When vaccine strains do not match the epidemic strains, this can potentially lead to higher morbidity and mortality [83].

Different formulations of inactivated vaccines are used for parenteral administration: whole virion, split virion and subunit vaccines. Split virion and subunit vaccines, initially developed to overcome adverse reactions associated with whole virion vaccines [84], were shown to be of comparable immunogenicity but were less reactogenic than whole virion preparations. Since the 70's, inactivated trivalent split virion vaccines have most commonly been used as seasonal vaccines. Paradoxically, the efficacy of these vaccines in age groups that are most at risk (the young and the elderly) is actually lower than for healthy adults [85-88].

An alternative to the inactivated formulations is live attenuated influenza vaccines (LAIV) that are produced by reassortment of gene segments encoding the desired HA and NA glycoproteins and those of a cold adapted (attenuated) strain. As these vaccines are administered intranasally they can induce mucosal immunity, in addition to systemic antibody and T cell responses, more closely mimicking the immune response induced after natural influenza virus infection. Because of low immunogenicity of inactivated vaccines in children, LAIV may be better suited to protect this age group [89]. Indeed it was shown that after intranasal administration of LAIV to children between 3-17 years of age, significant increases in B-cell and T-cell responses could be induced that were sustained at least 1 year after vaccination [90, 91]. However, whether universal vaccination of all immunologically naive children is in fact an advisable strategy remains a topic of debate. Vaccination of children at risk of developing severe complications due to influenza is of course highly recommended, vaccination of otherwise healthy children not at risk for developing severe complications with inactivated vaccines may interfere with development of heterosubtypic immunity that is otherwise induced following natural infections [92, 93].

Even though in some situations, such as childhood vaccination, LAIV may have advantages over TIV [94], they suffer from similar problems regarding production. Like inactivated vaccines, the production process of LAIV is still predominantly egg-based and difficult to scale-up. Vaccine-induced antibodies are also directed mostly against the head domain of HA and thus at risk of losing effectiveness in the face of antigenic drift or shift. In addition, LAIV production has some challenges of its own like the incompatibility of certain HA and NA combinations with the backbone virus to create a replication competent vaccine virus [95].

Clearly, currently available influenza virus vaccination strategies leave a lot to be desired. The induction of strain-specific antibodies directed to the head domain of the HA may be efficacious if the vaccine strains match the anticipated epidemic strains. In case of antigenic drift or in the case of a pandemic outbreak caused by newly emerging influenza viruses, the availability of vaccines that induce more broadly protective immunity is desirable to overcome this important public health issue. Such vaccines should induce antibodies against more conserved proteins or regions thereof and activate other arms of the immune system, like cell-mediated immune responses to conserved proteins. In other words, such vaccines should hit the nail (but not just on the head).

Numerous approaches have been employed to develop these elusive universal vaccines. They have been outlined and discussed in more detail in [78]. Briefly, compared to current regimens, novel approaches to vaccination against influenza can be improved in two

important ways, either by inducing more broadly protective immune responses or by decreasing the time of production using novel vaccine platforms.

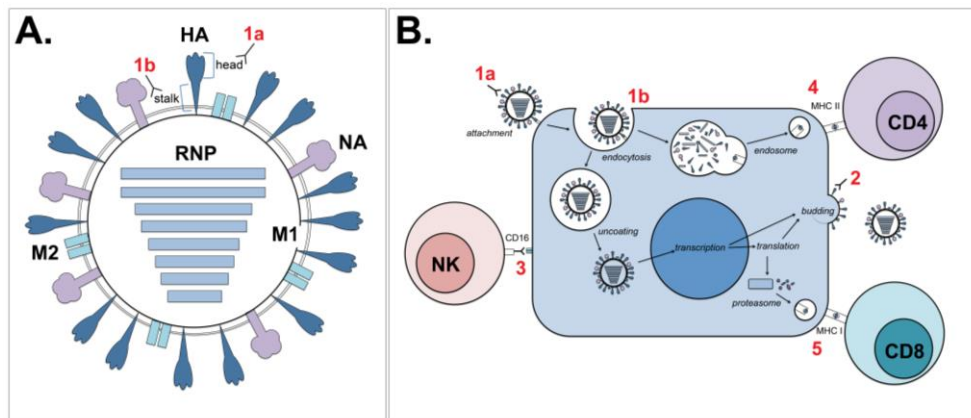


Figure 1 Schematic representation of possible immunological correlates of protection. Numerals in red show various immunological correlates of protection as indicated below. **(A)** Cartoon of an influenza virion, showing the hemagglutinin (HA) surface glycoprotein (stem and head), the neuraminidase (NA) surface glycoprotein, the matrix 2 (M2) ion channel, the matrix 1 (M1) structural protein and the ribonucleoproteins (RNPs: the combination of genomic RNA, viral polymerases PA, PB1 and PB2 and nucleoproteins (NP)). Antibodies directed against HA can either target the globular head (1A) or stem region (1B). **(B)** Interference of production of progeny virus by infected cells by various immunological correlates of protection, including (1) antibodies against HA head, interfering with binding or HA stem, potentially interfering with post-entry functions of HA, like endosomal membrane fusion; (2) antibodies against NA, limiting the production of progeny virus; (3) antibodies against M2e, HA or NA, followed by ADCC through CD16 signaling in NK cells (or phagocytosis, not shown); (4) virus-specific CD4⁺ T lymphocytes; and (5) virus-specific CD8⁺ T lymphocytes that possess cytolytic activity.

Inducing broadly protective immune responses

The influenza genome encodes 11 major proteins on 8 segments of RNA: HA, NA, NP, M1, M2, NS1, NS2, PA, PB1, PB1-F2 and PB2. These proteins are variably conserved among avian and human virus isolates and this information may be of use when attempting to identify conserved targets required to make a universal vaccine. A large study that analyzed more than 36,000 sequences of virus isolates collected over the past 30 years showed that PB1-F2, NA, M2, NS1 and NS2 proteins contain no sequences that were completely conserved in at least 80% of the viruses. However, comparison of the sequences of PB2, PB1, PA, NP, and M1 proteins showed that 55 sequences of 9-58 amino acids were completely conserved in at least 80%, or even as much as 95 to 100%, of the avian and human influenza A virus isolates and, although HA is generally considered to be highly variable, there was one 9 amino acid sequence that was conserved in all type A viruses [96].

When humoral immunity is induced, resultant antibodies can exert their effects by directly neutralizing virus particles, but can also mediate a number of non-neutralizing immunologic functions, including blocking of fusion between the viral and endosomal membrane, innate immune system activation, complement-mediated lysis, phagocytosis and antibody dependent cell-mediated cytotoxicity (ADCC). Broadly protective antibodies currently under investigation include those specific for membrane proteins such as M2, NA and HA. The latter deserves special mention as some exciting breakthroughs have been made very recently. In contrast to the head, the stem of the HA protein is highly conserved and the development of vaccines using so-called 'headless HA' have been the focus of intense research. However, until recently the instability of the stem in absence of the head posed a serious limitation on this vaccine candidate. Using very different methods but with similar results, two different groups were able to stabilize headless HA immunogens that induced broadly cross-reactive antibodies. In one study, vaccination completely protected mice and partially protected ferrets [97] and in the other, mice were protected from lethal infection and macaques showed decrease in fever after sublethal challenge [98].

Antibodies can also be directed at more highly conserved internal proteins. These are generally non-neutralizing and therefore alone they may not be sufficient to provide broad immunity, but evidence is mounting that they are of importance in conjunction with, for example, cell mediated immunity [99, 100].

Although cell mediated immunity (CMI) to influenza virus infections does not prevent infection, it can significantly decrease viral shedding, reduce disease severity and mortality. As T lymphocytes ($CD4^+$ or $CD8^+$) tend to preferentially recognize the more conserved internal proteins such as the nucleoprotein and matrix 1 (M1) protein, there is a greater potential for broad responses [101]. Indeed, CMI has repeatedly been shown to contribute to responses to both homologous and heterologous virus challenge [102-105]. Protection against virus of heterologous subtypes is known as heterosubtypic immunity [106], and it has been demonstrated that T cells play a crucial role in its development in animal models such as mice [107], ferrets [108] and macaques [109, 110]. In humans, a protective role of pre-existing virus specific $CD8^+$ and $CD4^+$ T cells has also been demonstrated against experimental infections [111, 112] and natural infection with the pandemic virus of 2009 [113-115]. Studies employing adoptive transfer of T cells from primed donor to naive recipient mice have contributed to our understanding of the function of both $CD4^+$ and $CD8^+$ cells in protection [116]. The isogenic guinea pig model that is discussed in Chapter 2, 3 and 4 is a new model that will allow for such adoptive transfer studies and additionally allows for investigation into the effect of CMI on transmission.

Novel vaccine platforms

With progressively improved knowledge of the protective antigenic targets described above and the advent of new techniques, an ever-increasing number of platforms for the generation of a universal vaccine are becoming available. These techniques can be employed in numerous ways to deliver the desired antigens. Additionally, these systems often allow for different routes of administration, which in turn can steer the type of immune response induced. Novel platforms offer promise for both of the two improvements of influenza vaccines; induction of more broadly protective immunity and reduced production time.

Novel approaches include viral vectors (further discussed below), DNA vaccines that employ DNA plasmids encoding influenza viral antigens, virus-like particles (VLPs) that serve as vehicles for antigens and virosomes that are essentially empty influenza virus envelopes that lack genetic material. A common limitation of some of these novel platforms, but also of existing influenza vaccines, remains limited immunogenicity. Adjuvants such as aluminium salts have been used to boost immunogenicity of human vaccines for decades, but novel approaches include improved adjuvants. Besides solely increasing immunogenicity, adjuvants can play an important role in facilitating increased speed of vaccine availability, because less viral antigen is required per dose (dose-sparing) meaning that more doses can become available in short period of time. Adjuvants may also help to broaden the humoral immune response [117] and some, such as ISCOMS have even been shown to result in increased virus specific CD8⁺ T-cell responses as was demonstrated in animal models and in clinical trials [118-121].

One novel approach, viral vectors, will be discussed in more detail as it was evaluated for efficacy in the ferret model in Chapter 5 of this thesis. Viral vectors are recombinant, non-influenza viruses engineered to express influenza viral proteins. There are several advantages of using (attenuated or replication deficient) viral vectors as vaccine platforms for universal vaccines. As previously mentioned, cellular immune responses appear to play a pivotal role in protection from influenza infection, especially when a broad (heterosubtypic) immunity is desired. Subunit proteins, and whole or split inactivated viruses, often induce antibody and CD4⁺ T-cell responses due to exclusive antigen presentation by MHC class II. The advantage of using viral vectors is that they drive *de novo* synthesis of proteins in infected cells and facilitate endogenous antigen processing and presentation by both MHC class I and II molecules, thus inducing the complete spectrum of cellular and humoral immune responses. Additionally, they may stimulate mucosal immunity (depending on the route of administration) and thus function much like the existing LAIV vaccines, but without many of the safety or production issues. Viral vectors may actually be able to act as their own adjuvants as the immune system can

mount a response to both the protein of interest and the vector. Consequently, these vaccines even have the potential to be used as bivalent vaccines, protecting against the vector itself as well as the transgenic influenza virus protein(s). Conversely, this may require that the host is immunologically naive for the vector, as pre-existing immunity to the vector could potentially interfere with induction of immunity against the foreign protein of interest. Other concerns with some of the vectors, for example the use Newcastle disease virus, include the possibility of recombination and reversion to virulence in chickens [122].

DNA viruses such as adenovirus [123], herpesvirus [124], baculovirus [125] and poxvirus [126] have been used for the generation of recombinant influenza virus vaccines. RNA viral vectors, including paramyxovirus, flavivirus, retrovirus, coronavirus, alphavirus, bunyavirus and rhabdovirus [127-129], have also been considered for expression of influenza virus proteins. To date, vectors expressing influenza virus HA genes are most commonly used but recently other antigens such as NP and M1 have also been employed, either alone or in combination with HA. Notably, Price *et al* have shown that immunization with a mixture of adenoviruses expressing NP and M2 confers heterosubtypic immunity [130], and can even reduce transmission in a mouse model [131]. The simultaneous expression of surface and internal proteins has the potential to induce both humoral and cell mediated immunity, therefore making these platforms interesting candidates for the development of universal vaccines.

One particularly promising candidate for universal influenza vaccine production is the Modified Vaccinia Ankara (MVA) vector [132, 133]. MVA is avian adapted and does not produce infectious progeny upon infection of most mammalian cells [134]. It does, however, express early, intermediate and abundant late gene products in these cells, therefore making it both safe and effective. Of importance, potentially pre-existing immunity to the MVA vector induced after vaccinia virus vaccination against small pox before 1975, or after repeated vaccination with the vector, does not interfere with immunogenicity [135]. Many different influenza virus proteins have been expressed in MVA vectors; including HA of pandemic H1N1, H7N9 (Chapter 5) and H5N1 [136-140], HA combined with NP [135] and NP combined with M1 [141]. Interestingly, it was shown that priming with an adenoviral vector with NP and M1 followed by an MVA-NP-M1 boost, provided better heterologous protection than using either vector alone [142]. Recombinant MVAs have been evaluated in clinical trials and were shown to be effective, safe and practical alternatives to current vaccination strategies [143, 144]. Therefore MVA is considered as a promising alternative vaccine platform for universal influenza vaccine development.

CORONAVIRUSES

Although progress has been made, at present there are no licensed vaccines for SARS-CoV or MERS-CoV. The previously discussed limitations of the available animal models have had significant effects on the development of effective prevention and intervention strategies. A brief overview of the basic principles of adaptive immunity to coronaviruses and how this knowledge has so far been employed in the quest for efficacious coronavirus vaccines will be given below.

Humoral and Cell Mediated Immunity

As is the case for influenza, coronavirus surface proteins are attractive targets for the induction of humoral immunity. Studies with SARS-CoV have shown that the S protein is a promising vaccine target as it induces high titers of neutralizing antibodies in sera of recovered patients [145] and in animal models [146]. However, neutralizing antibodies appear short lived in recovered patients and display narrow specificity for the viral strain that elicited them [147]. In addition, when inducing humoral immunity to coronaviruses, special attention must be paid to a phenomenon known as antibody dependent enhancement (ADE). For SARS-CoV it was shown that immunizing ferrets with an MVA-vectored, full-length S protein resulted in hepatic necrosis and enhancement of disease [148]. It is postulated that the full-length S protein may contain non-neutralizing epitopes that induce increased uptake of virus and can cause severe immunopathology [148, 149]. Therefore attempts were made to identify only the epitopes that induce high levels of neutralizing antibody. They were mapped to the RBD domain *in vitro* [150, 151] and were shown to induce protective antibodies in the mouse model [152]. In the case of MERS-CoV, experiments in mice have so far shown that MVA vectored full-length S protein induced high levels of neutralizing antibodies that did not appear to enhance disease [153].

Relatively little is known about the T cell response to human coronaviruses, and most that is known has been learned from SARS-CoV (reviewed in [154]). Importantly for vaccine development, in contrast to the relatively short-lived humoral immune response, cellular immunity appears longer lived [155]. Both SARS-CoV and MERS-CoV initially cause marked leukopenia and in SARS-CoV infected patients with severe disease this was shown to delay the development of the adaptive immune response and resulted in prolonged clearance [156]. Several SARS-CoV T cell epitopes on the S and N proteins have been identified using peripheral blood monocytes (PBMCs) obtained from recovered patients [157, 158] and these proteins are both capable of inducing CD4⁺ and CD8⁺ T-cell responses. Equally, numerous CD4⁺ and CD8⁺ T-cell epitopes have been identified on S and N proteins in mice

[154] and T cell responses have been shown to contribute to increased clearance and decreased clinical disease. Notably, adoptive transfer experiments of SARS-CoV specific CD4⁺ and CD8⁺ cells in mice accelerated viral clearance and reduced symptoms in challenged recipient mice [159].

Although information on immune responses is relatively limited, it appears clear that both S and N are capable of inducing potentially protective humoral (S) and cellular (S and N) immune responses and should therefore be considered the most attractive vaccine candidates.

Vaccine platforms

The available options for vaccine development for coronaviruses parallel those discussed for influenza and include inactivated or live-attenuated, subunit, DNA, VLPs and viral-vectored vaccines. Also, different adjuvants, including alum and MF59, have been tested to enhance immunogenicity of these vaccines. However all strategies have so far proven less successful than for their influenza counterparts.

It has been shown in several animal models that it is possible to induce potent immune responses against SARS-CoV using inactivated or live attenuated (especially E attenuated [160]) vaccines [161-166]. However, the potential of attenuated vaccine strains to revert to virulence makes them less suitable, especially for use in immunosuppressed individuals, which for MERS-CoV would be the target population. Also, Th2 immunopathology suggestive of hypersensitivity associated with eosinophilic infiltration has been observed with SARS-CoV inactivated whole virus vaccine in ferrets and nonhuman primates, which warrants caution when further development of such vaccine candidates is considered [167]. However this may have merely been an effect of the adjuvant as recently a new formulation of inactivated whole-virus with a novel delta inulin-based polysaccharide adjuvant was shown to provide protection without inducing such eosinophilic immunopathology in the murine model [168].

As previously mentioned, subunit vaccines based on well-defined immunogenic epitopes of the RBD and excluding potentially ADE-inducing non-neutralizing epitopes of the S protein may be attractive vaccine candidates for both SARS-CoV and MERS-CoV [169-171]. DNA vaccines encoding SARS-CoV S protein have been shown to induce both humoral immunity and CMI and they have proven effective in the mouse model [172] and have progressed to Phase I clinical trials [155]. However, immunogenicity of such vaccine formulations remains relatively low [72].

VLPs can be generated in various mammalian and plant expression systems and one of the most successful coronavirus VLP formulations to date has been chimeric and consisted of

E, M and N proteins of mouse hepatitis virus-CoV and SARS-CoV S protein. It was effective at inducing neutralizing antibodies and protecting from mice challenge [173].

MVA, Vesicular Stomatitis virus, adenovirus, rhabdovirus and attenuated parainfluenza virus have been assessed as potential vectors for S, N and M proteins in the development of viral vectored vaccines against SARS-CoV. Although efficacy at inducing both humoral and cell mediated immunity of such vaccines has been shown [169], as mentioned above; attention must be paid to the exact formulation of the vectored antigen to avoid induction of ADE. Also, pre-existing immunity to the vector may pose problems, as can be the case for adenovirus [174]. For MERS-CoV, MVA [153, 175] and adenoviruses [176, 177] appear to be promising candidates. The advantage of such viral vectored vaccines is that, as is shown in Chapter 5, they allow for rapid deployment in the face of a newly emerging pathogen.

OUTLINE OF THIS THESIS

The objective of the work presented in this thesis was to improve understanding of, and response to, emerging zoonotic respiratory viruses. To this end, various animal models were employed to represent respiratory viral infections in humans. The introduction serves to provide a background on the currently available animal models and (potential) vaccine strategies for human influenza and coronavirus infections.

For the work presented in this thesis, animal models were used in three distinct ways, underlining that the choice of animal model depends largely on the research question. In Chapter 2-4 a new isogenic guinea pig model was developed that provides unique features compared to established influenza virus models. The baseline parameters of influenza infection in this model were assessed to determine its suitability for use to simultaneously study transmission and cell mediated immunity to influenza infections. In Chapter 5, an established model was used to test a novel intervention strategy for an emerging influenza subtype. We showed that the modified vaccinia ankara (MVA)- H7 vaccine is effective against the newly emerging influenza A/H7N9 virus in the ferret model and that it satisfies one of the main aims of the novel influenza vaccines: rapid availability. Finally in Chapter 6, a new model was explored to gain understanding of the pathogenesis of a recently emerged coronavirus. Cynomolgous macaques were used to study underlying mechanisms that appear to restrict MERS-CoV replication in some hosts and data was compared to two other coronaviruses SARS-CoV and NL63-CoV.

In the summarizing discussion (Chapter 7), further attention is paid to the parallels and differences between coronaviruses and influenza viruses, what questions remain to be answered and how we may hope to answer them.

CHAPTER 2

PATHOGENESIS OF INFECTION WITH 2009 PANDEMIC H1N1 INFLUENZA
VIRUS IN ISOGENIC GUINEA PIGS AFTER INTRANASAL OR
INTRATRACHEAL INOCULATION

Wiersma LC, Vogelzang-van Trierum SE, van Amerongen G, van Run P, Nieuwkoop NJ, Ladwig M, Banneke S, Schaefer H, Kuiken T, Fouchier RA, Osterhaus AD, Rimmelzwaan GF

The American journal of pathology, 2015. Mar;185(3):643-50

ABSTRACT

To elucidate the pathogenesis and transmission of influenza virus, the ferret model is typically used. To investigate protective immune responses, the use of inbred mouse strains has proven invaluable. Here, we describe a study with isogenic guinea pigs, which would uniquely combine the advantages of the mouse and ferret models for influenza virus infection. Strain 2 isogenic guinea pigs were inoculated with H1N1pdm09 influenza virus A/Netherlands/602/09 by the intranasal or intratracheal route. Viral replication kinetics were assessed by determining virus titers in nasal swabs and respiratory tissues, which were also used to assess histopathologic changes and the number of infected cells. In all guinea pigs, virus titers peaked in nasal secretions at day 2 after inoculation. Intranasal inoculation resulted in higher virus excretion via the nose and higher virus titers in the nasal turbinates than intratracheal inoculation. After intranasal inoculation, infectious virus was recovered only from nasal epithelium; after intratracheal inoculation, it was recovered also from trachea, lung, and cerebrum. Histopathologic changes corresponded with virus antigen distribution, being largely limited to nasal epithelium for intranasally infected guinea pigs and more widespread in the respiratory tract for intratracheally infected guinea pigs. In summary, isogenic guinea pigs show promise as a model to investigate the role of humoral and cell-mediated immunities to influenza and their effect on virus transmission.

INTRODUCTION

Influenza viruses are an important cause of respiratory tract infections in humans. Seasonal influenza A/H1N1, A/H3N2 and B-viruses cause epidemics in the human population annually [178]. Occasionally, novel antigenically distinct influenza viruses cause pandemic outbreaks with increased morbidity and mortality. The last pandemic occurred in 2009 and was caused by A/H1N1 viruses of swine origin [179, 180]. Furthermore, zoonotic transmissions of avian influenza virus of various subtypes (e.g H7N9 and H5N1) have been reported, and may cause relatively large numbers of fatalities [12, 181, 182]. To obtain understanding of these viruses regarding pathogenesis, virulence, transmissibility and immunity, various animal models are being employed [46, 55, 58, 183]. Commonly, infection of ferrets is considered the preferred animal model for human influenza virus infections, as the pathogenesis in ferrets most closely resembles that

observed in humans [55, 184]. Additionally, ferrets and humans show similarities in receptor distribution in the respiratory tract, thus allowing for virus replication in the upper and/or lower respiratory tract, depending on the origin of the viruses tested and the route of inoculation [185, 186]. Since virus replication in the ferret upper respiratory tract is considered indicative for transmissibility of influenza viruses between humans, ferrets are also used for transmission studies [55, 58]. Other species that may be used to study transmission include (outbred) guinea pigs [58, 187] and, as recently identified, the common marmoset [188].

The animal models mentioned above each have their advantages and limitations. It has proven difficult to correlate parameters of cellular immunity with pathogenesis and transmission in these animal species.

For investigating (cellular) immunity to influenza virus infections inbred mouse strains have commonly been used, in part because many reagents are available for the identification and isolation of cells of the murine immune system. These models have provided a wealth of information on immune function [54]. The use of inbred animals also allows performing adoptive transfer experiments with isolated T or B lymphocyte populations or other cells of the immune system to assess their contribution to protective immunity [116]. However, mice transmit influenza viruses inefficiently and it is doubtful whether the pathogenesis of infection resembles that of humans [58].

The choice of animal model for any given study should therefore be selected based on the research question. Ideally, an animal model is used that combines the advantages of the ferret and the mouse model. Therefore, we were interested in using inbred guinea pigs (*Cavia porcellus*). We used strain 2 guinea pigs; a designation that follows the principles devised by geneticist Sewall Wright, a pioneer in animal (specifically guinea pig) inheritance patterns. Currently the only inbred strains still available are strain 2 and strain 13. It has already been demonstrated that transfer of lymphocyte populations is possible in these animals [189, 190]. In addition, sufficient immunological reagents are available to identify and isolate lymphocyte subsets [191]. Other advantages of the use of (isogenic) guinea pigs is that they are susceptible to both unadapted avian and human influenza viruses and can be used to investigate transmissibility of these viruses in relation to the presence of (cellular) immunity [58].

Typically, guinea pigs are inoculated with influenza virus by the intranasal (IN) route [55, 58], presumably because of the ease of administration. Intratracheal (IT) inoculation through intubation has been described [192] but is challenging because the diameter of the trachea is small and the cervicocranial anatomy of the guinea pig precludes simple visualization of the larynx via the mouth. To overcome these obstacles, inoculation with

virus by the IT route can be performed transcutaneously (surgically), which has been used previously with inactivated influenza virus [193] and other pathogens [194].

The aim of the present study was to investigate the pathogenesis of influenza virus infection in inbred strain 2 guinea pigs and to compare different routes of inoculation, as it has been shown in ferrets that the route of inoculation has a profound effect on the pathogenesis [186].

For infection of isogenic strain 2 guinea pigs, we used 2009 pandemic A/H1N1 influenza virus, which has continued to circulate as a seasonal virus since 2009.

Although studies have been conducted into its transmission [195], knowledge about pathogenesis and virus replication kinetics of this virus strain in particular, and influenza viruses in general, is still limited in guinea pigs [196].

In order to pave the way for new lines of research into viral transmission and cellular immunity, this study was performed to assess replication kinetics and pathogenesis of influenza A(H1N1)pdm09 virus infection via IN or IT inoculation in strain 2 isogenic guinea pigs.

MATERIALS AND METHODS

Animals and experimental design

All experiments were performed in accordance with an animal experimentation protocol approved by an independent Animal Welfare Committee (DEC Consult) and in compliance with national and European legislation. Twenty-two female, 12-16 week old (320-520 grams) isogenic strain 2 guinea pigs were purposely bred at the Federal Institute for Risk Assessment (BfR) in Berlin, Germany. Before the start of the experiment, animals were tested for the presence of serum antibodies to circulating influenza viruses A/H1N1, A/H3N2 and B/Yamagata-like using epidemic and corresponding vaccine strains with the haemagglutination inhibition assay, as described [197]. Influenza virus specific antibodies were not detected in any of the animals.

Animals were housed in groups of 4 or 6 per negatively pressurized BSL3 isolator unit at the animal facilities of the Erasmus Medical Center, on a 12-hour light/dark cycle and with ad-libitum access to food and water.

Twelve animals were inoculated by the IN route under ketamine and medetomidine anesthesia by instilling 150 μ L of virus per nostril (total volume 300 μ L per guinea pig, containing 2×10^6 tissue culture infectious dose (TCID₅₀) of influenza virus A/Netherlands/602/2009) with the animal in an upright position. The anesthetic was antagonized with atipamezole and during recovery of the animals, the head and nose

were kept slightly elevated with respect to the rump to prevent the inoculum from flowing out of the nostrils. Nasal, pharyngeal and rectal swabs were taken daily and animals were weighed prior to inoculation on day 0 and on days 1, 2, 3, 4 (n=12) and 7 (n=6) post-inoculation (p.i.) under isoflurane anesthesia (4% induction, 2% maintenance). On day 4 and 7, 6 animals were sacrificed by exsanguination under anesthesia with ketamine and medetomidine and autopsy was performed.

Ten animals were inoculated via the IT route. To this end, animals were anesthetized with ketamine and medetomidine, and 500 μL PBS containing 2×10^6 TCID₅₀ of virus was injected transcutaneously (surgically) directly into the trachea, while the animal was in dorsal recumbency. The anesthetic was antagonized with atipamezole and during recovery animals were again positioned with their heads slightly elevated with respect to the rump to prevent the inoculum from flowing out via either the pharyngeal or nasal cavity. Nasal, pharyngeal and rectal swabs were taken daily. Nasal swabbing was performed by inserting a thin (urethral) swab carefully into the nasal vestibule. Rectal and pharyngeal swabbing was performed by inserting the swab ca. 3 cm until slight resistance was felt, the swab was carefully twisted several times and retracted. Animals were weighed and swabbed prior to inoculation on day 0 and on days 1 (n=10), 2 (n=8), 3 (n=6), 4 (n=4) and 7 (n=2) p.i. under isoflurane anesthesia. On day 1, 2, 3, 4 and 7 p.i., two animals were sacrificed per time point by exsanguination as described above and autopsies were performed.

Virus preparation

Influenza virus A/Netherlands/602/2009 (A(H1N1)pdm09) was propagated in confluent Madin-Darby Canine Kidney (MDCK) cells. Culture supernatants were harvested after the appearance of cytopathic changes, cleared by low-speed centrifugation and stored at -80°C . The virus titer was determined in MDCK cells as described previously[198]. Virus was diluted in Phosphate Buffered Saline (PBS) to the desired concentration of 2×10^6 TCID₅₀ per 300 μL for IN and 500 μL for IT inoculation.

Pathological examination and Immunohistochemistry

Autopsies were carried out according to standard procedures. The trachea was clamped before opening the thorax and inflated lungs were visually inspected to assess the percentage of pulmonary tissue affected. Samples of nasal turbinate, nasal septum, trachea, tracheobronchial lymph node, bronchus, lung, cerebrum (including the olfactory bulb), cerebellum, heart, liver, kidney, spleen, duodenum and colon were fixed in 10% neutral-buffered formalin. For improved histological assessment, the entire right lung was inflated with formalin prior to fixation. Formalin-fixed tissues were paraffin embedded,

sectioned at 4 μm and stained with haematoxylin and eosin (HE) for histological evaluation. For immunohistochemical (IHC) evaluation, antigen was retrieved using 0.1% protease in PBS at 37°C for 10 minutes and tissues were stained with an immunoperoxidase method using a monoclonal antibody against influenza nucleoprotein (to assess influenza antigen distribution) or against major basic protein antibody, clone BMK-13 (AbD Serotec, for identification of eosinophils). For IHC, IgG2a isotype controls of each tissue and a positive control (for influenza) were included. All slides were evaluated by light microscopy without knowledge of the identity of the animals. Cranial and caudal lung lobes were sectioned both longitudinally and cross-sectionally and HE stained slides were semi-quantitatively assessed using previously described criteria [199].

Influenza antigen IHC was semi-quantitatively evaluated without knowledge of the identity of the animals by visually estimating the number of infected cells.

Assessment of virus titers in tissues and swabs

Nasal, pharyngeal and rectal swabs were stored at -70°C in transport medium (Hanks' balanced salt solution with 0.5% lactalbumin, 10% glycerol, 200 U/ml penicillin, 200 $\mu\text{g}/\text{ml}$ streptomycin, 100 U/ml polymyxin B sulfate, 250 $\mu\text{g}/\text{ml}$ gentamicin, and 50 U/ml nystatin (ICN Pharmaceuticals, Zoetermeer, Netherlands)). Samples of nasal turbinates, trachea, lung, cerebrum (including olfactory bulb), cerebellum, liver, spleen, lung, duodenum and colon were stored at -70°C. For determination of viral titers in tissue, tissues were weighed and homogenized (FastPrep-24 homogenizer (MP Biomedicals, Eindhoven)) in transport medium and cleared of tissue debris by centrifugation (1 min at 10000 rotations per minute (rpm)). Tenfold serial dilutions of swabs and processed tissue samples were used to infect MDCK cells in quadruplicate. On day 5 post-infection of cells, haemagglutination activity of the culture supernatants was assessed to demonstrate the presence of progeny virus [198]. Mean tissue culture infectious dose 50 (TCID₅₀ expressed per milliliter for swabs and per gram for tissue samples) was calculated using the Spearman-Kärber standard equation.

RESULTS

Clinical signs

Animals displayed few clinical signs. Two days p.i., recovery from isofluorane anesthesia was slower for all animals and animals in the IT inoculated group additionally displayed ruffled fur and slightly decreased activity. From day 0 to day 1 animals displayed modest mean weight loss of 5.4% and 4.4% for the IT and IN inoculated animals, respectively.

Virus replication

Two days p.i., virus titers in the nasal swabs reached a peak in all animals. By day 7 p.i., infectious virus was no longer detectable in the nasal swabs (<0.75 TCID₅₀/ml (10log)). After IN inoculation, higher virus titers were observed in nasal secretions than after IT inoculation (peak titers of 4.2 (standard deviation (SD) 1.2) and 2.5 (SD 1.5) TCID₅₀/ml (10log) - Figure 1). Pharyngeal swabs were intermittently positive for all animals but did not show a clear pattern of virus excretion (data not shown). Infectious virus was not detected in any of the rectal swabs.

In all animals that were inoculated via the IN route, infectious virus was detected in the nasal turbinates on day 4 p.i. (n=6) with virus titers ranging from 3.0 to 5.9 TCID₅₀/gr (10log) (mean 4.1 TCID₅₀/gr (10log) SD 1.2). At this time point, virus could not be isolated from remaining tissues, with the exception of the cerebrum of one out six animals, with a titer of 2.5 TCID₅₀/gr (10log) (data not shown).

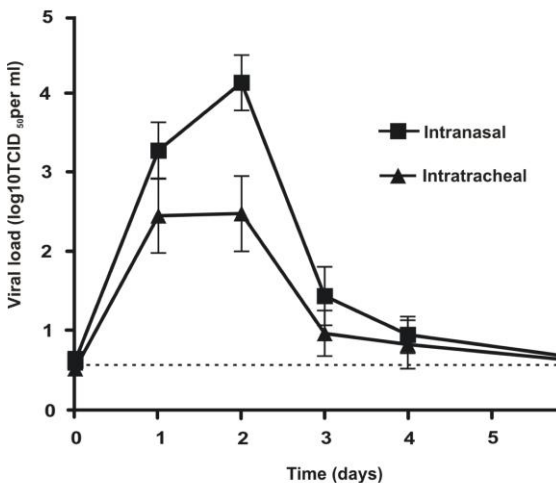


Figure 1 Viral load in nasal swabs after intranasal or intratracheal inoculation with influenza A(H1N1)pdm09 virus. Intranasal n=12 for day 0-4, n=6 day 7 p.i.. Intratracheal n=10 for day 0-1, n=8 day 2, n=6 day 3, n=4 day 4, n=2 day 7 (dashed line indicates limit of detection <0.75 TCID₅₀/ml (10log))

To investigate the kinetics of virus replication in various tissues after IT inoculation, ten strain 2 guinea pigs were inoculated and at various time points p.i., two animals were sacrificed. Based on the results obtained after IN inoculation, autopsies at earlier time points (days 1, 2 and 3) were included. Widespread virus replication was observed (Figure 2) with infectious virus detected in the nasal turbinates on days 1, 2, 3 (n=2 out of 2 animals) and 4 p.i. (n=1/2) (mean peak virus titer on day 1; 8.1 TCID₅₀/gr (10log) SD 1.7), trachea on day 1 (n=2/2) and 2 p.i. (n=1/2) (mean peak virus titer on day 1; 4.6 TCID₅₀/gr (10log) SD 0.6), lung on day 1, 2, 3 (n=2/2) and 4 (n=1/2) (mean peak virus titer on day 1; 6.7 TCID₅₀/gr (10log) SD 0.4) and cerebrum on day 1 (n=1/2) and 2 (n=2/2) p.i. (mean peak virus titer on day 2; 3.7 TCID₅₀/gr(10log) SD 0.1).

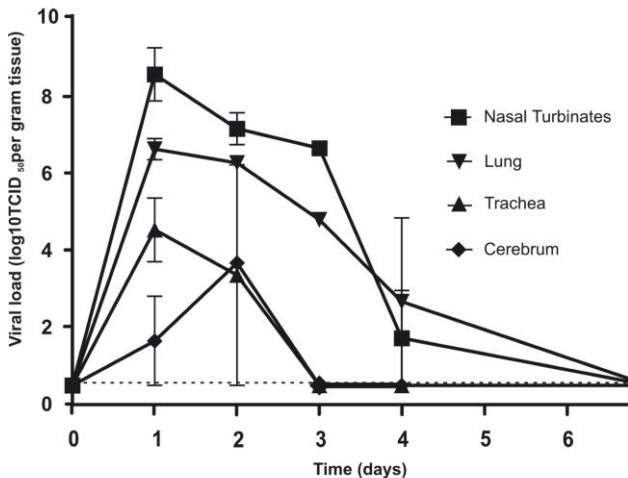


Figure 2 Tissue viral load after intratracheal inoculation with influenza A(H1N1)pdm09 virus, n=2 per time point (dashed line indicates limit of detection <0.75 TCID₅₀/gr(10log)).

Macroscopic and Microscopic findings

Macroscopically, lungs of IN inoculated animals showed multifocal small areas of consolidation affecting <15% of lung tissue. At day 4 and 7 p.i., a moderate quantity of mucopurulent exudate was present in the nasal cavity and the mucosa showed diffuse hyperaemia.

Lungs of IT inoculated animals were visibly more severely affected, with up to 30% of tissue showing randomly distributed, well-demarcated, firm, dark red foci in pulmonary parenchyma (Figure 3). Within the nasal cavity, especially posteriorly, a large quantity of mucopurulent exudate was present from day 2 to 7 p.i. and the mucosa was diffusely hyperaemic. Other tissues showed no notable macroscopic changes.

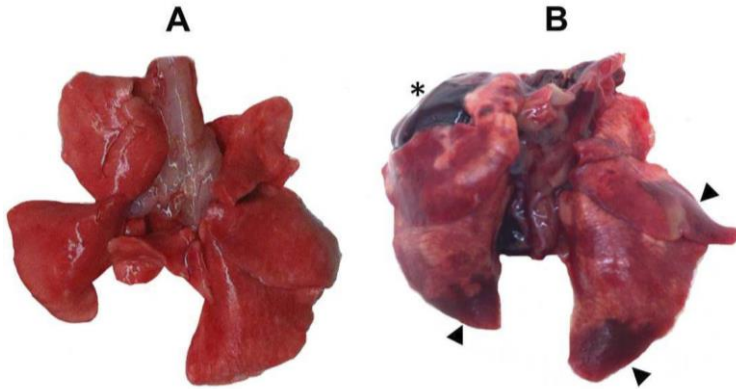


Figure 3 Macroscopic photo of guinea pig lung. (A) Normal guinea pig lung (B) Guinea pig lung at 2 days after intratracheal inoculation; arrowheads indicate multiple areas of consolidation, asterisk shows heart (not present in control).

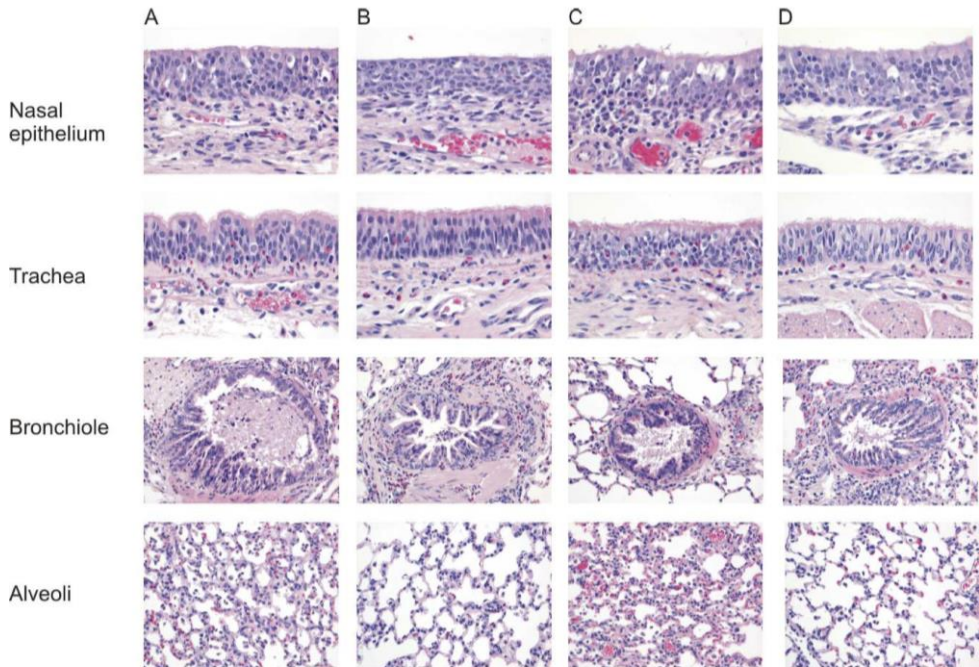


Figure 4 Histopathology (Haematoxylin & Eosin (HE)) of nasal epithelium and trachea (x40) and bronchiole and alveoli (x20). (A) Intratracheal inoculation 4 d.p.i. (B) Intranasal inoculation 4 d.p.i. (C) Intratracheal inoculation 7 d.p.i. (D) Intranasal inoculation 7 d.p.i.. Inflammatory changes are more pronounced after intratracheal inoculation.

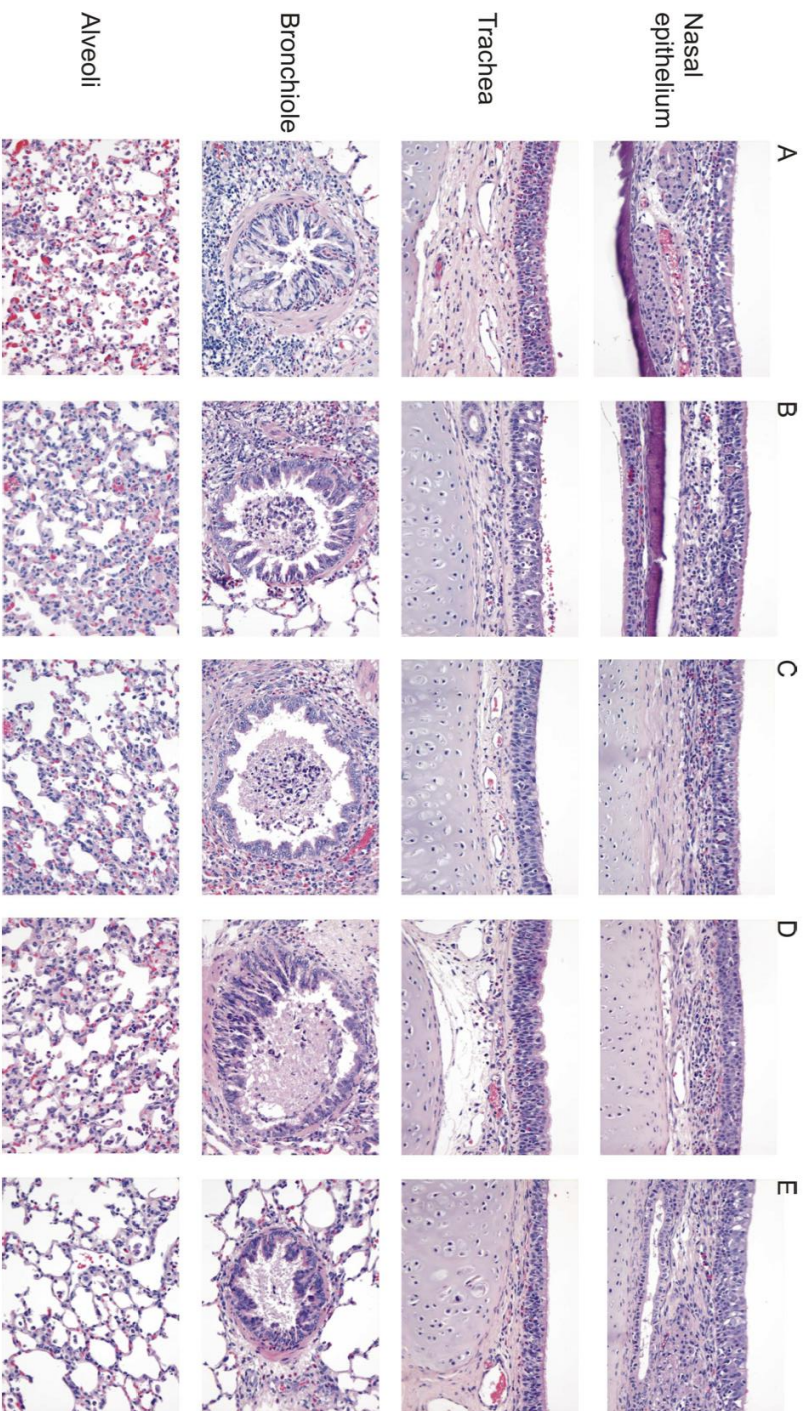


Figure 5 Histopathology (HE) of respiratory tissues (x20) after intratracheal inoculation at days 1 (A), 2 (B), 3 (C), 4 (D) and 7 (E) post inoculation. Acute inflammatory changes and necrosis are most prominent at days 2 and 3 post-inoculation.

Histological evaluation of tissues from IN inoculated animals revealed moderate inflammation of the nasal epithelium and mild inflammation in the remaining respiratory tract, with an inflammatory infiltrate composed predominantly of polymorphonuclear cells morphologically consistent with eosinophils, fewer heterophils and, especially in the pulmonary parenchyma, mononuclear cells morphologically consistent with macrophages. On days 4 and 7 p.i., all respiratory tract tissues and particularly alveoli from IT inoculated animals showed more widespread and more severe inflammation of the alveolar walls and respiratory epithelium (and, where present, the submucosa), than those of IN inoculated animals (Figure 4). After IT inoculation, the extent of acute inflammation was most marked around day 2 and 3 p.i. (Figure 5) and infrequently accompanied by intra-alveolar oedema and deposition of fibrin. Pyknosis, karyorrhexis and karyolysis (necrosis), flattening (attenuation) and/or loss of cilia of epithelial cells of nasal cavity, bronchi(oli) and alveoli were more frequently observed with this route of inoculation than with IN inoculation. Necrotic debris frequently accumulated in alveolar and airway lumina and on nasal epithelium. Some type II pneumocyte hyperplasia was seen in the alveoli by day 7 p.i. (regeneration).

Other tissues examined, including the cerebrum, showed no notable microscopic changes apart from one IN inoculated animal that showed perivascular cuffing with mononuclear cells (ca. 5 cells thick) in the olfactory lobe at day 7 p.i.. However, this animal showed no detectable virus titers or antigen positivity by IHC in the brain.

Immunohistochemical findings

After IN inoculation, moderate numbers of viral antigen positive cells were detected in the nasal epithelium at day 4 and, to a lesser extent, day 7 p.i.. Virus-infected cells were not detected in any other (respiratory) tissues (data not shown).

After IT inoculation, moderate numbers of virus-infected (epithelial) cells were detected by IHC in all respiratory tissues (Figure 6). Nasal epithelium showed a peak in positivity at day 2 p.i. with a steady decline on day 3 and 4, and was negative by day 7. Trachea was antigen positive on day 2 p.i. only. Bronchi(oli) showed peak positivity on day 1, followed by a steady decline on day 2, 3 and 4 and by day 7, antigen was no longer detectable. Antigen in alveoli also peaked at day 2 p.i. and thereafter declined steadily with only a few cells positive by day 7. The number of virus-infected cells in the respiratory tract therefore roughly correlated with the virus titers that were measured in the respective tissues (Figure 2).

Cell types that showed intranuclear antigen were epithelial cells of the upper respiratory tract and airways, and type II pneumocytes and alveolar macrophages in the pulmonary parenchyma (see inset Figure 6). These cells were identified based on their location and morphology. Other tissues inspected, including the cerebrum, showed no virus antigen positivity.

Major basic protein antibody (clone BMK-13) was used to definitively distinguish eosinophils from heterophils. In respiratory tissues, the predominant polymorphonuclear cell type present was confirmed to be eosinophils (Figure 7).

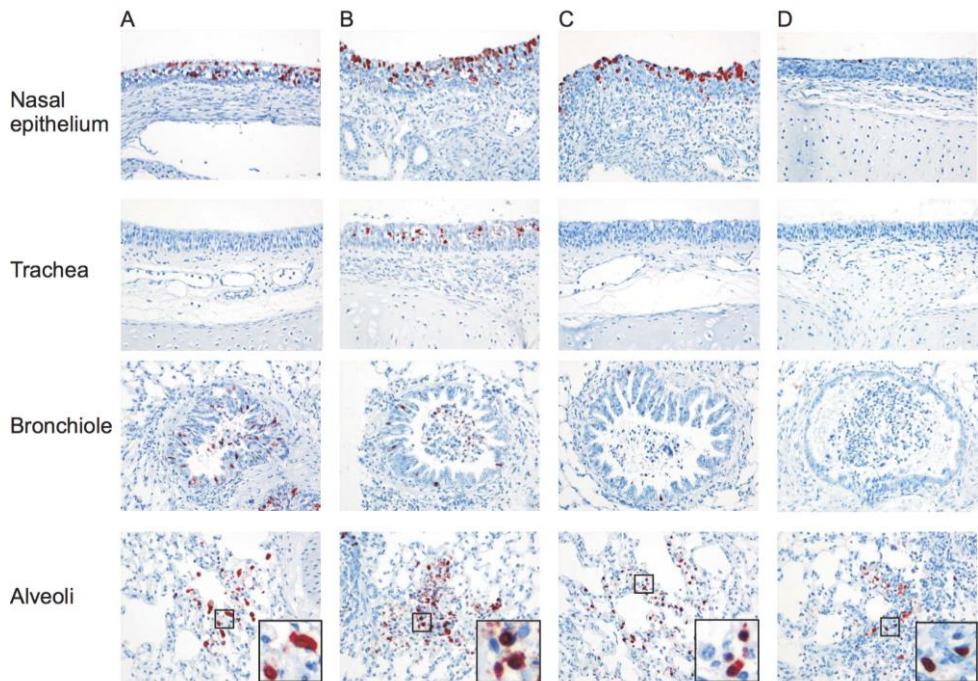


Figure 6 Immunohistochemistry (IHC) of respiratory tract tissues after intratracheal inoculation (x20). (A) 1 d.p.i. (B) 2 d.p.i. (C) 3 d.p.i. (D) 4 d.p.i.. Intranasal inoculation resulted in infection of cells in the nasal epithelium only (results not shown).

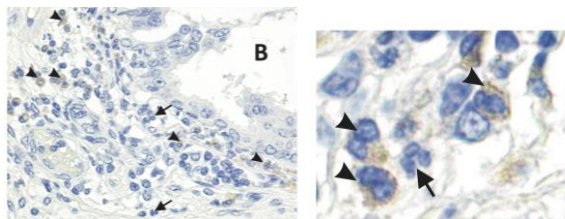


Figure 7 Immunohistochemistry of inflammatory infiltrate surrounding a bronchus (*) at day 2 post-intratracheal inoculation (A) x20, (B) cells at higher magnification. Arrowheads show eosinophils with granules that stain positive (brown) with major basic protein antibody (BMK-13), arrows show heterophils.

DISCUSSION

In the present study we investigated virus replication and pathogenesis of infection with A(H1N1)pdm09 influenza virus in strain 2 isogenic guinea pigs after intranasal (IN) or intratracheal (IT) inoculation. For both inoculation routes, virus excretion from the nose peaked around day 2 p.i., although after IN inoculation higher virus titers were observed in the nose swabs than after IT inoculation. After IN inoculation, virus replication in the respiratory tract was restricted to the nasal epithelium. In one animal virus was also detectable in the cerebrum on day 4 p.i.. In contrast, IT inoculation appeared to result in more widespread replication. On days 1, 2, 3 and 4 p.i., infectious virus was not only detected in the nasal epithelium, but also in the lungs and on days 1 and 2 in the trachea and the cerebrum. Due to the limited breeding capacity at present and restrictions imposed by the ethical committee, it was not possible to test virus replication in the respective organs at earlier time points after IN inoculation. It therefore remains unclear whether the virus replicated in the respective respiratory tissues before day 4 p.i.. Previous studies do not consistently report spread of influenza viruses to the lower respiratory tract after IN inoculation but the histological lesions observed in the lungs of the IN inoculated guinea pigs were consistent with those previously described for infection with influenza viruses of other subtypes [196, 200-202]. However, in the present study we could not confirm viral replication (by detection of infectious virus or infected cells) in tissues other than the nasal epithelium after IN inoculation.

For IT inoculation, the immunohistochemistry results (Figure 6 and 7) corresponded with the virus titers in the respective tissues (Figure 2), confirming the presence of virus in epithelial cells of the nasal turbinates, trachea, bronchi(oli), alveoli and in pulmonary macrophages between day 1 and 4 p.i.. Low virus titers were detected in the cerebrum at day 1 (n=1/2) and 2 (n=2/2), however no antigen positive cells were detected by IHC. No histological changes were noted in the cerebrum of any of the animals apart from one IN inoculated animal that showed minimal histological changes in the olfactory lobe at day 7 p.i., but did not show detectable viral titers or viral antigen positivity. The relevance of this finding and the potential importance of the olfactory route of entry into the guinea pig central nervous system therefore remains unknown.

Interestingly, IT inoculation resulted in effective spread of replicating virus to both the upper and lower respiratory tract. In ferrets, IT inoculation with 2009 pandemic A(H1N1) virus typically results in viral replication predominantly in the lower respiratory tract [140, 184, 203]. If IT inoculation becomes the preferred route of inoculation for guinea pigs, this is especially relevant for future transmission studies. For both routes of inoculation, the trachea appeared to be relatively spared. Histological lesions in the trachea were mild,

replicating virus was only demonstrated in 3 out of 10 IT inoculated animals and IHC was positive in only 1 animal. This may be explained by the relatively small number of cells available for infection in the trachea compared to the lower respiratory tract.

Overall, histological lesions corresponded generally with those reported in the few pathogenesis studies previously conducted in guinea pigs [196, 200-202] and consisted of rhinitis, tracheitis, bronch(iol)itis and alveolitis with mild (IN inoculation) and moderate (IT inoculation) infiltrates consisting of numerous eosinophils, fewer heterophils, and in the lower respiratory tract, macrophages. Epithelial attenuation and necrosis was noted multifocally throughout the respiratory tract and was more marked especially in the lower respiratory tract after IT inoculation.

In two of the previous guinea pig influenza studies that report on viral pathogenesis, the authors comment on the presence of neutrophils [201, 202]. Guinea pig polymorphonuclear cells that correspond to neutrophils are more correctly referred to as heterophils [204]. Guinea pig heterophils and eosinophils are easily confused at first glance due to the presence of a segmented nucleus and abundant eosinophilic cytoplasmic granules in both cell types. They can be distinguished to some extent on the basis of nuclear and granule morphology; heterophils are slightly smaller, have a more segmented nucleus and fewer and smaller cytoplasmic granules than eosinophils. However, when an infiltrate is composed of only one of these two cell types, these relative distinguishing features are less useful and so additional methods may become of interest, especially considering that the functional differences of these cell types parallel those in other species. Major Basic Protein is a constituent of eosinophil granules [205] and here we show that antibody directed against this protein (clone BMK-13) can be used to definitively distinguish eosinophils from heterophils. To our knowledge, there is no existing literature using this method in guinea pigs, and we hereby recommend its use in cases where accurate description of the inflammatory infiltrate is of importance. Using major basic protein antibody immunohistochemistry, we found that eosinophils were the predominant polymorphonuclear cell type in airway infiltrates of infected animals. Tang et al also report the presence of eosinophils in the airways of infected animals and speculate that this finding is suggestive of airway hypersensitivity [201]. Inbred guinea pigs have previously been shown to mount a delayed hypersensitivity response to influenza A infections using nasal washes and peritoneal exudates [206], a finding that would be consistent with these observations. However, the exact significance of this finding in the pathological response to influenza remains to be elucidated.

In summary, we have explored, for the first time, infection of isogenic strain 2 guinea pigs with pandemic H1N1 influenza virus as an influenza animal model. The IT and IN route of inoculation were compared and for both procedures, productive infection of the upper

respiratory tract was achieved, with a peak in viral replication around day 2 p.i.. IT inoculation appeared to result in more widespread viral replication and associated histological lesions in both the upper and lower respiratory tract whereas after IN inoculation histopathological changes were more restricted to the nasal cavity. Thus, compared to IN inoculation, the pathogenesis of infection of guinea pigs after IT inoculation may mimic viral pneumonia in humans more closely. However, IT administration is a technically more demanding procedure. In addition to these findings, we presented a novel way to accurately distinguish heterophils from eosinophils in guinea pig formalin-fixed, paraffin embedded tissue sections using major basic protein antibody (BMK-13).

The use of this particular inbred strain of guinea pigs seems a promising model for human infections with influenza virus. Furthermore, it would allow investigation of virus specific cellular immunity and identification of immune correlates of cross-protection against influenza virus infection by adoptive transfer of selected lymphocyte subsets. Since guinea pigs transmit influenza virus efficiently, the model also allows studying the impact of immunity on virus transmission.

CHAPTER 3

VIRUS REPLICATION KINETICS AND PATHOGENESIS OF INFECTION WITH
H7N9 INFLUENZA VIRUS IN ISOGENIC GUINEA PIGS UPON
INTRATRACHEAL INOCULATION

Wiersma LC, Kreijtz JH, Vogelzang-van Trierum SE, van Amerongen G, van Run P, Ladwig M, Banneke S, Schaefer H, Fouchier RA, Kuiken T, Osterhaus AD, Rimmelzwaan GF

Vaccine, 2015. Dec 8;33(49):6983-7

ABSTRACT

Since 2013, avian influenza viruses of subtype H7N9 have been transmitted from poultry to humans in China and caused severe disease. Concerns persist over the pandemic potential of this virus and further understanding of immunity and transmission is required. The isogenic guinea pig model uniquely would allow for investigation into both. Eighteen female isogenic guinea pigs 12-16 weeks were inoculated intratracheally with either A/H7N9 virus (n=12) or PBS (n=6) and sacrificed on days 2 and 7 post-inoculation. Nasal and pharyngeal swabs were taken daily to assess viral replication kinetics and necropsies were performed to study pathogenesis. All animals showed peak virus titers in nasal secretions at day 2 post-inoculation and by day 7 post-inoculation infectious virus titers had decreased to just above detectable levels. At day 2, high virus titers were found in nasal turbinates and lungs and moderate titers in trachea and cerebrum. At day 7, infectious virus was detected in the nasal turbinates only. Histology showed moderate to severe inflammation in the entire respiratory tract and immunohistochemistry (IHC) demonstrated large numbers of viral antigen positive cells in the nasal epithelium at day 2 and fewer at day 7 post-inoculation. A moderate number of IHC positive cells was observed in the bronchi(oli) and alveoli at day 2 only. This study indicates that isogenic guinea pigs are a promising model to further study immunity to and transmission of H7N9 influenza virus.

INTRODUCTION

In 2013, the first human cases of infection with avian influenza viruses of subtype H7N9 were reported in China. As of February 23rd, 2015 a total of 571 laboratory-confirmed infections have been reported to WHO, of which 212 had a fatal outcome [207]. Infections have thus far been the result of direct transmission from birds predominantly and only a few human-to-human transmission clusters have been reported [208-210]. Although recent studies have shown that adaptation of the virus incurs a fitness cost in ferrets [211], concerns persist over the probability that the virus will acquire the necessary mutations for sustained human-to-human transmission. As this subtype has not previously circulated in the human population, humoral immunity is virtually absent and the impact of a pandemic could therefore be substantial. Both viral transmission and the effect of pre-existing (cellular) immunity are crucial elements in determining the pandemic potential of H7N9 influenza virus. Therefore, further investigation into both these factors

is of key importance. Typically, the ferret model is used to investigate certain aspects of influenza virus infections such as pathogenesis and transmission [212-214]. However, possibilities to study virus-specific immunity and its effect on pathogenesis and transmission are limited.

Isogenic guinea pigs have recently been identified as a model for studying influenza viruses [215] and may offer some advantages over the ferret model. Guinea pigs have been used as models for influenza virus transmission [187, 216] and strain 2 (isogenic) guinea pigs additionally offer the possibility for more in depth study of cellular immunity through adoptive transfer of immune cell subsets [190, 193].

Another advantage of this model is that guinea pigs have been shown to be susceptible to unadapted mammalian and avian influenza viruses [187]. Avian influenza viruses bind predominantly to α -2,3-linked sialic acid (SA) receptors and mammalian influenza viruses preferentially bind α -2,6-linked SA receptors [217]. In guinea pigs, both α -2,3-linked and α -2,6-linked SA receptors are abundantly present in the nasal cavity and trachea, whereas α -2,3-linked SA receptors predominate in the lungs [57]. Similarly in humans, the upper airways express relatively more α -2,6-linked SA receptors and the lower airways express more α -2,3-linked SA receptors [218]. H7N9 is a virus of avian origin and therefore binds more readily to α -2,3-linked SA receptors, and the overall pattern of H7N9 attachment in guinea pig tissue was found to be similar to that observed in humans. In both species, the virus attached (albeit to a slightly different extent) to ciliated epithelial cells in the nasal turbinates, trachea, and bronchus, ciliated and nonciliated cells in the bronchioles, and both type I and type II pneumocytes in the alveoli [219]. Although the ferret is one of the most commonly used animal models for influenza virus infection and transmission, the attachment pattern of H7N9 virus was rather dissimilar to humans [219] and use of guinea pigs may therefore offer an additional advantage for studying this particular viral subtype. In this study we determined the virus replication kinetics and pathogenesis of intratracheal influenza A H7N9 virus infection in strain 2 isogenic guinea pigs to assess the suitability of this model for future transmission and immunity studies.

MATERIALS AND METHODS

Virus preparation

Influenza virus A/Anhui/1/2013 was propagated in embryonated chicken eggs three times and confluent Madin-Darby Canine Kidney (MDCK) cells once. Culture supernatants were harvested after the appearance of cytopathic changes, cleared by low-speed

centrifugation and stored at -70°C . MDCK cells were used to determine virus titre, as described [198]. Virus was diluted in Phosphate Buffered Saline (PBS) to the desired concentration, 2×10^6 TCID₅₀ per 500 μL , for intratracheal inoculation.

Animals and experimental design

The animal experimentation protocol was approved by an independent animal welfare committee (DEC Consult) and experiments were performed in compliance with national and European legislation. The Federal Institute for Risk Assessment (BfR) in Berlin, Germany provided eighteen 12-16 week old (320-600 grams) isogenic strain 2 guinea pigs. Animals were tested prior to the start of the experiment for presence of antibodies to circulating influenza viruses A/H1N1, A/H3N2 and B/Yamagata-like and their respective vaccine strains using the haemagglutination inhibition assay, as previously described [197]. No antibodies against these viruses were detected in any of the animals.

Three groups of 6 animals were held in biosafety level 3 conditions at the animal facilities of the Erasmus Dierexperimenteel Centrum, on a 12-hour light/dark cycle with ad-libitum access to food and water.

Intratracheal inoculation was performed under ketamine and medetomidine anesthesia on all 18 animals by injecting 500 μL of either 2×10^6 tissue culture infectious dose (TCID₅₀) H7N9 virus A/Anhui/1/2013 (n=12) or Phosphate Buffer Saline (PBS) (n=6) transcutaneously (surgically) directly into the trachea, with the animal in dorsal recumbency. The anesthetic was antagonized with atipamezole and during recovery animals were placed with the head slightly elevated to prevent loss of the inoculum. Nasal, pharyngeal and rectal swabs were taken daily and animals were weighed on day 0, 1 and 2 (n=18), 3, 4 and 7 (n=9) post-inoculation (p.i.) under isoflurane anesthetic. On day 2 and day 7 p.i., 6 animals from the virus infected group and 3 animals from the PBS control group were anesthetized with ketamine and medetomidine, exsanguinated and necropsied.

Pathological examination and Immunohistochemistry

Necropsies were conducted following standard procedures. Before opening the thoracic cavity, the trachea was clamped to prevent deflation of lungs and allow for accurate visual assessment of the percentage of lung tissue affected. Nasal turbinates, nasal septum, trachea, tracheobronchial lymph node, bronchus, lung, olfactory bulb, cerebrum, cerebellum, liver, heart, kidney, spleen, duodenum and colon were sampled and fixed in 10 % neutral buffered formalin. Prior to fixation, the right lung was inflated with formalin to improve histological assessment.

Formalin fixed tissues were embedded in paraffin and cut to 4 μm . For histological and immunohistochemical evaluation, tissue was stained with either haematoxylin and eosin (HE), or with an immunoperoxidase method using a monoclonal antibody against influenza nucleoprotein, respectively. IgG2a isotype controls of each tissue and a positive control were included for the immunoperoxidase method. Identity of the animals was concealed prior to evaluation of the slides and lung lobes were sectioned according to a standard protocol to avoid bias. HE stained slides were semi-quantitatively evaluated using standardized criteria [199] and IHC slides were assessed semi-quantitatively by visually estimating the proportion of cells that showed a positive nuclear stain.

Assessment of virus titers in swabs and tissue

All swabs were stored at $-70\text{ }^{\circ}\text{C}$ in transport medium (Hanks' balanced salt solution with 0.5 % lactalbumin, 10 % glycerol, 200 U/ml penicillin, 200 $\mu\text{g}/\text{ml}$ streptomycin, 100 U/ml polymyxin B sulfate, 250 $\mu\text{g}/\text{ml}$ gentamicin, and 50 U/ml nystatin (ICN Pharmaceuticals, Zoetermeer, Netherlands)). Tissue samples of cerebrum (including olfactory bulb), cerebellum, nasal turbinates, trachea, lung, liver, spleen, duodenum and colon were stored at $-70\text{ }^{\circ}\text{C}$.

In order to determine virus titers in tissues, samples were weighed and homogenized (FastPrep-24 homogenizer (MP Biomedicals, Eindhoven)) in the aforementioned transport medium and centrifuged. MDCK cells were infected with tenfold serial dilutions of supernatant of swabs and processed tissue samples (in quintuplicate for respiratory and central nervous system tissue samples and nasal swabs and in quadruplicate for samples from PBS inoculated animals, remaining tissues and pharyngeal and rectal swabs). Haemagglutination activity of the culture supernatants of MDCK cells was assessed on day 5 after inoculation to demonstrate the presence of virus [198]. The Spearman-Kärber standard equation was used to calculate the tissue culture infectious dose 50 (TCID₅₀ expressed per milliliter for swabs and per gram for tissue samples).

RESULTS

Infection with H7N9 virus resulted in minor clinical signs

Animals displayed few clinical signs. On day two, the group inoculated with virus showed ruffled fur, decreased activity and animals were slower to recover from isoflurane anesthetic. From day 0 to day 1 virus inoculated animals showed minimal weight loss (1.6%) compared to the PBS group. A small amount of serous nasal exudate was only observed upon anesthesia with isoflurane in all animals.

Virus replicated in the entire respiratory tract and peaked at day 2 post-inoculation

All animals showed a peak in viral titer in nasal secretions at day 2 p.i. (mean titer 3.0 TCID₅₀/ml (10log) standard deviation (SD) 1.8) (p.i.) and by day 7 p.i., only two out of six animals still showed detectable titers (2.3 and 2.1 TCID₅₀/ml (10log)), detection limit <0.5 TCID₅₀/ml (10log) (Figure 1 (A)). Pharyngeal swabs were intermittently positive for all virus infected animals but no clear pattern of virus excretion was observed. Infectious virus was not isolated from any of the rectal swabs.

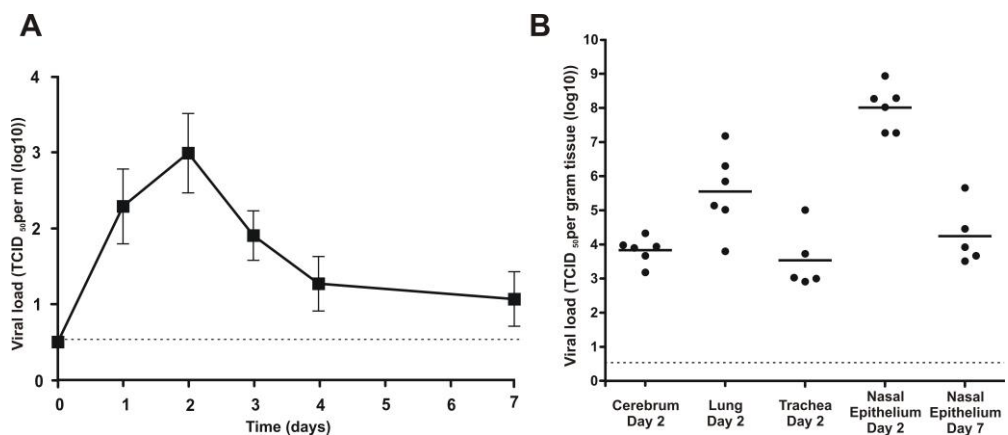


Figure 1 (A) Tissue viral load after IT inoculation with influenza A/H7N9. Cerebrum day 2 p.i., Lung day 2 p.i., Trachea day 2 p.i., Nasal turbinates day 2 p.i. and Nasal turbinates day 7 p.i. (dashed line indicates limit of detection < 0.5 TCID₅₀ per gram (10log)). **(B) Viral load in nasal swabs after IT inoculation with influenza A/H7N9 virus.** For day 0, 1 and 2: n=12, for day 3, 4 and 7: n=6 (dashed line indicates limit of detection < 0.5 TCID₅₀ per milliliter (10log)).

At day 2 p.i., infectious virus was isolated from nasal turbinates (mean titer 8.0 TCID₅₀/gr (10log) SD 0.7, n= 6/6), trachea (3.0 TCID₅₀/gr (10log) SD 1.7, n= 5/6), lung (5.6 TCID₅₀/gr (10log) SD 1.2, n= 6/6) and cerebrum (3.8 TCID₅₀/gr (10log) SD 0.4, n=5/6) (Figure 1 (B)). Virus could not be isolated from remaining tissues, with the exception of one animal that showed low titers in kidney (2.7 TCID₅₀/gr (10log)) and liver (2.5 TCID₅₀/gr (10log)) at day 2. By day 7 p.i., virus could be isolated only from nasal turbinates (3.5 TCID₅₀/gr (10log) SD 1.9, n= 5/6) (Figure 1 (B)).

All PBS inoculated animals tested negative for viral excretion.

Infection with H7N9 causes rhinitis, tracheitis, bronch(iol)itis and brochointerstitial pneumonia

Macroscopically, lungs of virus inoculated animals showed multifocal to coalescing well-demarcated areas of hyperaemia and consolidation affecting up to 30% of lung tissue. On day 2, and to a lesser extent day 7, a moderate quantity of mucopurulent exudate was present in the nasal cavity of all infected animals, especially caudally, and the mucosa was diffusely hyperaemic.

Histological evaluation of tissues of infected animals revealed moderate to marked inflammation of the epithelium and submucosa of the nasal cavity, trachea and bronchi, with an inflammatory infiltrate composed predominantly of eosinophils and fewer heterophils. (Figure 3 A, B, C) Epithelial cells of the nasal cavity, and to a lesser extent, the trachea and bronchi frequently showed karyopyknosis, karyorrhexis and karyolysis (necrosis) (Figure 3). In the nasal cavity this was multifocally associated with formation of a necropurulent exudate, especially on day 2 p.i. (Figure 2 and 3). The lumen of smaller airways frequently contained necrotic debris and flocculent eosinophilic material (mucus). Pulmonary parenchyma showed multifocal to coalescing areas of dense cellular infiltrates consisting of eosinophils, heterophils and macrophages in the walls and lumen of alveoli, frequently accompanied by epithelial cell necrosis (Figure 3D).

Lesions in the respiratory tract were of similar nature on both day 2 and day 7 p.i., however on day 2 they were generally more severe and on day 7, there was evidence of moderate mononuclear cell infiltration around the airways and type II pneumocyte hyperplasia in the alveoli (regeneration) (Figure 2). The cerebrum (including the olfactory bulb) and the cerebellum showed no macroscopic or histopathological changes.

Tissues collected from PBS inoculated animals showed minimal to mild presence of eosinophils in the epithelium and, where present, submucosa, throughout the respiratory tract. One animal showed mild focal pyogranulomatous tracheitis with intralesional bacteria at day 2 p.i., likely as a consequence of the inoculation.

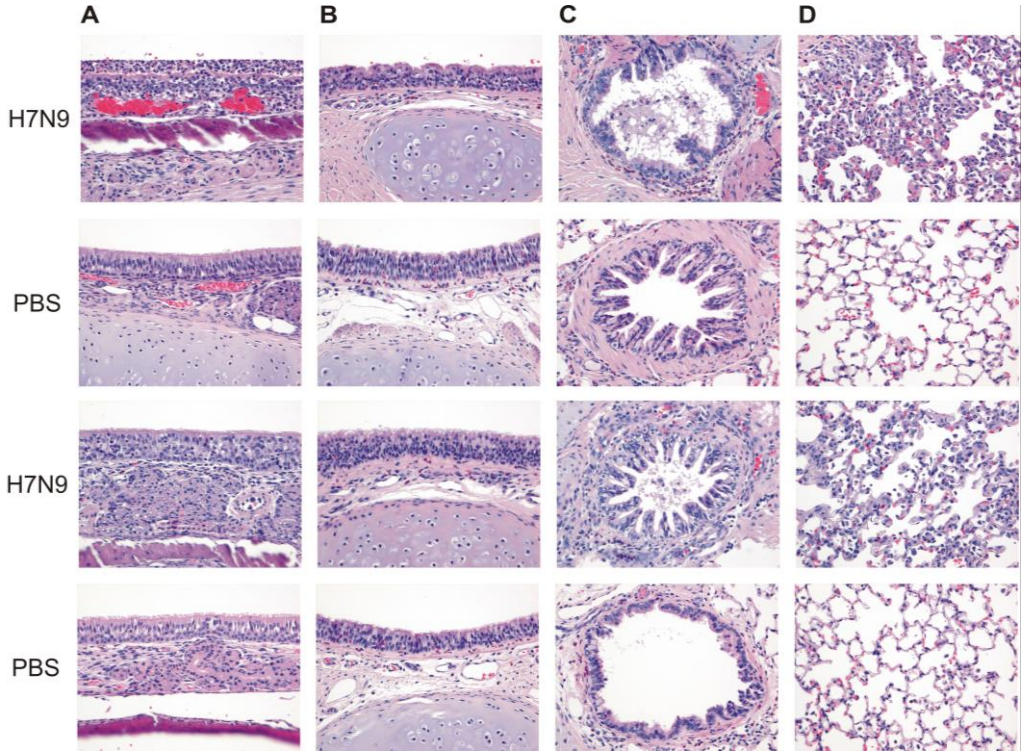


Figure 2 Haematoxylin and Eosin (HE) stain (x20). Respiratory tissues of A/H7N9 inoculated animals and PBS inoculated control animals at day 2 (top two rows) and day 7 (bottom two rows) post-inoculation (A) Nasal turbinates (B) Trachea (C) Bronchi (D) Alveoli.

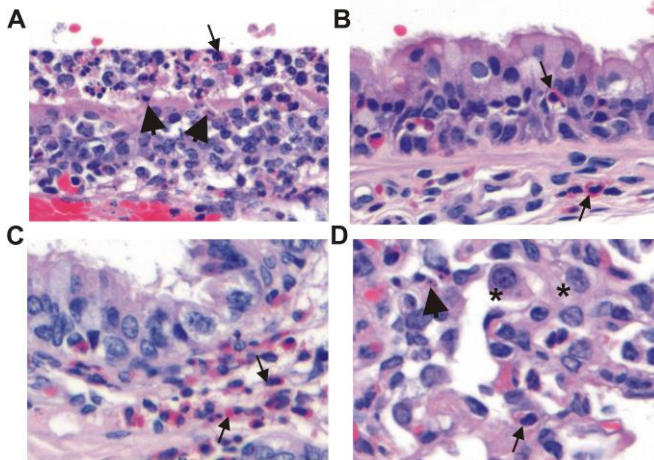


Figure 3 Hematoxylin and eosin (HE) (40x). Close up of histopathological lesions in respiratory tissues of A/H7N9 inoculated animals day 2 post-inoculation. Arrowheads indicate necrosis, arrows indicate heterophilic and eosinophilic inflammatory cells, asterisk indicates macrophages: (A) nasal epithelium showing a layer of exudate composed of inflammatory cells and necrotic debris; (B) trachea showing inflammatory infiltrates in the epithelium and submucosa; (C) bronchiole showing inflammatory infiltrates predominantly in the submucosa; (D) alveoli showing thickened alveolar septae with inflammatory infiltrates and necrosis.

Virus-infected cells were detected in the entire respiratory tract at day 2

Moderate numbers of viral antigen positive cells were found only in the nasal epithelium, bronchi(oli) and alveoli 2 days p.i.. On day 7 p.i., antigen positive cells were found in nasal epithelium only (Figure 3). No viral antigen was detected in any other tissues, including the olfactory bulb.

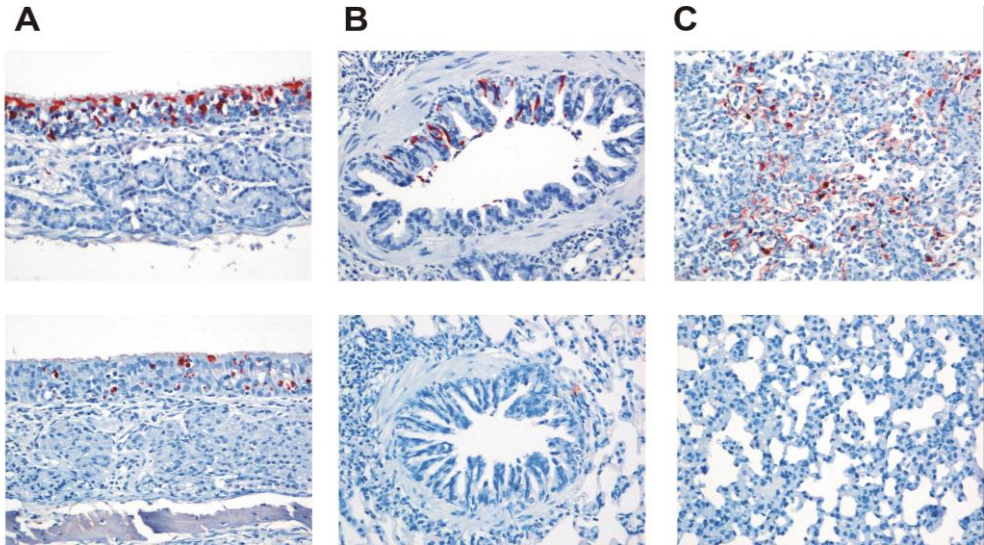


Figure 12 Immunohistochemistry (IHC) (x20) A/H7N9 inoculated animals at day 2 (top row) and day 7 (bottom row) post-inoculation (A) Nasal turbinates (B) Bronchi (C) Alveoli.

DISCUSSION

The present study shows the virus replication kinetics and pathogenesis of influenza A/H7N9 virus infection in strain 2 isogenic guinea pigs after intratracheal inoculation.

At day 2 p.i., virus inoculated animals showed a peak in viral titers in nasal secretions, infectious virus was isolated from nasal turbinates, trachea, lung and cerebrum and viral antigen was demonstrated in nasal turbinates, bronchi and alveoli by IHC. By day 7, infectious virus and viral antigen was only found in nasal turbinates and mean infectious virus titers in nasal secretions had decreased to just above detectable levels. Histology showed moderate to severe acute necrotizing rhinitis and (broncho)interstitial pneumonia and mild to moderate tracheitis.

Although infectious virus was found in the cerebrum at day 2, no viral antigen was detected by immunohistochemistry in the olfactory bulb or other central nervous tissues at this time point, nor were any histopathological changes noted. The ability of this virus to infect the brain of these guinea pigs therefore remains uncertain.

Virus replication kinetics correspond to previous reports of H7N9 virus infection in outbred guinea pigs, where peak virus titers also occurred at day 2 [216]. However in that particular study, animal numbers were low and inoculation was intranasal rather than intratracheal. Although they found infectious virus in the lungs, virus infected cells were not demonstrated in the airways or alveoli using IHC. The study in these outbred animals also showed a predominantly mononuclear inflammatory reaction in the respiratory tract, especially later in infection, which we did not observe in our model [216].

The ferret model is still considered to best mimic the pathogenesis of influenza infections in humans and when compared to intratracheal H7N9 virus infection in ferrets, the guinea pig model shows similar pathogenesis and replication kinetics. H7N9 virus reaches higher titers and persist longer in the nasal turbinates of guinea pigs than ferrets and, in contrast to ferrets, submucosal glands are not affected. For similar inoculatory doses, ferrets generally show more prominent clinical signs and a higher percentage of lung tissue affected than strain 2 guinea pigs as a result of H7N9 virus infection [213, 214].

The distribution of the virus in the respiratory tract resembles what was shown by virus binding [219] and what would be expected knowing receptor distribution in the guinea pig; namely that it is found in both the upper and lower respiratory tract.

Histopathological changes following intratracheal H7N9 inoculation were more severe, necrotizing and widespread than after intratracheal inoculation with H1N1pdm09 virus in this strain of guinea pigs [215]. H7N9 virus infected animals also showed higher average peak viral titers and more prolonged virus shedding from the nose than H1N1pdm09 infected animals [215].

This experiment confirms that the use of this strain of isogenic guinea pigs is very useful for investigating influenza viruses with pandemic potential, including the newly emerging H7N9 viruses. The model allows simultaneous examination influenza virus pathogenesis, immunity, and transmission.

CHAPTER 4

HETEROSUBTYPIC IMMUNITY TO H7N9 INFLUENZA VIRUS IN ISOGENIC GUINEA PIGS AFTER INFECTION WITH PANDEMIC H1N1 VIRUS

Wiersma LC, Kreijtz JH, Vogelzang-van Trierum SE, van Amerongen G, van Run P, Ladwig M, Banneke S, Schaefer H, Fouchier RA, Kuiken T, Osterhaus AD, Rimmelzwaan GF

Vaccine, 2015. Dec 8;33(49):6977-82

ABSTRACT

Heterosubtypic immunity is defined as immune-mediated (partial) protection against an influenza virus induced by an influenza virus of another subtype to which the host has not previously been exposed. This cross-protective effect has not yet been demonstrated to the newly emerging avian influenza A viruses of the H7N9 subtype. Here, we assessed the induction of protective immunity to these viruses by infection with A(H1N1)pdm09 virus in a newly developed guinea pig model. To this end, ten female 12-16 week old strain 2 guinea pigs were inoculated intratracheally with either A(H1N1)pdm09 influenza virus or PBS (unprimed controls) followed 4 weeks later with an A/H7N9 influenza virus challenge. Nasal swabs were taken daily and animals from both groups were sacrificed on days 2 and 7 post inoculation (p.i.) with A/H7N9 virus and full necropsies were performed. Nasal virus excretion persisted until day 7 in unprimed control animals, whereas only two out of seven H1N1pdm09-primed animals excreted virus via the nose. Infectious virus was recovered from nasal turbinates, trachea and lung of all animals at day 2 p.i., but titers were lower for H1N1pdm09-primed animals, especially in the nasal turbinates. By day 7 p.i., relatively high virus titers were found in the nasal turbinates of all unprimed control animals but infectious virus was isolated from the nose of only one of four H1N1pdm09-primed animals. Animals of both groups developed inflammation of variable severity in the entire respiratory tract. Viral antigen positive cells were demonstrated in the nasal epithelium of both groups at day 2. The bronchi(oli) and alveoli of unprimed animals showed a moderate to strong positive signal at day 2, whereas H1N1pdm09-primed animals showed only minimal positivity. By day 7, only viral antigen positive cells were found after H7N9 virus infection in the nasal turbinates and the lungs of unprimed controls. Thus infection with H1N1pdm09 virus induced partially protective heterosubtypic immunity to H7N9 virus in (isogenic) guinea pigs that could not be attributed to cross-reactive virus neutralizing antibodies.

INTRODUCTION

In addition to the enormous public health burden of seasonal influenza viruses, newly emerging and pandemic viruses pose a constant threat. In 2009, an influenza A(H1N1) (H1N1pdm09) virus of swine-origin emerged in humans [180], caused a worldwide pandemic and has continued to circulate [220]. In 2013, H7N9 virus crossed the species barrier from poultry in China and new cases are still being reported [207]. In such

situations, when an influenza virus of a novel subtype is introduced into a naive population, specific immunity to the new virus is limited. However, it has long been recognized that infection with an influenza virus of one subtype can confer a certain degree of protection to infection with a virus of another subtype [221]. This type of cross-protection is known as heterosubtypic immunity and, although it generally does not offer sterile protection, it can contribute significantly to decreasing disease severity and virus shedding [106]. Besides antibody mediated immunity, cell mediated immunity, particularly mediated by CD8⁺ cytotoxic lymphocytes (CTLs), has repeatedly been demonstrated to contribute to heterosubtypic immunity to influenza virus infections (reviewed in [222]).

Heterosubtypic immunity has been demonstrated in several species including mice [102, 107], macaques [109, 110], ferrets [108], pigs [223, 224], ducks [225, 226], chickens [227, 228], cotton-rats [229] and has also been confirmed following natural infection in humans [113]. Previous infection with H3N2 has been shown to have an effect on viral transmission of pandemic H1N1 virus in outbred guinea pigs [195] but to date, the existence of heterosubtypic immunity has not been ascertained in (isogenic) guinea pigs and, although it has been speculated that prior infection with H1N1pdm09 would provide a certain degree of protection against H7N9 infection [230], this combination of viruses has never been studied in an animal model.

Strain 2 isogenic guinea pigs have recently been identified as a model for influenza virus infection [215]. The fact that these guinea pigs are inbred, and therefore isogenic, offers exciting new possibilities to study immune mediated mechanisms of protection against influenza virus infections. For example, adoptive transfer experiments can be conducted by isolating lymphocytes from a donor that has been infected with an influenza virus to a naive recipient, that is subsequently challenged with a heterologous virus subtype, as has been performed in mice [116, 231]. In addition, guinea pigs, like ferrets, may transmit influenza viruses efficiently and therefore this model would offer the unique possibility to study the effect of cell-mediated immunity on transmission of influenza viruses. Reagents for studying cell-mediated immunity in guinea pigs are more abundantly available than those for ferrets [191, 232].

To explore the induction heterosubtypic immunity in strain 2 isogenic guinea pigs, animals were intratracheally inoculated with H1N1pdm09 virus or PBS as a control. Four weeks later, H1N1pdm09 primed and unprimed animals were challenged with H7N9 virus. Virus titers, as well as histopathological and immunohistochemical parameters were compared between the two groups.

MATERIALS AND METHODS

Virus preparations

H7N9 influenza virus A/Anhui/1/2013, isolated from a fatal human case and kindly provided by the WHO Pandemic Influenza Preparedness (PIP) framework, was propagated in embryonated chicken eggs three times and confluent Madin-Darby Canine Kidney (MDCK) cells once. Influenza virus A/Netherlands/602/2009 (A(H1N1)pdm09) was propagated in confluent MDCK cells twice. After the appearance of cytopathic changes, culture supernatants were harvested, cleared by low-speed centrifugation and stored at -70°C . Virus titer was determined in MDCK cells, as described [198]. Virus was diluted in Phosphate Buffered Saline (PBS) to 2×10^6 tissue culture infectious dose (TCID₅₀) per 500 μL , for intratracheal inoculation. The choice of dose and inoculatory route was based on previous experiments with H1N1pdm09 in isogenic guinea pigs [215].

Animals and experimental design

Experiments were performed in compliance with national and European legislation and an independent animal welfare committee (DEC Consult) approved the animal experimentation protocol. The Federal Institute for Risk Assessment (BfR) in Berlin, Germany supplied ten 12-16 week old (320-600 grams) female isogenic strain 2 guinea pigs. A haemagglutination inhibition assay was performed as previously described [197] to test for the presence of antibodies to circulating influenza viruses A/H1N1, A/H3N2 and B/Yamagata-like and their respective vaccine strains. All animals were found to be negative for antibodies to influenza prior to the start of the experiment.

Two groups, one group of 3 and one group of 7 animals, were housed in two separate glove boxes (biosafety level 3 conditions) at the animal facilities of the Erasmus Dierexperimenteel Centrum, on a 12-hour light/dark cycle with ad-libitum access to food and water.

All 10 animals were anesthetized with ketamine and medetomidine and inoculated intratracheally by keeping the animals in dorsal recumbency and injecting a total volume of 500 μL transcutaneously directly into the trachea. The anesthetic was antagonized with atipamezole, and animals were placed with their heads slightly elevated to prevent loss of the inoculum.

The group of 3 animals received Phosphate Buffer Saline (PBS) followed 4 weeks later by 2×10^6 TCID₅₀ influenza virus A/Anhui/1/2013 (H7N9) (further referred to as unprimed animals). The group of 7 animals received 2×10^6 TCID₅₀ H1N1pdm09 virus

A/Netherlands/602/09 followed four weeks later by 2×10^6 TCID₅₀ of the H7N9 virus (further referred to as H1N1pdm09-primed animals).

After inoculation with H1N1pdm09, nasal swabs were taken on day 2 to verify that all animals were indeed productively infected. On day 0, 1, 2, 3, 4 and 7 after H7N9 inoculation, all animals were weighed and nasal, pharyngeal and rectal swabs were taken under isofluorane anesthesia. Animals were anesthetized with ketamine and medetomidine, exsanguinated and necropsied on day 2 post inoculation (one unprimed animal and three H1N1pdm09-primed animals) and on day 7 p.i. (2 unprimed and four H1N1pdm09-primed animals). Unless otherwise specified, days p.i. refers to time points after inoculation with H7N9 virus.

Assessment of virus titers in swabs and tissue

All swabs were stored at -70°C in transport medium (Hanks' balanced salt solution with 0.5% lactalbumin, 10% glycerol, 200 U/ml penicillin, 200 µg/ml streptomycin, 100 U/ml polymyxin B sulfate, 250 µg/ml gentamicin, and 50 U/ml nystatin (ICN Pharmaceuticals, Zoetermeer, Netherlands)). Tissue samples of cerebrum (including olfactory bulb), cerebellum, nasal turbinates, trachea, lung, liver, spleen, duodenum and colon were stored at -70°C.

Virus titers in tissues were determined by weighing and homogenizing samples (FastPrep-24 homogenizer (MP Biomedicals, Eindhoven)) in the transport medium, followed by centrifugation. MDCK cells were infected with tenfold serial dilutions of supernatant of swabs and processed tissue samples (in quintuplicate for respiratory and central nervous system tissue samples and nasal swabs and in quadruplicate for remaining tissues and pharyngeal and rectal swabs). Haemagglutination (HA) activity of the culture supernatants of MDCKs was assessed on 5-7 days after infection to demonstrate the presence of virus [198]. The tissue culture infectious dose 50 (TCID₅₀ expressed per milliliter for swabs and per gram for tissue samples) was calculated using the Spearman-Kärber standard equation. The detection limit was <0.5 TCID₅₀/ml.

Virus Neutralization

In order to detect virus-neutralizing antibodies, heat inactivated sera from day 0 and day 28 p.i. with H1N1pdm09 and day 2 and 7 p.i. with H7N9 virus were prepared in 60 µl volumes of 2-fold serial dilutions starting at 1:10. Virus (H1N1pdm09 and H7N9) was diluted to 20 TCID₅₀/ml in infection medium (Lonza BioWhittaker Modified Eagle's Medium (EMEM), with Earle's Balanced Salt Solution, HEPES, Sodium Bicarbonate, 200 U/ml penicillin, 200 µg/ml streptomycin, L-Glutamine, 10% fetal calf serum and trypsin) and 50 µl was added to all wells containing antibody dilutions and incubated at 37°C for

2 hours. MDCK cells were washed and the virus-serum mixture was transferred onto the cells and incubated overnight at 37 °C. The next day, medium was removed and replaced with 200 µl of infection medium. Cells were incubated for 5-7 days after which an HA assay was performed [198].

Pathological examination and Immunohistochemistry

Standard necropsy procedures were followed. The trachea was clamped before opening the thoracic cavity to prevent deflation of lungs, and allow for accurate visual assessment of pulmonary tissue. Nasal turbinates, nasal septum, trachea, tracheobronchial lymph node, bronchus, lung, olfactory bulb, cerebrum, cerebellum, liver, heart, kidney, spleen, duodenum and colon were sampled and fixed in 10 % neutral buffered formalin. Prior to fixation, the right lung was inflated with formalin to improve histological assessment.

Paraffin embedded, formalin fixed tissues were cut to 4 µm. For histological evaluation, tissue was stained with haematoxylin and eosin (HE). For immunohistochemical evaluation, tissue was stained with an immunoperoxidase method using a monoclonal antibody against influenza nucleoprotein. IgG2a isotype controls were used for each tissue and one positive control was included. Animals were anonymized before evaluation of the slides and lung lobes were sectioned according to a standard protocol to avoid bias. Standardized criteria were used to semi-quantitatively evaluate HE stained slides [199] and IHC slides were assessed by visually estimating the proportion of cells that showed a positive nuclear stain.

RESULTS

Clinical signs

All animals displayed limited clinical signs upon challenge infection with H7N9 virus. On day two, animals from both groups showed ruffled fur, decreased activity and were slower to recover from isofluorane anesthetic. A small amount of serous nasal exudate was only observed upon anesthesia with isofluorane in all animals. Most animals showed a small decrease in body weight (< 5%) from day 0 to day 2 p.i.

Virus titers

Unprimed animals showed peak virus titers in nasal swabs at day 2 p.i. (mean $10^{2.5}$ TCID₅₀/ml SD 0.8), on day 3 and 4 p.i. titers dropped below detectable levels and by day 7 p.i. virus was again detectable ($10^{1.9}$ TCID₅₀/ml SD 0.28).

H1N1pdm09-primed all animals were productively infected with pH1N1, as confirmed by virus excretion in nasal swabs on day 2 following inoculation. Following H7N9 inoculation, only two animals showed detectable virus titers in nasal secretions. One animal showed detectable virus on day 1 ($10^{2.7}$ TCID₅₀/ml) and day 2 ($10^{2.3}$ TCID₅₀/ml), the other was positive on day 3 ($10^{2.7}$ TCID₅₀/ml) and day 4 ($10^{2.3}$ TCID₅₀/ml) and virus was not detected in any animal on day 7. All other animals in this group were uniformly negative for virus in nasal secretions (Figure 1).

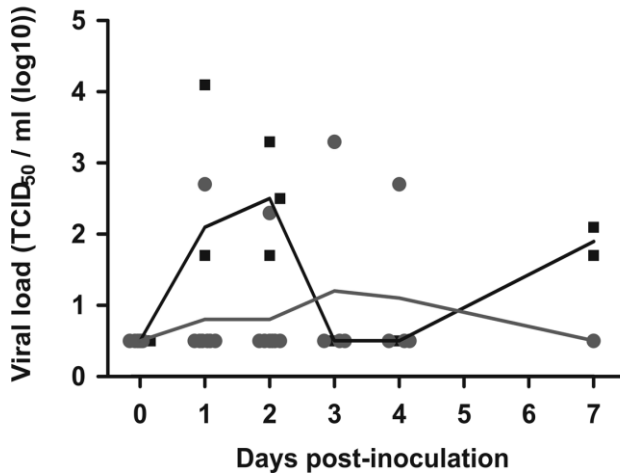


Figure 1 Viral load in nasal swabs (TCID₅₀ per milliliter (log₁₀)) after inoculation with A/H7N9/Anhui/1/2013 influenza virus. Individual unprimed animals are shown in black squares and the black line represents the average (day 0-2 p.i. $n=3$, day 3-7 p.i. $n=2$) Individual H1N1pdm09-primed animals are shown in grey circles and the red line represents the average (day 0-2 p.i. $n=7$, day 3-7 p.i. $n=4$) (limit of detection < 0.5 TCID₅₀/ml (log₁₀)).

Pharyngeal swabs showed intermittent low viral titers for all virus infected animals but no clear pattern of virus excretion was demonstrated.

Infectious virus was isolated from the one unprimed animal that was sacrificed at day 2 p.i., from nasal turbinates ($10^{7.6}$ TCID₅₀/gr), trachea ($10^{5.0}$ TCID₅₀/gr), lung ($10^{5.2}$ TCID₅₀/gr) and cerebrum ($10^{2.0}$ TCID₅₀/gr). From the two animals that were sacrificed on day 7 p.i., virus was isolated from nasal turbinates (mean $10^{4.9}$ TCID₅₀/gr SD 0.9, $n=2/2$) and cerebrum ($10^{2.3}$ TCID₅₀/gr SD 0.4, $n=2/2$). Virus was not isolated from remaining tissues.

Infectious virus was isolated from H1N1pdm09-primed animals at day 2 p.i., from nasal turbinates ($10^{4.6}$ TCID₅₀/gr SD 1.4, $n=3/3$), lung ($10^{4.1}$ TCID₅₀/gr SD 0.5, $n=3/3$), trachea

($10^{3.4}$ TCID₅₀/gr SD 0.6, n= 3/3) and cerebrum ($10^{2.0}$ TCID₅₀/gr SD 1.8, n= 2/3). The one animal that shed virus from the nose on day 1 and 2 had significantly higher virus titers in the nasal turbinates at day two than the animals that showed no nasal shedding at this time point ($10^{6.1}$ TCID₅₀/gr compared to $10^{4.4}$ and $10^{3.3}$ TCID₅₀/gr). By day 7 p.i., virus could be isolated from nasal turbinates of only one animal ($10^{3.1}$ TCID₅₀/gr, n= 1/4), which was the same animal that showed nasal shedding on day 3 and 4. Virus could not be isolated from remaining tissues. Although virus titres in all respiratory tissues at day 2 p.i. and nasal turbinates at day 7 p.i. were visibly lower in H1N1pdm09 primed animals than in unprimed animals (and historical H7N9 controls, see accompanying paper), small sample sizes precluded statistical analysis (Figure 2).

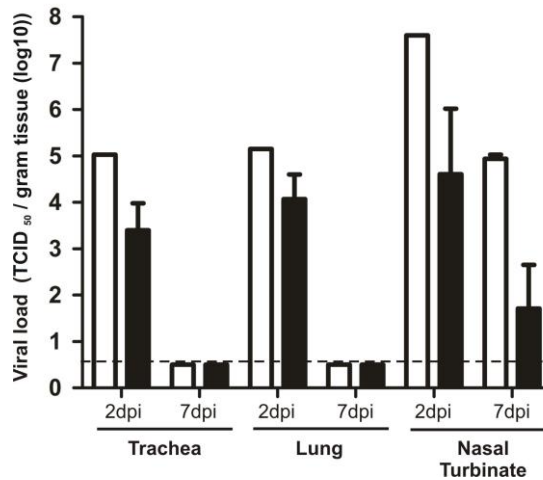


Figure 2 Viral load in respiratory tract tissues (TCID₅₀ per gram tissue (log₁₀)) after inoculation with A/Anhui/1/2013 (H7N9) influenza virus. Titers in trachea, lung and nasal turbinates of unprimed animals (white bars) and H1N1pdm09-primed animals (black bars) at 2 and 7 days post-inoculation (dpi). (limit of detection < 0.5 TCID₅₀/ml (log₁₀))

Virus Neutralization

Sera from unprimed animals did not neutralize either H1N1pdm09 or H7N9 virus at any time point. Pre-infection sera from H1N1pdm09-primed animals did not neutralize H1N1pdm09 virus but sera obtained at day 28 p.i. displayed virus neutralizing antibody titers ranging from 1:40 to 1:160. These sera failed to neutralize the H7N9 virus.

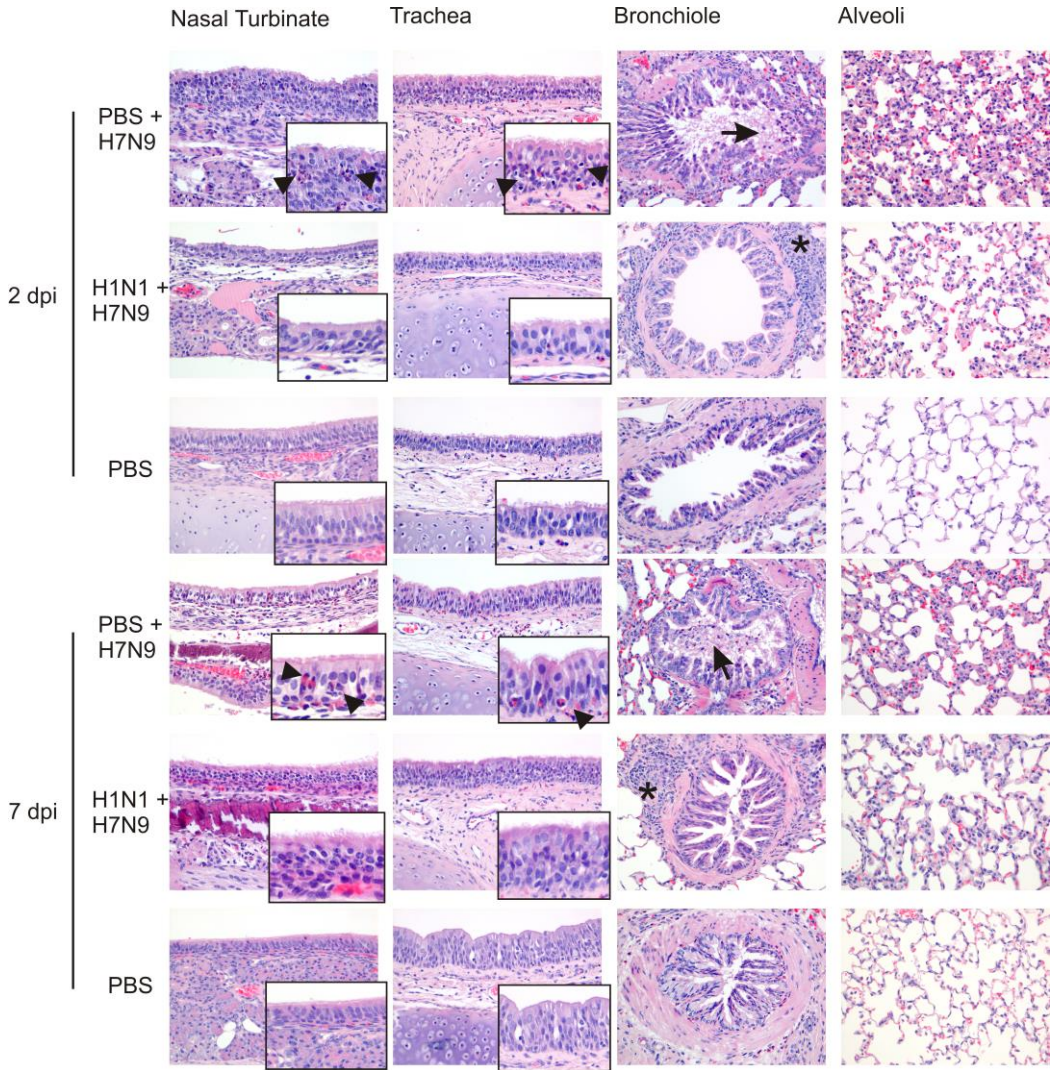


Figure 3 Haematoxylin and Eosin (HE) stain (x20). Histopathological changes in respiratory tissues of unprimed (PBS + H7N9), H1N1pdm09-primed (H1N1 + H7N9) and mock infected (PBS) animals at 2 and 7 days post-inoculation (dpi) with influenza A/H7N9/Anhui/1/2013 virus. Arrowheads show inflammatory infiltrates and necrosis, arrows show inflammatory cells and debris in bronchiolar lumina, and asterisks indicate peribronchiolar lymphocytic infiltrates.

Macroscopic and Microscopic findings

Macroscopically, lungs of virus inoculated animals showed multifocal to coalescing well-demarcated areas of hyperaemia and consolidation affecting 20-30% of lung tissue in unprimed animals, and 10-20% of lung tissue in H1N1pdm09-primed animals. On day 2, and to a lesser extent day 7, moderate (unprimed) or small (H1N1pdm09-primed) quantities of mucopurulent exudate were present in the nasal cavity, especially caudally, and the mucosa was diffusely hyperaemic.

For unprimed animals, the epithelium and submucosa of the nasal cavity, trachea and bronchi revealed varying severity of inflammation, with an inflammatory infiltrate composed predominantly of eosinophils and fewer heterophils. Necrotic epithelial cells were frequently observed in the nasal cavity, and to a lesser extent, the airways. On day 2 p.i. multifocal necropurulent exudate covered parts of affected nasal epithelium. Lumina of smaller airways were frequently filled with necrotic debris and eosinophilic material.

Alveoli showed multifocal areas of densely cellular infiltrates consisting of eosinophils, heterophils and macrophages in the walls and lumen of alveoli, frequently accompanied by epithelial cell necrosis. Lesions were of similar nature on both day 2 and day 7 p.i., however on day 2 lesions were generally more severe and necrotizing and on day 7, there was more evidence of mononuclear cell infiltration around the airways in the H1N1pdm09-primed animals.

Although the nature of the lesions was the same for both groups, the H1N1pdm09-primed group was less severely affected and showed fewer lesions in the lungs (Figure 3)

The cerebrum (including the olfactory bulb) and the cerebellum showed no macroscopic or histopathological changes in any of the animals.

Detection of virus-infected cells

Unprimed animals showed moderate numbers of viral antigen positive cells in the nasal epithelium, bronchi(oli) and alveoli at 2 days p.i.. On day 7 p.i., small numbers of antigen positive cells were found in nasal epithelium and lung. H1N1pdm09-primed animals showed moderate amounts of viral antigen in the nasal epithelium at day 2 p.i. and nearly no antigen in airways or alveoli. By day 7 p.i., H1N1pdm09-primed animals were uniformly negative for viral antigen (Figure 4).

No viral antigen was detected in any other tissues, including the olfactory bulb, in any of the groups.

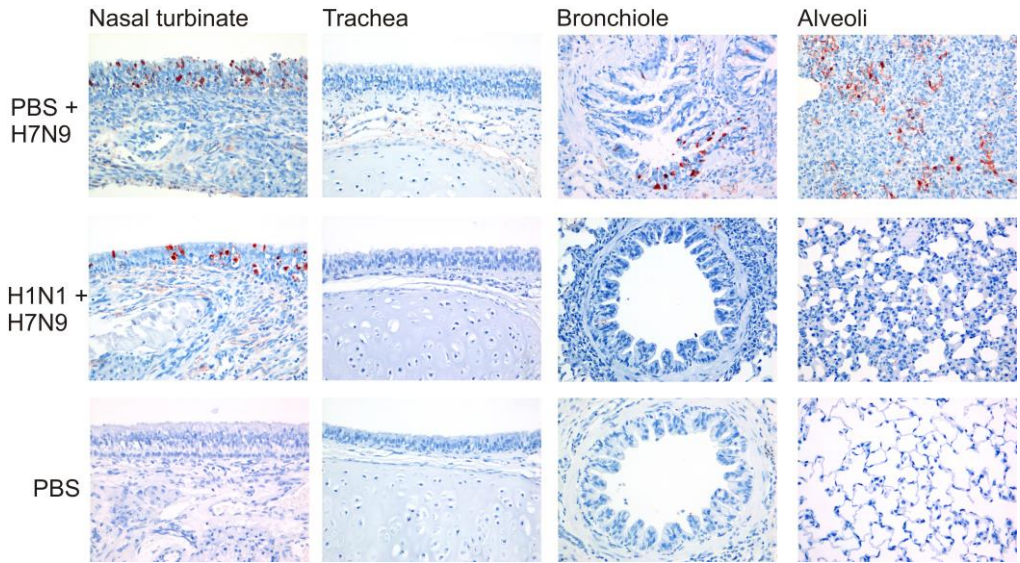


Figure 4 Influenza virus immunohistochemistry (IHC) (x20). Respiratory tract tissues of unprimed (PBS + H7N9), H1N1pdm09-primed (H1N1 + H7N9) and mock infected (PBS) animals at 2 days post-inoculation (dpi) with influenza A/H7N9/Anhui/1/2013 virus.

DISCUSSION

In the present study we demonstrate that a prior infection with a A(H1N1)pdm09 influenza virus can induce heterosubtypic immunity to challenge infection with an avian influenza virus of the H7N9 subtype in isogenic guinea pigs.

Similar observations were made in others studies that demonstrated that infection with seasonal influenza viruses afforded mice and ferrets protection against infection with highly pathogenic avian influenza viruses of the H5N1 subtype [50, 107, 108].

Of interest, in humans prior infections with heterosubtypic strains of influenza virus also have an impact on susceptibility to infection with a pandemic influenza virus of a novel subtype, as was demonstrated by Epstein et al. This study showed that subjects who experienced H1N1 influenza virus infection prior to the 1957 pandemic were less likely to develop symptomatic influenza caused by the pandemic strain of the H2N2 subtype [233]. It was suggested that cellular immunity played a role in the observed protection.

One of the hallmarks of heterosubtypic immunity is that, in most cases, sterile immunity is not achieved but the extent of viral shedding from the respiratory tract is reduced. This suggests that the extent of virus transmission between individuals will also be reduced, although this never has been studied properly.

During the last decade, the quest for universal influenza vaccines has spurred the elucidation of immune correlates of protection that contribute to heterosubtypic immunity. Antibodies have been identified that are specific for conserved proteins such as the M2 protein or conserved regions of an otherwise variable protein, such as the stem region of the HA molecule (reviewed in [234]). It has been demonstrated that after passive administration or hyperimmunization these antibodies can be broadly protective against infection with influenza viruses of various subtypes. However, after infection these antibody responses are subdominant and other correlates of protection may be more important for infection-induced heterosubtypic immunity. In the present study, serum obtained after infection with the A(H1N1)pdm09 strain neutralized the homologous strain but failed to neutralize the A(H7N9) virus. Most likely, cross-reactive T cells contributed to protective immunity, which concurs with the observation of mononuclear cell infiltrates surrounding airways of H1N1pdm09-primed guinea pigs. Indeed in mouse, ferret and macaque models heterosubtypic immunity correlated with the induction of cross-reactive T cells [116, 235] [107, 236]. It is important to note that virus-specific CD8⁺ T cells display a high degree of cross-reactivity and T cells induced after infection with seasonal human influenza viruses can recognize cells infected with avian influenza viruses of the H5N1 subtype [103, 237] and the H7N9 subtype [104] or swine-origin viruses such as H1N1pdm09 viruses [105]. By performing adoptive transfer of T cells obtained from mice

that experienced an influenza virus infection it was demonstrated that indeed T cells can confer protective immunity [116, 231]. Of interest, during the 2009 pandemic it was also demonstrated that the frequency of pre-existing virus-specific CD8⁺ T cells inversely correlated with disease severity caused by infection with the A(H1N1)pdm09 viruses [113]. However, the correlation with viral shedding was not studied, but this has been established previously after experimental infection of subjects that lacked antibodies against the strain that was used for infection [112]. In our study, protection against the development of severe disease was observed. Not only did the H1N1pdm09-primed guinea pigs show less viral shedding from the upper respiratory tract, they also showed lower virus titers, less severe histopathological lesions and less widespread distribution of viral antigen positive cells in the respiratory tract than the unprimed control animals.

This study shows that infection with a A(H1N1)pdm09 virus induced protective immunity against challenge infection with the newly emerging avian viruses of the H7N9 subtype in guinea pigs. For this purpose we used isogenic strain 2 guinea pigs, which offers some important advantages. The use of these animals would allow the elucidation of correlates of protection more precisely by adoptive transfer of antibodies or subsets of lymphocytes. Since the guinea pig is a preferred species to study transmission of influenza viruses, the impact of immunity induced by prior infection and individual arms of the immune system on transmission can also be investigated, and will be the subject of future experiments. This model may help advancing our understanding of influenza dynamics in the human population.

CHAPTER 5

A SINGLE IMMUNIZATION WITH MODIFIED VACCINIA VIRUS ANKARA-BASED
INFLUENZA VIRUS H7 VACCINE AFFORDS PROTECTION IN THE INFLUENZA
A(H7N9) PNEUMONIA FERRET MODEL

Kreijtz J H, Wiersma LC, De Gruyter HL, Vogelzang-van Trierum SE, van Amerongen G,
Stittelaar KJ, Fouchier RA, Osterhaus AD, Sutter G, Rimmelzwaan GF

The Journal of infectious diseases, 2015. Mar 1;211(5):791-800

ABSTRACT

Since the first reports in early 2013, >440 human cases of infection with avian influenza A(H7N9) have been reported including 122 fatalities. After the isolation of the first A(H7N9) viruses, the nucleotide sequences became publically available. Based on the coding sequence of the influenza virus A/Shanghai/2/2013 hemagglutinin gene, a codon-optimized gene was synthesized and cloned into a recombinant modified vaccinia virus Ankara (MVA). This MVA-H7-Sh2 viral vector was used to immunize ferrets and proved to be immunogenic, even after a single immunization. Subsequently, ferrets were challenged with influenza virus A/Anhui/1/2013 via the intratracheal route. Unprotected animals that were mock vaccinated or received empty vector developed interstitial pneumonia characterized by a marked alveolitis, accompanied by loss of appetite, weight loss, and heavy breathing. In contrast, animals vaccinated with MVA-H7-Sh2 were protected from severe disease.

INTRODUCTION

In spring of 2013, avian influenza A viruses of the H7N9 subtype caused an outbreak of severe respiratory illness in humans in China. These viruses re-emerged in the winter of 2013-2014 to cause a second outbreak [238-240]. So far, more than 440 human cases have been reported of which 122 had a fatal outcome [241]. Based on the absence of a multi-basic cleavage site in the viral hemagglutinin and the phenotype of the virus in the intravenous pathogenicity index test (IVPI), the H7N9 virus is categorized as a low pathogenic avian influenza virus [12]. Despite the low pathogenic phenotype, the virus is able to attach to the lower respiratory tract in humans and H7N9-infected patients present at the hospital with severe respiratory illness [238, 242]. Furthermore, it was demonstrated that intratracheal inoculation of ferrets with an influenza A/H7N9 virus causes severe broncho-interstitial pneumonia [213]. More widespread circulation of these viruses is feared and therefore there is interest in the development of vaccines that could prevent infection or mitigate disease severity.

The conventional production of such (pre)pandemic vaccines fell short during the last pandemic (H1N1) in 2009 [243, 244]. The evaluation of (pre) pandemic vaccines against avian influenza viruses of the H5N1 and H7N9 subtypes indicated that these vaccines are poorly immunogenic and the use of adjuvants is required to improve their immunogenicity

[245, 246]. However, the use of adjuvants may have some limitations and adverse side effects [247].

These issues underscore the need for new production platforms with capacity to produce large quantities of efficacious vaccines in a short period of time [248]. So far, various H7 vaccine candidates have been evaluated for their immunogenicity and protective capacity with variable success [249-257]. Recombinant DNA technology may facilitate the production of purified recombinant viral proteins, DNA vaccines, but also viral vectors such as MVA [253-256, 258].

MVA is a highly attenuated and replication-deficient orthopoxvirus that is biologically and genetically well-characterized, has successfully been developed as next generation smallpox vaccine as well as having been evaluated as a viral vector for numerous prophylactic and therapeutic vaccines [259, 260]. Recombinant MVA has also been tested extensively as a vaccine candidate against various influenza viruses [132]. Recently it was shown that influenza H5N1 vaccines based on the MVA technology were found to be safe and immunogenic in mice, chickens and macaques. Currently, a prototype MVA-H5 vaccine is under clinical development in a phase I/IIa clinical trial [137, 261-264]. In addition, MVA-based universal influenza vaccines, that elicit heterosubtypic-immunity, are in various stages of development [135, 265-267].

Here we evaluate the first H7N9 viral vector vaccine, based on Modified Vaccinia virus Ankara (MVA), in a ferret model for influenza A/H7N9 virus induced pneumonia. The immunogenicity and protective capacity of the vaccine was investigated after a single and two immunizations. To assess the possibility for dose sparing also a 100-fold lower vaccine dose was investigated.

MATERIAL & METHODS

Vaccine construction

The HA gene sequence of influenza virus A/Shanghai/2/2013 (GISAID accession number: EPI439502(H7-Sh2)) was codon optimized for stable insertion and expression in the context of vaccinia virus MVA. Silent mutations were introduced in H7-Sh2 to remove runs of four or more G/C and stop signal sequences (TTTTTNT) for early MVA-specific transcription. The tailor-made H7-Sh2 sequence with *HpaI* and *NotI* restriction sites added to the 5' and 3' termini was obtained as synthetic gene (Baseclear, Leiden, the Netherlands) and cloned into the MVA vector plasmid pMKIIIred [268] under control of the synthetic promoter

psynII and containing the mCherry sequence as marker gene, resulting in pMKIIIred-H7 (Figure 1) [269]. Subsequently, chicken embryo fibroblasts (CEF) cultured under serum-free conditions in VP-SFM medium (Life technologies, Breda, The Netherlands) were infected with MVA and transfected with pMKIIIred-H7 DNA using Fugene HD (Promega, Leiden, The Netherlands) to generate recombinant MVA containing the H7-Sh2 sequence and mCherry as a fluorescent marker. Recombinant viruses were clonally isolated in plaque passages on CEF screening for foci of red fluorescent cells. Finally, the mCherry marker gene was removed from the viral genomes due to a second step of intragenomic homologous recombination resulting in the final marker-free recombinant MVA-H7-Sh2. To generate vaccine preparations MVA-H7-Sh2 was purified by ultracentrifugation through sucrose, resuspended in physiological saline and stored at -80°C . Virus amplifications, titrations, and quality control experiments were performed as described previously [268]. Expression of the H7 protein was confirmed using immunocytochemistry and Western blot analysis as described previously using a hyperimmune rabbit serum against influenza virus A/Seal/Massachusetts/1/80 (Figure 1F) [268].

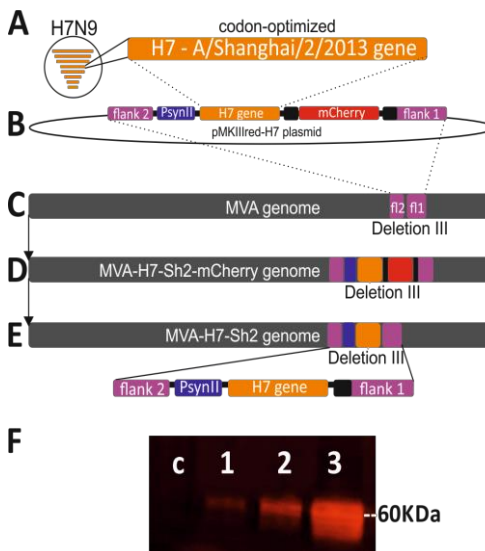


Figure 1 Construction of the MVA-H7-Sh2 vector (A-E) and H7 protein expression (F). The HA gene sequence of influenza virus A/Shanghai/2/2013 (H7-Sh2) was codon-optimized, obtained as synthetic gene (A) and cloned between the flank 2 and flank 1 regions of the MVA vector plasmid pMKIIIred under control of the PsynII promoter and containing the mCherry sequence as marker gene, resulting in pMKIIIred-H7 (B). Subsequently, chicken embryo fibroblasts (CEF) were infected with MVA (C) and transfected with pMKIIIred-H7 DNA using Fugene HD (Promega, Leiden, The Netherlands) to generate recombinant MVA containing the H7-Sh2 sequence and mCherry as a fluorescent marker, inserted in the MVA genome through homologous recombination (D). Finally, the mCherry marker gene was removed from the viral genome due to a second step of intragenomic homologous recombination resulting in the final marker-free recombinant MVA-H7-Sh2 (E). H7 protein expression was confirmed by Western blot analysis of cell lysates from MVA-H7-Sh2 infected Baby Hamster Kidney cells (BHK-21) using a hyperimmune rabbit serum against influenza virus A/Seal/Massachusetts/1/80 and a Goat anti-Rabbit IRDye Infrared antibody (Westburg BV, Leusden, The Netherlands) (lanes: c=negative control, 1=MVA-H7-Sh2 1:50, 2=MVA-H7-Sh2 1:10, 3=MVA-H7-Sh2 undiluted)(F).

Animals

Twenty-eight healthy female ferrets (*Mustela putorius furo*) of around 12 months of age were used and assigned to experimental groups as indicated below. Before use the absence of antibodies against Aleutian disease virus and seasonal influenza viruses was confirmed. The animals were housed under standard conditions, provided with commercial food pellets and water ad libitum and placed in BSL-3 isolator units just before challenge inoculation with H7N9 virus. An independent animal ethics committee (DEC consult) approved the experimental protocol before the start of the experiment.

Immunization and challenge infection

Animals were immunized once (group A, n=6) or twice (group B, n=6) intramuscularly with MVA-H7-Sh2 at 10^8 plaque forming units (pfu) per dose and an interval of 3 weeks. Empty vector control (wildtype MVA (wtMVA) at a dose of 10^7 pfu) (group C, one immunization n=3, group D two immunizations, n=3) and PBS (group E, n=4) were used as negative control immunizations. To assess the possibility of dose sparing also a group of ferrets was immunized twice with 10^6 pfu MVA-H7-Sh2 (Group F, n=6). Before each immunization and before the challenge, blood was drawn from the animals to test for the induction of influenza virus specific antibodies. Four weeks after the last immunization the animals were inoculated under anesthesia (ketamine/medetomidine (reversed with atipamezole), with 3 ml containing $10^{5.5}$ TCID₅₀ influenza virus A/Anhui/1/2013 (H7N9) by the intratracheal route. This virus was isolated from a fatal human case in China and kindly provided under conditions of the Pandemic Influenza Preparedness (PIP) Framework. The virus was passaged three times in embryonated chicken eggs and passaged once in Madin Darby Canine Kidney (MDCK) cells. The infectious titer was determined as described previously and expressed as tissue culture infectious dose 50% (TCID₅₀) [198]. The challenge dose was based on the outcome of a dose-finding study showing substantial levels of virus replication in the upper respiratory tract (URT) and lower respiratory tract (LRT) as well as lung damage, but no mortality during a four day follow up. Nasal and pharyngeal swabs were taken prior to influenza virus inoculation (day 0) and on day 2 and 4 post inoculation (p.i.) and stored in transport medium (Hanks medium (MEM) with lactalbumin, glycerol, penicillin, streptomycin, polymyxin B, nystatin, gentamicin) at -70°C until use. Four days p.i. all animals were euthanized. From the time point of influenza virus inoculation onwards the animals were housed in bio-safety level 3 containment facilities and were monitored for clinical signs.

Serology

The serum samples collected prior to immunization and on day 21 and 49 post immunization were tested for the presence of influenza A/H7N9 virus specific antibodies in the hemagglutination inhibition (HI) assay with a 6+2 reassortant strain of influenza virus A/Anhui/1/2013 (containing the HA and NA of the H7N9 virus and the remaining 6 gene segments of influenza virus A/Puerto Rico/8/34 (A/PR/8/34)) [270]. Sera were also tested for the presence of virus-neutralizing antibodies using a virus microneutralization (VN) assay, performed as described previously and using the reverse genetics virus described above [271]. Rabbit serum raised against influenza virus A/Seal/Massachusetts/1/80 (H7N7) was used as positive control in both assays. For calculation purposes serum samples with an antibody titer of <10 were arbitrarily assigned a titer of 5. Seroconversion is defined as a post-vaccination titer of ≥ 40 or a fourfold rise in the antibody titer when the baseline titer was >10. Antibody titers of ≥ 40 were considered to be seroprotective.

Virus replication in the respiratory tract and the central nervous system (CNS)

Upon necropsy of the animals on day 4 p.i. samples were collected from their right lung lobes and accessory lobe, nasal turbinates, trachea, bronchi and tracheobronchial lymph nodes and stored at -70°C until further processing. In addition to the respiratory tract, the cerebrum and olfactory bulb were also sampled. Tissue samples were homogenized and processed as described previously [140]. Ten-fold serial dilutions of nasal and pharyngeal swab supernatants (quadruplicate) and the homogenate supernatants of lungs (quintuplicate), other respiratory tract samples (triplicate; quadruplicate) and the CNS (triplicate; quadruplicate) were used to determine the presence of infectious virus titers in confluent layers of MDCK cells as described previously [198].

Pathological examination and Immunohistochemistry

Necropsies were carried out according to standard protocols. The trachea was clamped prior to opening the thorax and inflated lungs were assessed visually to determine the percentage of lung grossly affected. Lungs were weighed and relative lung weight was calculated as a percentage of total body weight. Nasal turbinates, nasal septum, trachea, tracheobronchial lymph node, bronchus, lung, cerebrum (including the olfactory bulb) and cerebellum were sampled and fixed in 10% neutral buffered formalin. To optimize histological assessment, the right lung was inflated with formalin prior to fixation and, after fixation, right cranial and caudal lung lobes were sectioned in a longitudinal and cross-sectional plane in a standardized manner. Formalin fixed tissues were embedded in paraffin, cut to $4\mu\text{m}$ and either stained with haematoxylin and eosin (HE) for

histopathological evaluation or with an immunoperoxidase method using a primary monoclonal antibody (Clone HB65 IgG2a (American Type Culture Collection)) against the nucleoprotein of influenza A virus and a secondary goat-anti-mouse IgG2a HRP antibody (Southern Biotech, Birmingham, Alabama, USA), for immunohistochemical (IHC) evaluation. A positive control and IgG2a isotype controls of each slide were included. All slides were evaluated without prior knowledge of the identity of the animals and HE slides were assessed semi-quantitatively using previously described criteria (Table 3) [272]. IHC was evaluated qualitatively to confirm association of histological lesions with the presence of viral antigen.

Statistics

Differences in antibody titers and virus titers were tested for statistical significance using unpaired Student T-tests. Differences were considered significant at $p < 0.05$.

RESULTS

Influenza virus specific immune responses

After one immunization with 10^8 pfu MVA-H7-Sh2, 92% of the animals (Group A and B) seroconverted upon vaccination as measured in the HI assay (Table 1). In these groups 75% of the animals reached titers of ≥ 40 , which are considered to be protective.

A second vaccination boosted the serum antibody titers as seen in animals of group B. The HI GMT increased from 31.7 (SD=2.8) to 127 (SD=2.0). All animals in this group reached antibody titers ≥ 40 . In general the results obtained with the HI assay were in agreement with those obtained in the VN assay. After two immunizations, a GMT of 160 (SD=3.5) was achieved.

To assess if dose sparing was possible with MVA-H7-sh2 ferrets were also immunized twice with 100-fold lower dose. However, only one out of these six animals (group F) seroconverted after the first immunization and GMT of the group was 6.3 (SD=1.8). The second immunization with 1:100 diluted vaccine dose increased the GMT to 12.6 (SD=2.8), but out of six ferret only three seroconverted and two reached HI serum antibody titers of ≥ 40 . Again, similar results were obtained with the VN assay, in which a GMT of 17.8 (SD=2.0) was reached. Antibodies directed to influenza virus A/Anhui/1/2013 were not detectable in any of the control animals that received wtMVA (Group C, D) or PBS (Group E) by HI or VN assay.

Table 1 Serology after MVA-H7-Sh2 immunization

Group	Serology	HI		VN		
		1 st imm.	2 nd imm.	1 st imm.	2 nd imm.	
A	MVA-H7-Sh2 10 ⁸ pfu ¹	Seroconverted ²	6/6	d.n.a.	6/6	d.n.a.
		Seroprotected ³	5/6	d.n.a.	3/6	d.n.a.
		GMT (SD)	50.4 (1.8)*	-	28.3 (1.5)	-
B	2x MVA-H7-Sh2 10 ⁸ pfu	Seroconverted	5/6	6/6	6/6	6/6
		Seroprotected	4/6	6/6	4/6	5/6
		GMT (SD)	31.7 (2.8)*	127.0 (2.0)*	44.9 (2.0)*	160.0 (3.5)*
F	2x MVA-H7-Sh2 10 ⁶ pfu	Seroconverted	1/6	3/6	2/6	5/6
		Seroprotected	0/6	2/6	0/6	1/6
		GMT (SD)	6.3 (1.8)	12.6 (2.8)	7.9 (2.0)	17.8 (2.0)

¹Animals were immunized at the moment of the second immunization in group B and F. Post-immunization sera were obtained four weeks post immunization. The sera after the first immunization in group B and F were obtained three post immunization (on the day of the second immunization).

²Seroconverted: when an animal has a \geq four-fold increase in antibody titer after immunization. The numbers for seroconversion are cumulative: an animal that seroconverted after the first immunization is also accounted for as seroconverted after the 2nd immunization.

³Seroprotected: when an animal has an antibody titer of ≥ 40

*Titer is significantly higher than that of group F; d.n.a.= does not apply

No HI or VN antibody titers were detected against the H7N9 influenza A/Anhui/1/2013 virus in the sera from the animals in the PBS and wtMVA groups.

Clinical signs

Two days post inoculation with influenza virus A/Anhui/1/13, all animals but those immunized once or twice with 10⁸ pfu MVA-H7-Sh2 had loss of appetite. No other signs of disease were noticeable. On day 4 post challenge inoculation three different clinical phenotypes were observed: Group B (2x MVA-H7-Sh2 10⁸ pfu) animals did not display any signs of disease (ate well, normal posture and normal breathing), Group A (1x MVA-H7-Sh2 10⁸ pfu) and Group F (2x MVA-H7-Sh2 10⁶ pfu) animals ate slightly less, were a bit lethargic but displayed normal posture and normal breathing, Group C (1x wtMVA 10⁷ pfu), D (2x wtMVA 10⁷ pfu) and E (PBS) animals were lethargic, showed heavy breathing and alternately showed hunched or flat-stretched posture. Most animals that experienced clinical signs also suffered from weight loss with mean values of 9.7% (SD=5.1) in group C, 14.1% (SD=3.5) in group D and 8.3% (SD=3.4) and 8.6% (SD=3.7) in group E and F, respectively. In contrast, animals in group A (mean weight gain: 2.8% (SD=8.0)) and group B (mean weight gain: 4.3% (SD=5.5)) were protected from weight loss.

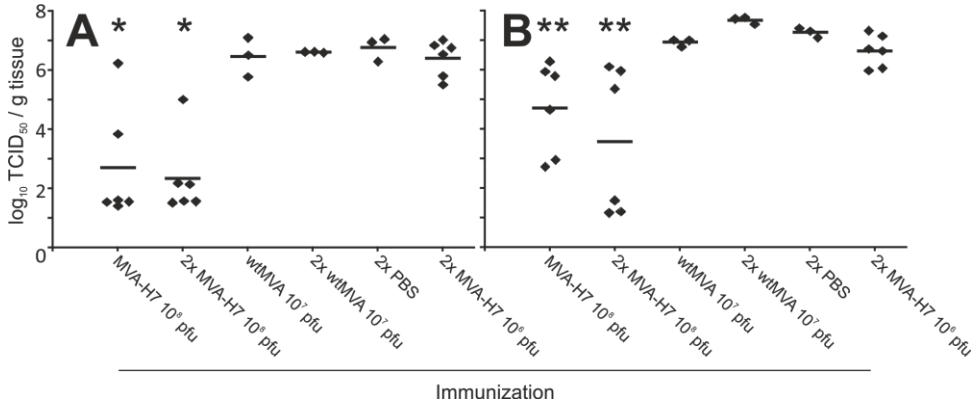


Figure 2 Virus replication in the trachea (A) and lung (B). MVA-H7 is an abbreviation for the MVA-H7-Sh2 vaccine. * indicates that the virus titers in the trachea of the animals in the two indicated groups are significantly lower than those of the other four groups. ** indicates that the virus titers in the lung of the animals in the two indicated groups are significantly lower than those of the other groups except the single shot wtMVA group.

Virus replication in the upper and lower respiratory tract

Swabs were taken on day 0, 2 and 4 p.i. from the nose and pharynx to assess viral shedding from the upper respiratory tract. All samples on day 0 were negative. Apart from one animal in group E that had a virus titer in its nose on day 2 p.i. ($10^{4.8}$), no virus was present in any of the other nasal swabs on day 2 and 4. The pharyngeal swabs on day 2 p.i. were virus-positive for animals from all six groups. In the groups A, B and F, all immunized with MVA-H7-Sh2, virus titers were lower on day 4 p.i. and in groups C, D and E pharyngeal virus titers increased between day 2 and day 4 p.i. (Table 2).

Highest virus titers were observed in the trachea and lung samples (Figure 2). Mean virus titers in groups A and B were significantly lower for both organs and 50% and 67% of the animals in these respective groups tested negative for the presence of infectious virus in their trachea. Also in the lungs of two out of six animals of group B, virus was undetectable. In addition, in none of the animals of this group virus was detectable in the nasal turbinates whereas in the other groups 17-100% of the animals virus was detectable in that anatomic site (Table 2). In the bronchi of animals from all groups virus was detectable but the lowest titers were observed in the bronchi of animals in groups A and B: and $10^{5.0}$ (SD= $10^{1.9}$) and $10^{3.1}$ (SD= $10^{2.2}$) respectively. Sporadically, low virus titers were detected in the tracheobronchial lymphnodes and the central nervous system (cerebrum and olfactory bulb) of some animals, but there was no clear pattern regarding the distribution of animals that tested positive over the experimental groups (Table 2).

Histopathological changes and immunohistochemistry

Macroscopically observed lesions consisted of multifocal to coalescing consolidation of pulmonary parenchyma, characterized by depressed areas of increased consistency and (dark) red discolouration. The total percentage of lung tissue affected varied between groups, with group B showing only minimal lesions and group D most severely affected (Table 3). All infections resulted in a similar expression of pulmonary pathology characterized by alveolitis, bronchiolitis, and to a lesser extent, bronchitis. Alveolar lesions consisted of thickening of septae and filling of alveolar spaces with variable quantities of (alveolar) macrophages and neutrophils, in severe cases accompanied by karyolytic and karyorrhectic (necrotic) cellular debris, red blood cells (haemorrhage), proteinaceous fluid (edema) and eosinophilic fibrillar material (fibrin) (Figure 3). In addition, multifocally alveolar epithelium showed hyperplasia of type II pneumocytes. Bronchiolar lesions consisted of necrosis of epithelial cells, luminal accumulations of aforementioned inflammatory cells and cellular debris, frequently accompanied by peribronchiolar accumulations of lymphocytes and fewer plasma cells, macrophages and neutrophils. Bronchi were similarly affected but to a far lesser extent and variably showed hyperplasia of bronchial associated tissue (BALT). Infrequently, perivascular spaces were infiltrated with predominantly lymphocytes (perivascular cuffing).

Remarkable differences between groups predominated in the extent and severity of alveolar lesions, with groups C, D and E showing significantly more extensive and more severely affected alveolar tissue. Severity of lesions in bronchioli was remarkably similar between groups. Groups A, B and F showed slightly more BALT hyperplasia (consistent with an active immune response)(Figure 3). Semi-quantitative assessment of IHC stain showed little positive nuclear staining in alveolar tissue of especially group C, F and, to a lesser extent, E when compared with remaining groups. Bronchioli showed fewer differences in IHC scores among groups, a finding that was consistent with the histological findings.

Table 2 Virus replication in and outside the respiratory tract

Group	Pharyngeal swab							
	Nasal Turbinates		Bronchi	Trachea-bronchial Lymphnode	Cerebrum	Olfactory Bulb		
	day 2	day 4						
A	MVA-H7-Sh2 10 ⁸ pfu	3.9; SD=1.2 (100%)	2.2; SD=1.8 (50%)	2.1; SD=2.1 (17%)	5.0; SD=1.9 (100%)	n.v.d.	1.6; SD=1.0 (33%)	1.8; SD=1.0 (17%)
B	2x MVA-H7-Sh2 10 ⁸ pfu	2.2; SD=1.8* (50%)	0.7; SD=0.3** (33%)	n.v.d. ²	3.1; SD=2.2*** (67%)	1.7; SD=0.3 (33%)	n.v.d.	n.v.d.
C	wtMVA 10 ⁷ pfu	1.1; SD=1.0* (33%)	3.2; SD=1.7 (100%)	1.3; SD=0.1 (33%)	6.8; SD=1.0 (100%)	2.5; SD=1.2 (67%)	n.v.d.	n.v.d.
D	2x wtMVA 10 ⁷ pfu	2.8; SD=2.0 (67%)	3.3; SD=2.0 (100%)	1.7; SD=0.4 (67%)	6.4; SD=0.2 (100%)	3.2; SD=1.6 (67%)	1.2; SD=0.0 (33%)	1.4; SD=0.2 (33%)
E	2x PBS	2.8; SD=1.6 (100%)	3.1; SD=2.4 (66%)	2.5; SD=1.6 (100%)	6.6; SD=1.1 (100%)	n.v.d.	1.3; SD=0.1 (33%)	n.v.d.
F	2x MVA-H7-Sh2 10 ⁶ pfu	2.2; SD=1.7 (83%)	1.1; SD=1.3 (33%)	1.2; SD=0.2 (17%) ²	6.6; SD=0.6 (100%)	1.8; SD=1.1 (17%)	n.v.d.	n.v.d.

Virus titers were determined in tissue samples obtained on day 4 p.i.;

Virus titers are expressed as mean log₁₀ TCID₅₀ per gram tissue, with standard deviation

¹ n.v.d. = no virus detected

² Values in parenthesis are the percentages of animals in that group with detectable virus in the respective tissue

*Titer is significantly lower than that of group A

**Titer is significantly lower than that of group C, D, E

***Titer is significantly lower than that of groups C, D, E and F.

Table 3 Histopathological and Immunohistochemistry scores

Group	A		B		C		D		E		F	
	MVA-H7-Sh2 10 ⁸ pfu n=6	Mean (SD)	2x MVA-H7-Sh2 10 ⁸ pfu n=6	Mean (SD)	wtMVA 10 ⁷ pfu n=3	Mean (SD)	2x wtMVA 10 ⁷ pfu n=3	Mean (SD)	2x PBS n=3	Mean (SD)	2x MVA-H7-Sh2 10 ⁶ pfu n=6	Mean (SD)
Score												
Percentage Lung Affected ¹	17.5 % (22.3)	5.2 % (2.9)	1.0 % (0.2)	30.0 % (15.0)	41.7 % (17.6)	33.3 % (27.5)	24.2 % (15.9)					
Relative Lung Weight	1.1 % (0.2)	1.0 % (0.2)	1.5 % (0.1)	1.7 % (0.1)	1.5 % (0.1)	1.5 % (0.4)	1.5 % (0.4)					
Extent Alveolitis ²	1.5 (0.5)	1.2 (0.4)	2.3 (0.6)	3.0 (0.0)	2.0 (1.0)	1.5 (0.8)						
Severity Alveolitis ³	1.3 (0.5)	1.3 (0.5)	2.3 (0.6)	2.3 (0.6)	2.0 (0.0)	1.2 (0.4)						
Severity Bronchiolitis	2.5 (0.5)	2.2 (0.4)	2.7 (0.6)	2.3 (0.6)	2.3 (0.6)	2.5 (0.5)						
Severity Bronchitis	1.2 (0.4)	1.2 (0.4)	1.0 (0.0)	1.0 (0.0)	0.7 (0.6)	0.7 (0.6)						
Severity Tracheitis	1.5 (0.5)	1.3 (0.5)	1.3 (0.6)	0.7 (0.6)	0.7 (0.6)	0.8 (0.8)						
Alveolar Oedema ⁴	0.2 (0.4)	0.5 (0.5)	1.0 (0.0)	1.0 (0.0)	0.7 (0.6)	0.7 (0.5)						
Alveolar Hemorrhage	0.5 (0.5)	0.5 (0.5)	1.0 (0.0)	1.0 (0.0)	0.7 (0.6)	0.7 (0.5)						
Type II Hyperplasia	1.0 (0.0)	1.0 (0.0)	1.0 (0.0)	1.0 (0.0)	1.0 (0.0)	1.0 (0.0)						
Peri-bronchiolar Infiltrates ⁵	2.5 (0.5)	2.5 (0.5)	2.0 (0.0)	2.3 (0.6)	2.3 (0.6)	2.2 (0.4)						
Peri-bronchial Infiltrates	2.0 (0.9)	1.5 (1.0)	1.3 (0.6)	1.3 (0.6)	1.3 (0.6)	1.0 (0.0)						
Perivascular Infiltrates	1.7 (0.5)	1.3 (0.5)	1.3 (0.6)	1.3 (0.6)	1.7 (0.6)	1.2 (1.0)						
BALIT Hyperplasia	1.5 (0.5)	1.7 (0.5)	1.0 (0.0)	1.0 (1.0)	1.3 (0.6)	1.7 (0.5)						
IHC Alveoli ⁶	1.0 (0.0)	1.2 (0.4)	2.0 (0.0)	3.0 (0.0)	2.7 (0.6)	1.8 (0.8)						
IHC Bronchioli	1.8 (0.8)	1.3 (0.5)	2.0 (0.0)	2.0 (0.0)	2.7 (0.6)	2.0 (0.0)						

¹ Histopathological and immunohistochemistry scoring system

² Percentage of lung affected was determined by examination of the intact lungs looking at consolidation of pulmonary parenchyma, characterized by depressed areas of increased consistency and (dark) red discoloration

³ Extent of alveolitis and alveolar damage: 0, 0%; 1, 1%-25%; 2, 25%-50%; 3, > 50%

⁴ Severity of alveolitis, bronchiolitis, bronchitis, and tracheitis: 0, no inflammatory cells; 1, few inflammatory cells; 2, moderate numbers of inflammatory cells; 3, many inflammatory cells.

⁵ Presence of alveolar edema, alveolar hemorrhage, and type II pneumocyte hyperplasia: 0, no; 1, yes.

⁶ Extent of peribronchial, peri-bronchiolar and perivascular infiltrates: 0, none; 1, 1-2 cells thick; 2, 3-10 cells thick; 3, more than 10 cells thick.

⁷ IHC score: 0, 0%; 1, <1%; 2, 5-10%; 3, 10-25%; 4, 25-50%; 5, >50% cell showing positive nuclear staining

⁸ Bold values indicate a marked difference in the respective score for the indicated group(s) compared to score of the others groups.

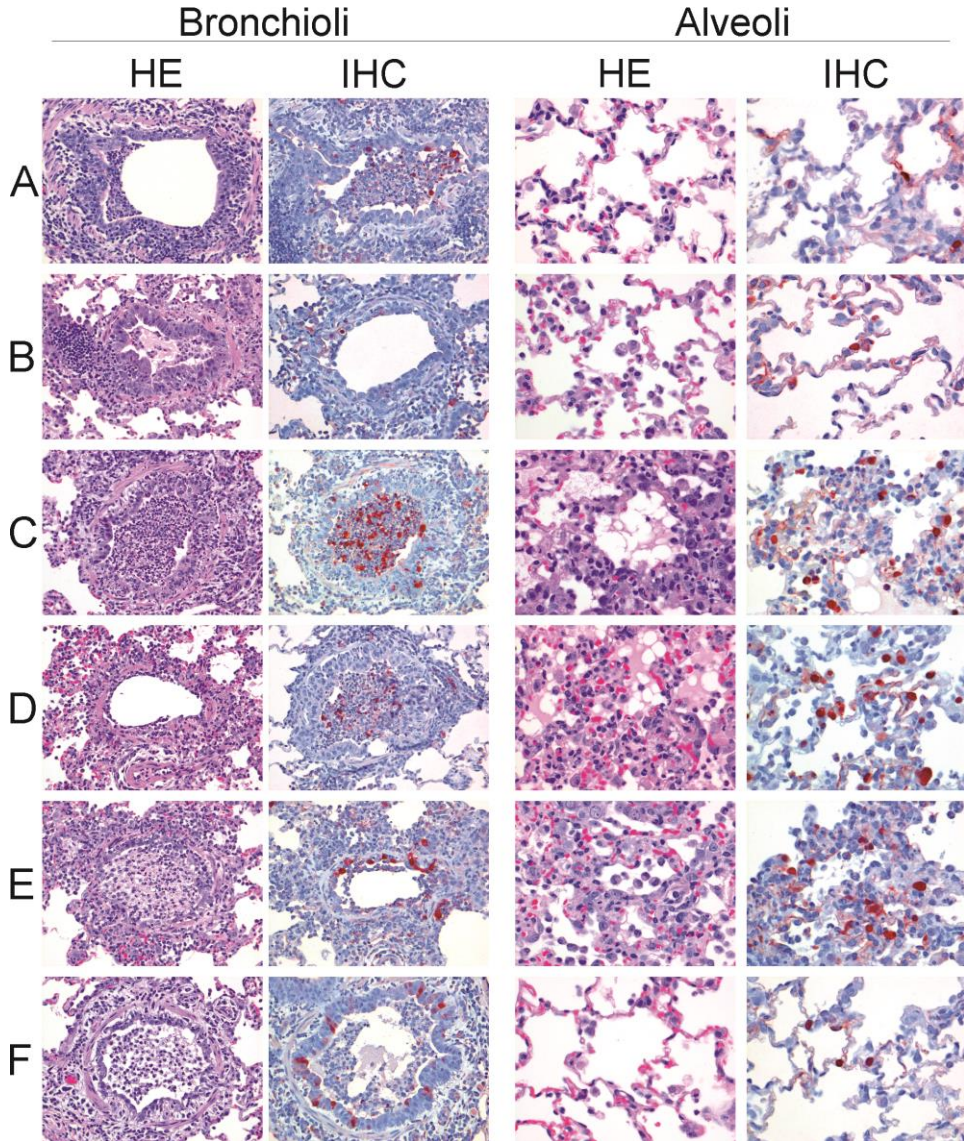


Figure 3 Histopathology (HE) and antigen expression (IHC) in bronchioli (x20) and alveoli (x40) of groups A-F. Histopathology of bronchioli shows peribronchiolar inflammatory infiltrates, epithelial necrosis and luminal accumulations of predominantly neutrophils and necrotic debris in all groups. Antigen expression in bronchioli is of similar extent for groups A, C-F and mild for group B. Histopathology of the alveoli shows a small increase in alveolar macrophages in groups A (MVA-H7-Sh2 10^3 pfu), B (2x MVA-H7-Sh2 10^8 pfu) and F (2x MVA-H7-Sh2 10^6 pfu). Groups C (wtMVA), D (2x wtMVA 10^7 pfu) and E (2x PBS) show marked interstitial and luminal accumulations of predominantly neutrophils and macrophages, (epithelial) necrosis and edema. Antigen expression in alveoli is minimal to mild for groups A, B and F and marked for groups C, D and E.

DISCUSSION

Here we describe the construction and preclinical evaluation of the first H7N9 influenza vaccine based on the MVA viral vector technology. Ferrets immunized with the MVA-H7-Sh2 vaccine developed protective antibody titers against the H7N9 influenza virus strain A/Anhui/1/2013 that was used for challenge infection. Animals that received one or two doses of 10^8 pfu seroconverted and after two immunizations all animals developed HI antibody titers of ≥ 40 , which are considered to be protective. Indeed animals with post vaccination HI titers of ≥ 40 displayed reduced virus replication in the respiratory tract, especially in the lungs. The histopathological changes caused by challenge infection were less severe in these animals in particular of the alveoli. Thus, MVA-H7-Sh2 immunization protected animals against weight loss and respiratory symptoms and the development of interstitial pneumonia and alveolitis but to a lesser extent against the development of bronch(iol)itis. A few animals in the control groups and the group that received a single immunization with MVA-H7-Sh2 had low virus titers in the CNS (olfactory bulb and brain). Spreading to the CNS, although to a minimal extent may be the result of infection of cells in the olfactory epithelium as was described previously [186, 273] after intranasal inoculation of ferrets with A/H5N1 viruses. In the present study, the ferrets were inoculated via the intratracheal route to model H7N9 induced pneumonia. Since the nasal turbinates also tested positive for the presence of infectious virus 4 days post inoculation, the olfactory bulb may have become infected indirectly.

Administration of a 100-fold lower dose of MVA-H7-Sh2 proved to be less immunogenic than the normal dose. Clearly the MVA-H7-Sh2 induced antibody response is strongly dose-dependent, which may be explained in part by the vectors replication deficiency. With a lower dose simply less cells become infected and express the transgene. However, in mice it was demonstrated that with an MVA-based H5N1 vaccine candidate substantial dose-sparing could be achieved [262].

Recently we have demonstrated that with an MVA-based vaccine partial protection of ferrets against infection with a A(H1N1)pdm09 virus could be achieved. Immunization with 10^8 pfu MVA-H7-Sh2 seems to afford stronger protection against virus replication in the respiratory tract than the MVA-H1 vaccine against infection with the pandemic A(H1N1)2009 virus [140]. However, in both models the MVA based vaccines did not induce sterile immunity as was observed against challenge infection with A(H5N1) influenza viruses in other species, including mice and cynomolgus macaques [136, 261-263].

Reduction of A/H7N9 virus titers in especially the upper respiratory tract after challenge infection by MVA-H7-Sh2 vaccination may reduce the risk of airborne transmission with

these viruses [274, 275]. In contrast to the partial protection from virus replication in the upper and lower respiratory tract shown here, Chen et al have shown that a live-attenuated H7N9 vaccine was capable of providing sterile immunity in ferrets against homologous and heterologous challenge infection [276]. Although it was not tested, mucosal IgA antibodies most likely have contributed to the protective capacity of the vaccine in their model in which vaccine and challenge virus were both inoculated intranasally. It would be of interest to test MVA-H7-Sh2 in a similar model to test if it can be used for the induction of mucosal immunity.

Apart from vaccines based on the actual novel H7N9 strain also vaccines based on historic H7Nx viruses have been shown to induce cross-reactive antibodies that are able to neutralize the novel H7N9 virus [250]. Goff et al demonstrated that a Newcastle disease virus expressing the HA gene of a historic H7N3 virus induced cross-reactive antibodies in mice that afforded protection against infection with an A/H7N1 influenza virus isolated in 1993 [253]. Chu et al demonstrated that a historic H7N9 virus-derived vaccine partially protected mice against infection with influenza virus A/Anhui/1/2013. Furthermore, live-attenuated H7N3 and H7N7 vaccines provided partial protection against the novel H7N9 strain in ferrets [277].

These examples illustrate the benefits of virus repositories containing prototypic strains of the respective HA and NA subtypes found in nature. Such a repository should be updated regularly based on influenza surveillance data in poultry, swine and humans. The HA nucleotide sequence of a prototypic strain is already enough to produce a viral-vector vaccine for viruses of that particular subtype and a logic next step would be to not only have an influenza virus repository [278] but to also establish a vaccine repository based for example on a versatile vaccine production platform such as MVA. To accelerate the further clinical development of MVA-based influenza vaccines, further expansion of the safety and efficacy track record of MVA as a viral vector is required. Finally, once advanced regulatory frameworks are in place, reaching beyond the national guidelines (e.g. pandemic influenza vaccines registration by EMA in Europe) MVA-based vaccine production technology could facilitate rapid availability of vaccines for emerging novel influenza viruses including those of the H7N9 subtype.

CHAPTER 6

CONFINED DPP4 EXPRESSION AND INTERFERON SIGNALING IN THE
RESPIRATORY TRACT OF NON-HUMAN PRIMATES ARE ASSOCIATED WITH
RESTRICTED MERS CORONAVIRUS REPLICATION

Wiersma LC*, Widagdo W*, Smits SL, de Vries RD, Getu S, Schipper D, Raj VS, Kuiken T,
Osterhaus AD, van den Brand JM, Haagmans BL

* both authors contributed equally to the paper

(manuscript in preparation)

ABSTRACT

Middle East respiratory syndrome coronavirus (MERS-CoV) may cause severe pneumonia in humans. To study the pathogenesis of this virus, young adult cynomolgus macaques were inoculated with MERS-CoV. Viral replication in the upper respiratory tract was limited as evidenced by relatively low levels of viral RNA in nasal and throat swabs and the absence of MERS-CoV nucleocapsid protein in nasal respiratory epithelium. Lack of MERS-CoV replication in the upper respiratory tract was consistent with the absence of its host receptor, dipeptidyl peptidase-4 (DPP4), in the nasal epithelium. In the lower respiratory tract, limited pathological changes were noted and infectious virus was eliminated by four days post inoculation. Consistent with the rapid clearance of MERS-CoV, IFN- β and phosphorylated STAT1 (pSTAT1) expression levels were enhanced in the lungs of infected animals. Different from SARS-CoV, which inhibits phosphorylation and translocation of STAT1, co-localization of pSTAT1 and MERS-CoV antigen indicates that virus-infected cells respond to interferon signaling. Therefore, DPP4 expression and the activation of interferon signaling pathways might be critically involved in controlling MERS-CoV replication *in vivo*.

INTRODUCTION

There are six coronaviruses (CoVs) known to cause respiratory illness in humans with clinical manifestations ranging from mild to fatal. Four of them, 229E-CoV, OC43-CoV, HKU1-CoV, and NL63-CoV commonly cause mild upper respiratory tract infection [279, 280]. The other two CoVs have been reported to cause severe lower respiratory tract infection [281]. One of them, severe acute respiratory syndrome coronavirus (SARS-CoV), rapidly spread across continents in 2003. However, the pandemic was contained within a year due to well-coordinated and stringent public health measures. By the end of the outbreak, SARS-CoV had affected ~8000 people resulting in ~800 fatal cases [281, 282]. Another CoV was isolated from a 60-year-old Saudi Arabian man with acute pneumonia. This virus, currently known as Middle East respiratory syndrome coronavirus (MERS-CoV), has infected more than 1500 people [32, 283]. Approximately 35% of infected patients succumb to severe infection with life-threatening complications, such as septic shock, acute kidney failure, and acute respiratory distress syndrome. These patients are mostly over 50 years of age and have underlying comorbidities, such as diabetes, immunocompromised state, chronic renal failure, and heart disease. The remaining two

thirds of MERS cases are either asymptomatic or develop mild pneumonia. This group mostly consists of young immunocompetent individuals without comorbidities but with close contact to MERS patients, such as family members and health-care personnel [283-286]. It is currently unclear how MERS-CoV infection can cause such differences in clinical manifestations. Our lack of understanding how MERS-CoV infection can cause such differences in clinical manifestations is due in part to the dearth of data on the pathogenesis of MERS infection in the respiratory tract.

To better understand MERS pathogenesis, we analysed experimental MERS-CoV infection in healthy young adult cynomolgus macaques. The replication capacity of this virus in both upper and lower respiratory tract tissues was thoroughly assessed. Distribution of the MERS-CoV host receptor, dipeptidyl peptidase-4 (DPP4) [287], was evaluated and compared to MERS-CoV tropism in the respiratory tract. Innate immune signaling in response to MERS-CoV infection, focusing on the expression of interferon-beta (IFN- β) and its surrogate marker pSTAT1, was also analyzed in lung tissue samples. In addition, the capacity of MERS-CoV to induce upper respiratory tract infection was compared to NL63-CoV, while MERS-CoV infection in the lower respiratory tract was compared to SARS-CoV. Unlike MERS-CoV, both NL63-CoV and SARS-CoV use angiotensin converting enzyme-2 (ACE2) as their host receptor [288, 289]. Our observations provide novel insights in the pathogenesis of MERS-CoV.

MATERIALS AND METHODS

Virus preparation

MERS-CoV (EMC/2012 isolate) [32] was passaged six times on Vero E6 cells. NL63-CoV was passaged four times on Vero E6 cells. All cell cultures were performed under biosafety level (BSL) 3 conditions.

In-vivo infection experiment

Experiments were performed under BSL 3 conditions at the Erasmus Medical Centre in Rotterdam using an animal research protocol approved by the Institutional Animal Welfare Committee (EMC2808, nr 122-12-32). Young adult cynomolgus macaques (*Macaca fascicularis*) seronegative for coronaviruses were purchased from commercial breeders (Harlan, Indianapolis, IN, USA), maintained in standard housing and provided with commercial food pellets and water *ad libitum* until the start of the experiment. Two weeks prior to inoculation with MERS-CoV, a telemetric sensor (DST micro-T ultra-small

temperature logger, Star-Oddi, Reykjavik, Iceland) was placed in the peritoneal cavity of only three macaques in the MERS-CoV inoculated group to record body temperature every 15 minutes. Before the inoculation, the macaques were examined clinically and determined as healthy by a registered veterinarian and were placed in negatively pressurized glove boxes. During the experiment, animals were checked daily for clinical signs, including assessment of appearance, behavior, weight, presence of any nasal or ocular secretions, food and water consumption.

All inoculations were performed under anesthesia ((ketamine® (Nimatek, Eurovet Animal Health BV, Bladel, the Netherlands) and domitor® (Orion Pharma, Espoo, Finland)). Ten macaques were inoculated intratracheally (4.5 ml) and intranasally (0.5 ml) with 1×10^6 50% Tissue Culture Infectious Dose (TCID₅₀) MERS-CoV. Prior to infection and at days 1, 2, 4, 8, and 11 pi, animals were anesthetized with ketamine, and oral and nasal swabs were taken and placed in 1 ml Dulbecco's modified Eagle's medium supplemented with 100 IU penicillin/ml and 100 µg streptomycin/ml (virus transport medium). The swabs were frozen at -70°C until analysis (see below). Four macaques were euthanized at each of days 1 and 4 pi, while the last two were euthanized at day 21 pi by exsanguination under anesthesia. Autopsies were performed according to a standard protocol. One lung from each monkey was inflated with 10% neutral-buffered formalin by intrabronchial intubation and suspended in 10% neutral-buffered formalin overnight. Samples were collected in a standard manner, embedded in paraffin, cut at 3 µm, and used for immunohistochemistry (see below), in situ hybridization (see below) or stained with hematoxylin and eosin (H&E) for examination by light microscopy. Tissue samples were also collected in virus transport medium (Hanks balanced salt solution supplemented with 10% glycerol, 200 U of penicillin per ml, 200 µg of streptomycin per ml, 100 U of polymyxin B sulphate per ml, 250 µg of gentamycin per ml, and 50 U of nystatin per ml). Tissue samples were weighed prior to homogenization in 2 ml virus transport medium, using Polytron PT2100 tissue grinders (Kinematica). After centrifugation, the homogenates were frozen at -70°C until virus titration (see below) and RT-qPCR (see below).

NL63-CoV and SARS-CoV infections were used as a contrast to further understand the pathogenesis of MERS-CoV infection. Experimental NL63-CoV infection was performed in four macaques. They were inoculated intratracheally (2.5 ml) and intranasally (0.5 ml) with 1×10^5 TCID₅₀ of HCoV-NL63. Two animals were euthanized at each of days 4 and 21 pi. All animals were euthanized by exsanguination under anesthesia. Meanwhile, experimental SARS-CoV infection had been previously performed in our center also in healthy young cynomolgus macaques [68]. They were infected intratracheally with 1×10^6 TCID₅₀ SARS-CoV (strain HKU-39849) and euthanized at day 4 pi. Left over lung tissue

samples from this experiment were analyzed together with lung tissue samples from MERS-CoV experiment.

Ex-vivo infection experiment

Nasal tissue and one entire lung lobe were harvested from a healthy 8 year-old cynomolgus macaque and transferred immediately to ice. Lung tissue was prepared as described previously [290]. Nose and lung tissue were sliced and transferred to 24-well plates (Corning, Wiesbaden, Germany) containing culture medium and incubated overnight at 37°C in 5% (v/v) CO₂. Each tissues were prepared in triplicate. Either 3×10^6 TCID₅₀ MERS-CoV or culture medium (mock infected group) was added to the wells under BSL3 conditions. After 1 hour incubation at 37°C, 500 µl fresh medium was added to each well and incubated overnight at 37°C in 5% (v/v) CO₂. All tissue pieces were then fixed in formalin and embedded in paraffin. MERS-CoV was detected using 5 µg/ml mouse IgG1 anti-MERS-CoV nucleocapsid protein (Sino Biological Inc, Beijing, China) and 1:100 peroxidase labeled goat anti-mouse IgG1. Red signal was revealed using 3-amino-9-ethyl-carbazole substrate [77].

Virological analysis

Viral RNA was isolated using viral RNA Mini kit (Qiagen, Hilden, Germany) and subsequently measured for viral load using reverse transcription-quantitative polymerase chain reaction (RT-qPCR) (Roche, Mannheim, Germany). Each MERS-CoV samples was only considered positive if both E and N gene were detected [291]. Meanwhile, NL63-CoV samples were detected by RT-qPCR targeting N gene [292]. Samples were also titrated on Vero E6 cells to further confirm the results of RT-qPCR. Ten-fold serial dilutions of the homogenates were prepared in Lonza IMDM medium containing 5% fetal bovine serum (FBS) for virus titration assay on Vero E6 cells [293]. The amount of infectious virus in lung homogenates was calculated according to the Spearman-Kärber standard equation [294]. The limit of viral detection for this assay was 0.5 log₁₀ TCID₅₀/ml.

Bacteriological analysis

One macaque developed severe suppurative bronchopneumonia in our study. Lung tissue samples of this macaque were used to isolate RNA and bacterial typing as described previously [295].

Immunohistochemistry

For immunohistochemistry (IHC), MERS-CoV antigen was detected using rabbit serum against SARS-CoV nucleocapsid (N) protein, which is known to cross-react with MERS-CoV [287]. NL63-CoV was detected using rabbit serum against its nucleocapsid protein (kind gift from Lia van den Hoek). Normal rabbit serum was used as negative control for both. Distribution of DPP4 and ACE2 expression was evaluated on the non-infected macaque tissues using polyclonal goat IgG anti-human DPP4 (R&D systems, Abingdon, UK) and polyclonal rabbit IgG anti-human ACE2 (Abcam, Cambridge, UK), respectively. Normal goat serum and rabbit IgG was used as a control. Peroxidase-labeled goat anti-rabbit IgG (DAKO, Glostrup, Denmark) was diluted 1:100 and used as secondary antibody for NL63-CoV, MERS-CoV, and ACE2 staining. Goat anti-rabbit IgG (Southern Biotech, Alabama, USA) diluted 1:200 was used as secondary antibody for DPP4 staining. For MERS-CoV, peroxidase was revealed using diaminobenzidine substrate, while other antigens were revealed with 3-amino-9-ethyl-carbazole substrate. Counterstaining was performed with hematoxylin.

We studied co-localization between pSTAT1 and nucleocapsid protein of either MERS-CoV or SARS-CoV in the infected lungs of macaques sacrificed at day 1 pi. Lung tissues derived from non-infected macaques were included as negative control tissues. Monoclonal antibodies against MERS-CoV nucleocapsid protein (SinoBiological, Beijing, China) and SARS-CoV nucleocapsid protein (Imgenex, Littleton, USA) were used in 5 µg/ml concentration [77, 296]. Goat anti-mouse IgG1 labeled with alkaline phosphatase was used as secondary antibody (DAKO, Glostrup, Denmark). The dark blue signal was revealed with BCIP/NBT substrate (DAKO, Glostrup, Denmark). Phosphorylated STAT1 protein was detected using rabbit anti-human pSTAT1 (ThermoScientific, Rockford, USA) at a 1:200 dilution [297]. Rabbit IgG in similar concentration was used as a negative control. Peroxidase labeled goat anti-rabbit IgG diluted at 1:100 was used as secondary antibody staining. Red signal was revealed using 3-amino-9-ethyl-carbazole substrate followed by hematoxylin counterstaining.

In situ hybridization

In situ hybridization (ISH) was performed according to the RNAScope platform [298]. Probes targeting the nucleocapsid gene of MERS-CoV and NL63-CoV were designed by Advanced Cell Diagnostics (Hayward, CA, USA).

Cytokine measurements

RT-qPCR was performed as described previously to detect cellular gene expression changes for IFN- β , IL-6, IL-8, CCL3, CCL20, and osteopontin [68, 296]. Differences in gene expression are represented as the fold change in gene expression relative to a calibrator and normalized to a reference, using the $2^{-\Delta\Delta Ct}$ method [299]. GAPDH (glyceraldehyde-3-phosphate dehydrogenase) was used as a reference endogenous control. The samples from the mock-infected macaques were used for calibration [299]. Data distribution was evaluated with D'Agostino and Pearson omnibus normality test. The data were presented either in mean \pm standard error of mean or median \pm interquartile range. Statistical analysis was performed with unpaired t test or Mann-Whitney test.

RESULTS

Clinical signs and gross pathology of MERS-CoV infected healthy young adult macaques

Ten young healthy adult cynomolgus macaques were inoculated both intranasally and intratracheally with MERS-CoV. Clinical signs, fever and body weight loss were minimal in all animals during the experiment (Fig. 1a). Upon autopsy, the macroscopic lung lesions were found to be generally mild, consisting of focal to multifocal consolidation in approximately 5% area of lung tissue, except for one macaque that developed severe suppurative bronchopneumonia (Fig. 1b). This macaque also showed elevated body temperature up to 40°C around day 4 post inoculation (pi) (Fig. 1a). Histological examination on the lung sample of this macaque revealed myriad intralesional small rod-shaped bacteria. Bacterial typing analysis on the lung sample of this animal revealed the presence of *Escherichia coli*, which suggests bacterial co-infection in this animal. The bronchial lymph nodes and tonsils were enlarged in all animals.

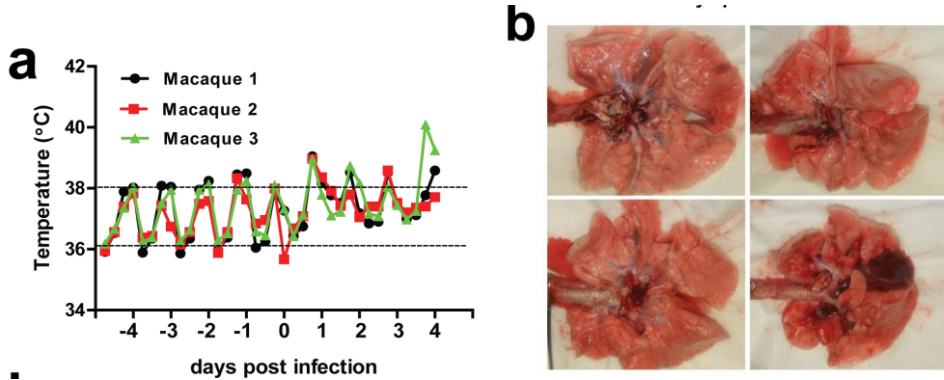


Figure 1 Body temperature and gross lesions of MERS-CoV infected macaques. All animals developed elevated body temperature (body temperature $>38^{\circ}\text{C}$) post MERS-CoV inoculation (a). One macaque (number 3) developed bacterial co-infection during the experiment. This macaque developed elevated temperature up to 40°C around day 4 pi (a) and had severe gross lesions (b, bottom right) compared to the other macaques. Gross pathology pictures were taken of four macaques sacrificed at day 4 pi.

Limited MERS-CoV infection in the upper and lower respiratory tracts

Nasal and throat swabs were collected at multiple time-points to assess MERS-CoV replication over time. MERS-CoV RNA was detected from day 1 pi but levels were in general relatively low (Fig. 2). This observation was consistent with the fact that all swabs, except for one throat swab sample from the macaque with bacterial co-infection (10 TCID₅₀/ml, labelled with asterisk in Fig. 2), were found negative in the virus titration assay. In lung homogenates, infectious virus was only observed at relatively high levels shortly after inoculation (Fig. 2). Other respiratory and extra-respiratory tissues tested did not contain infectious virus. However, MERS-CoV RNA was detected in the lungs of all animals (Fig. 2), and in the urine, large intestines, and kidney of only one macaque sacrificed at day 1 pi (data not shown). These results demonstrate that MERS-CoV replication in experimentally infected cynomolgus macaques is efficiently restricted; only when lung tissue samples were taken at very early time points post inoculation infectious virus was detected.

Replication of MERS-CoV in the upper and lower respiratory tract tissues was further analysed using immunohistochemistry (IHC). MERS-CoV nucleocapsid protein was detected mainly in the bronchiolar and the alveolar epithelial cells at day 1 pi (Fig. 3). *In*

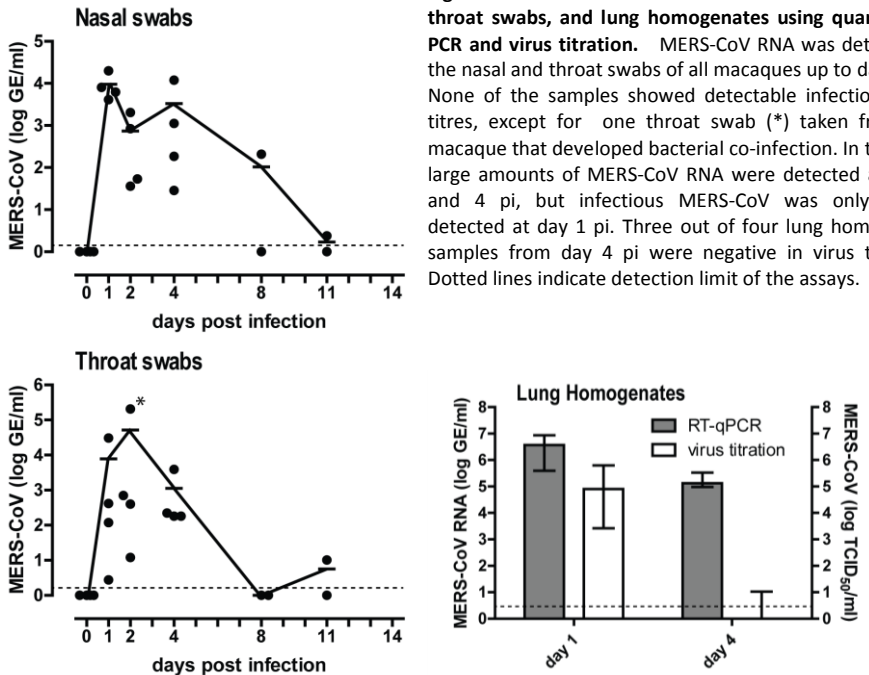


Figure 2 Detection of MERS-CoV in the nasal swabs, throat swabs, and lung homogenates using quantitative PCR and virus titration. MERS-CoV RNA was detected in the nasal and throat swabs of all macaques up to day 11 pi. None of the samples showed detectable infectious virus titres, except for one throat swab (*) taken from the macaque that developed bacterial co-infection. In the lung, large amounts of MERS-CoV RNA were detected at day 1 and 4 pi, but infectious MERS-CoV was only largely detected at day 1 pi. Three out of four lung homogenate samples from day 4 pi were negative in virus titration. Dotted lines indicate detection limit of the assays.

situ hybridisation with a MERS-CoV nucleocapsid probe confirmed the IHC results (Fig. 3). Consistent with the replication of MERS-CoV in the lungs, expression of dipeptidyl peptidase-4 (DPP4), the MERS-CoV receptor [287], was also observed in the bronchial and alveolar epithelial cells, although mainly in the type 2 alveolar epithelial cells. However, DPP4 expression gradually became undetectable from the lower to the upper respiratory tract. Whereas epithelial cells in the submucosal gland along the respiratory tract, terminal bronchioles, and trachea were DPP4 positive, both the olfactory and respiratory nasal epithelial cells were found to be DPP4 negative (Fig. 4). The lack of DPP4 expression in the upper respiratory tract corresponds with undetectable MERS-CoV replication in this location (Fig. 4). In addition to the lower respiratory tract, DPP4 is also widely expressed in other organs, including liver, kidney, and intestines (Fig. 5). MERS-CoV nucleocapsid protein, however, was not detected in these tissues. In addition, *ex-vivo* MERS-CoV infection of macaque nasal and lung tissues was performed. As shown in figure 6, both type I and II alveolar epithelial cells were successfully infected, while nasal respiratory epithelium was not. Together, these results reveal that MERS-CoV tropism in the respiratory tract corresponds to the distribution of DPP4.

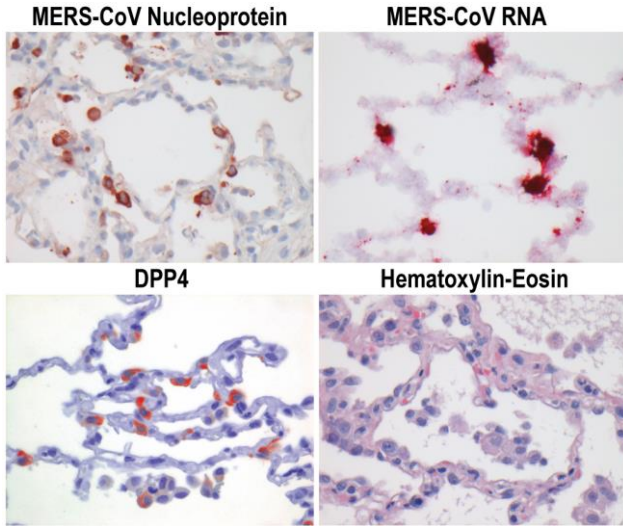


Figure 3 MERS-CoV and DPP4 were detected in the lower respiratory tract. MERS-CoV nucleocapsid protein and RNA was detected in the alveolar epithelium. Nucleocapsid protein and DPP4 were detected using immunohistochemistry staining, while MERS-CoV RNA with in-situ hybridization. Pictures were taken from macaques sacrificed at day 1 pi. DPP4 was also expressed in the alveolar epithelium. HE staining of the lungs showed mild histopathological changes. All pictures were taken at 40x objective magnification.

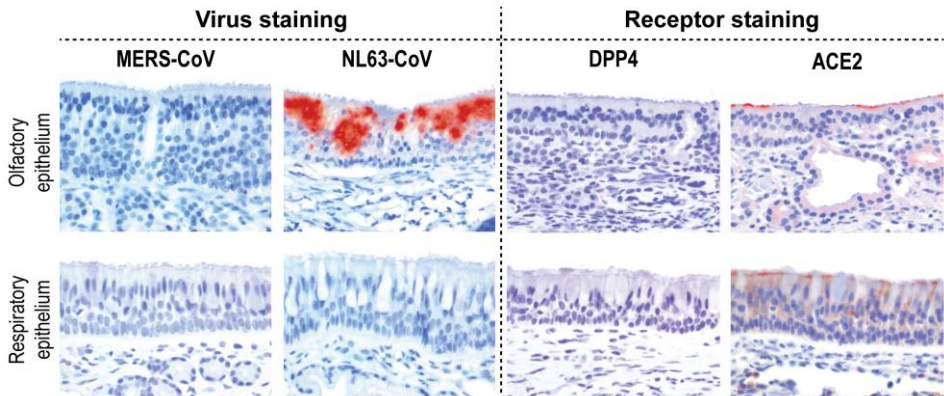


Figure 4 Immunohistochemistry staining of MERS-CoV, NL63-CoV, and their receptors in the nasal epithelium. Neither MERS-CoV nucleocapsid protein nor MERS-CoV receptor, DPP4, were detected in the nasal epithelium. In contrast, NL63-CoV nucleocapsid protein was detected in the nasal olfactory epithelium and NL63-CoV receptor, ACE2, was detected in both nasal olfactory and respiratory epithelium. All pictures were taken at 40x objective magnification.

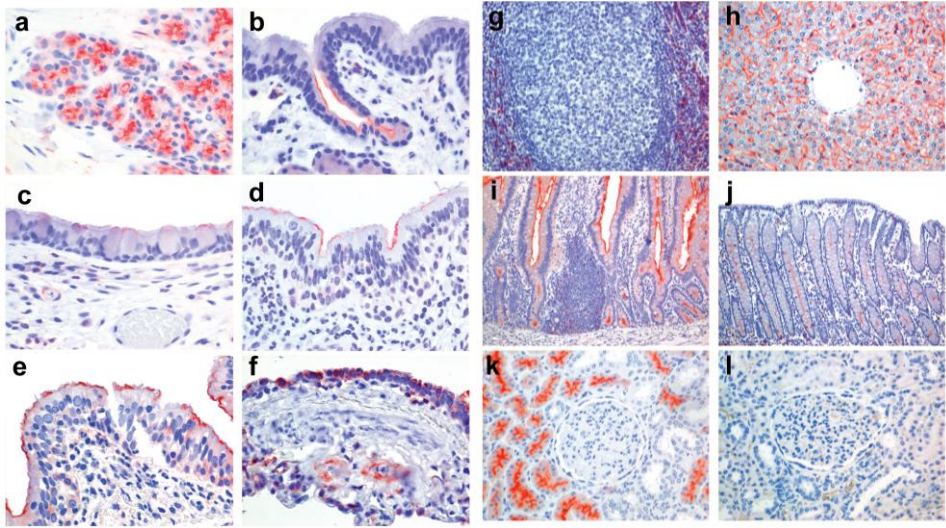


Figure 5 DPP4 expression in other macaque tissues. DPP4 was expressed on the apical surface of the nasal submucosal glands (A), the tracheal submucosal glands and their secretory ducts (B). It showed limited expression on the apical surface of the trachea (C). The expression was gradually increased in the bronchi (D), the bronchioles (E), and the terminal bronchioles (F), as it reached the lungs. In the tonsils, it was mainly detected in the paracortex and medulla, but not inside the lymphoid follicles (G). In the liver, it was predominantly found in the endothelium of the hepatic sinusoids (H). In the intestine, it was detected on the apical surface of small intestine (I) and colonic crypts (J). In the kidney cortex, it was mainly found in the apical surface of proximal tubules but not in the glomeruli (K). Negative control staining on kidney tissues showed no background in our staining (L). Small intestine and colon pictures were taken at 10x objective magnification; tonsil, liver, and kidney at 20x; while the rest at 40x.

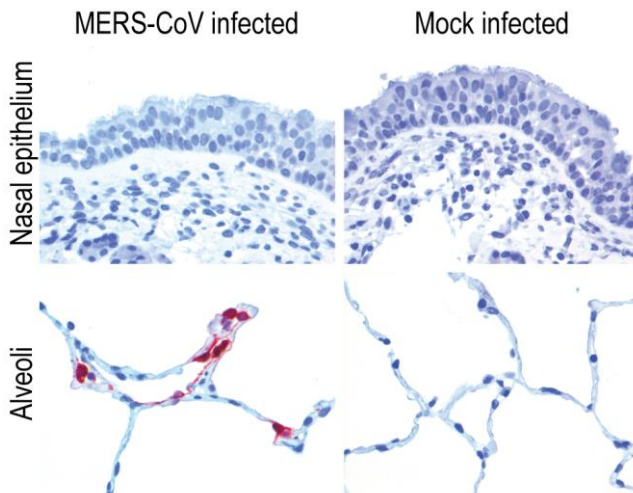


Figure 6 Ex-vivo MERS-CoV infection in the nasal and lung tissues. MERS-CoV nucleocapsid protein was detected in type I and II alveolar epithelial cells but not in the nasal epithelial cells. Non-infected tissues (mock) were used as negative control. All pictures were taken at 400x magnification.

Similar to DPP4, ACE2, the entry receptor of SARS-CoV and NL63-CoV [288, 289], is expressed in the alveolar epithelial cells [300]. Meanwhile in the upper respiratory tract epithelium, ACE2 is also expressed, unlike DPP4; ACE2 is present in the apical layer of both nasal respiratory and olfactory epithelium (Fig. 4). We subsequently performed experimental NL63-CoV infection of cynomolgus macaques. They showed mild clinical signs and no gross lesions upon autopsy, but did seroconvert (virus neutralization titres of 40-80). NL63-CoV antigen was detected by IHC in the nasal olfactory epithelial cells (Fig. 4), but not in the other tissues. This result was confirmed with ISH (data not shown). Localized replication of NL63-CoV was consistent with very low NL63-CoV RNA levels (Ct value above 36) in the lungs, nasal and pharyngeal swabs taken from days 1 to 4 pi and with the inability to culture virus from these samples (not shown). In line with the clinical signs and gross pathology data, histopathological evaluation of the lung tissues of NL63-CoV-infected macaques only showed mild increase of alveolar macrophages and neutrophils, and minimal hypertrophy and hyperplasia of type II cells. Based on these results, we conclude that NL63-CoV predominantly induces mild upper respiratory tract infection in cynomolgus macaques. Differences in tropism between MERS-CoV and NL63-CoV in the upper respiratory tract correspond with differences in the distribution of their receptors, DPP4 and ACE2, respectively.

MERS pathogenesis in the lower respiratory tract

MERS-CoV infected macaques showed minimal histopathological changes in the lungs. There was mild increase of alveolar macrophages and neutrophils in the alveolar lumina, and moderate type II hyperplasia and hypertrophy as compared to control mock inoculated animals (Fig. 3). Few syncytial cells were also seen in the alveolar lumina. MERS-CoV RNA was detected in the lungs at high levels at day 1 and 4 pi, but almost no infectious virus was found at day 4 pi (Fig. 2). This was consistent with the MERS-CoV nucleocapsid protein immunohistochemistry results, showing less viral antigen at day 4 pi compared to day 1 pi. This rapid clearance of MERS-CoV from the lungs might be associated with expression of type I interferon (IFN) and its downstream cellular signalling. It has been shown *in vitro* that MERS-CoV is highly sensitive to type I interferon [301]. We observed high level expression of IFN- β in lung tissue samples collected at day 1 pi (Fig. 7a). However this high expression was only observed in some lung tissue samples, suggesting localized expression of IFN- β in the lungs, consistent with variable levels of MERS-CoV RNA detected in different tissue samples. IFN- β expression has been reported to be correlated with presence of SARS-CoV in the lung [296]. Nevertheless, IFN- β levels in the lungs dropped significantly at day 4 pi, similar to other cytokines like IL-6, CCL3, and CCL20 (Fig. 7a).

In order to better contrast our MERS-CoV data with other CoV infections in cynomolgus macaques, samples from previous experimental SARS-CoV infections [68] were reanalysed together with samples obtained in this study. At day 4 pi, SARS-CoV RNA levels were $\sim 2 \log_{10}$ higher in the lungs compared to MERS-CoV. Infectious SARS-CoV also could be cultured at this time point [300]. IFN- β mRNA expression in the lungs of SARS-CoV infected macaques was also $\sim 2 \log_{10}$ higher compared to MERS-CoV infected macaques (Fig. 7b). This may reflect a strong correlation between IFN- β expression and virus titre [296]. Besides IFN- β , IL-6 and CCL3 expression levels were also significantly higher, while CCL20 was significantly lower in the SARS-CoV infected macaques (Fig. 7b).

To further characterize the type I IFN production in both MERS-CoV and SARS-CoV infections, pSTAT1 immunohistochemistry was performed on the lung tissues of the infected macaques. STAT1 becomes phosphorylated as a result of downstream IFN signalling [296]. We observed that pSTAT1 was expressed in nuclei of alveolar epithelial cells at day 1 pi, both in MERS-CoV- and SARS-CoV-infected macaques, but not in mock-infected macaques (Fig. 8a,b). pSTAT1 expression was localized to areas near blood vessels and virus infected cells consistent with localized IFN- β expression. MERS-CoV infected lung explants did not show staining for pSTAT1, suggesting that the type I IFN is initially produced by infiltrating immune cells (Fig. 8c). Interestingly, pSTAT1 translocation was observed in MERS-CoV-infected cells (Fig. 8a), but not in SARS-CoV-infected cells (Fig. 8b). It has been reported that SARS-CoV infection does block pSTAT1 translocation to the nucleus both *in vitro* and *in vivo* [296, 301]. Our results suggest that MERS-CoV infection does not block pSTAT1 translocation in the lungs of cynomolgus macaques, confirming previous *in vitro* findings [301].

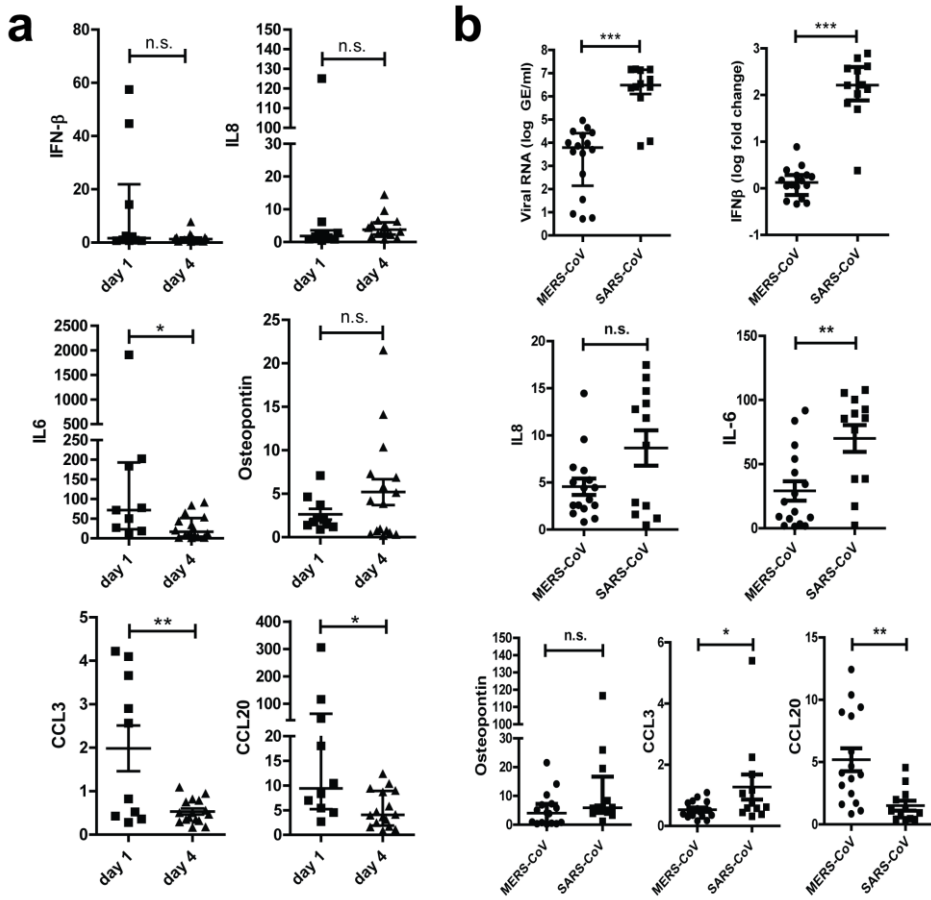


Figure 7 IFN β , IL-8, IL-6, osteopontin, CCL3, and CCL20 mRNA expression in the lungs of MERS-CoV infected macaques at day 1 and 4 pi (a); Viral RNA and mRNA expression of IFN β , IL-8, IL-6, osteopontin, CCL3, and CCL20 in the lungs of MERS-CoV and SARS-CoV infected macaques at day 4 pi (b). In figure (a), all data were presented in fold change unit as described in the methods section. Osteopontin and CCL3, were displayed in mean \pm standard error of mean and analysed with unpaired t-test due to their normal distribution. IFN β , IL-8, IL-6, and CCL20 were presented in median \pm interquartile range and analysed with Mann-Whitney test. Significant difference was found in IL6, CCL3, and CCL20. In figure (b), viral RNA, IFN β and osteopontin were displayed in median \pm interquartile range and analyzed with Mann-Whitney test. The graphs of viral RNA and IFN β are in the log₁₀ scale, while that of osteopontin, IL-8, IL-6, CCL3, and CCL20 were presented in mean \pm standard error of mean, graphed in linear scale, and analysed with unpaired t-test. Significant difference was detected in the viral RNA, IFN β , IL-6, CCL3, and CCL20 (**p value \leq 0,001; **p value \leq 0,01; *p value \leq 0,05; n.s. = not significant).

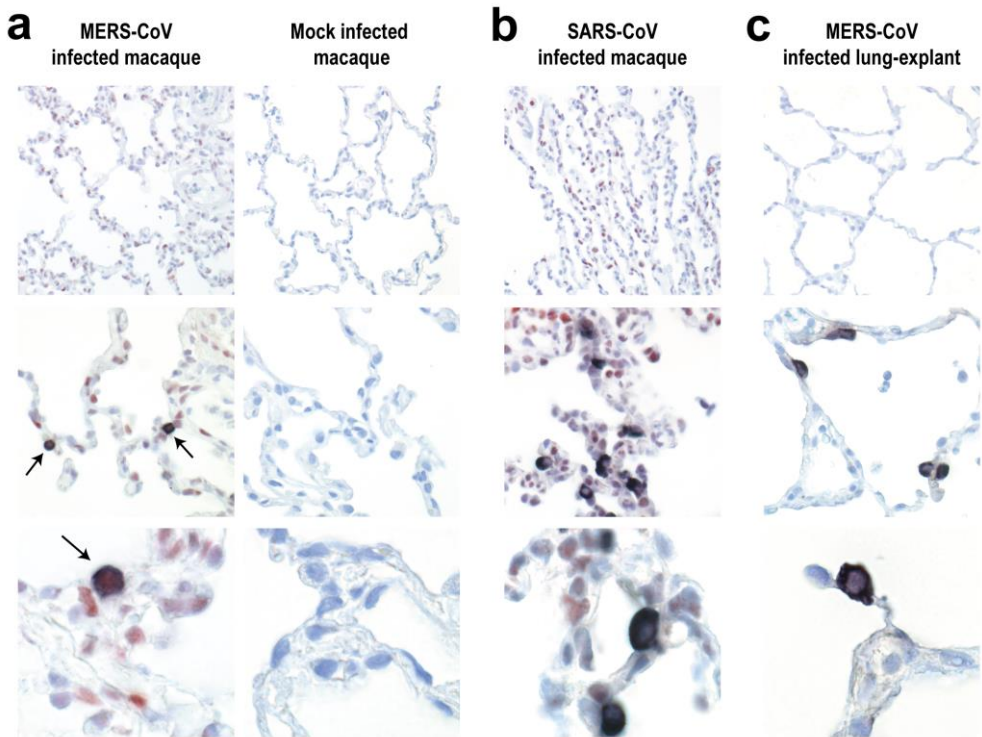


Figure 8 Double immunohistochemistry staining of pSTAT1 and virus nucleocapsid protein in the lungs of MERS-CoV infected macaques (A), the lungs of a SARS-CoV infected macaque (B), and MERS-CoV infected *ex vivo* lung tissues (C). pSTAT1 signal is shown in red, while MERS-CoV and SARS-CoV nucleocapsid protein are shown in dark blue. In the top row (200X magnification), pSTAT1 was abundantly detected in the lungs of MERS-CoV infected macaques at day 1 pi. Lung from mock infected macaques was used as negative control (A). Similar results were found in the lungs of SARS-CoV infected macaques (B), but not in the MERS-CoV infected *ex vivo* lung tissues (C). In the middle (40x objective magnification) and bottom row (100x), several MERS-CoV infected alveolar epithelial cells were positive for pSTAT1 (arrows) (A). Co-localization of pSTAT1 and virus nucleoprotein was not found in the lungs of SARS-CoV infected macaques (B) and in the MERS-CoV *ex vivo* infected lung tissues (C).

DISCUSSION

The pathogenesis of MERS is still not well understood, partly because of the lack of human lung tissue from MERS cases. Experimental infection in healthy young adult cynomolgus macaques was performed to gain some insights in the host factors that may restrict MERS-CoV replication *in vivo*. MERS-CoV-infected cynomolgus macaques developed a virtually asymptomatic infection, mimicking mild human MERS cases mostly observed in healthy

young individuals without comorbidities [285, 286]. We speculate that MERS-CoV replication in the respiratory tract of such individuals might be restricted in a similar manner as we observed in macaques. Limited MERS-CoV replication in the upper respiratory tract epithelium of the non-human primates corresponded with the absence of DPP4. The expression pattern of DPP4 is different from ACE2, another ectopeptidase, that serves as the NL63-CoV receptor [289]. In fact, ACE2 is expressed in the nasal epithelium, providing NL63-CoV the possibility to enter the upper respiratory tract. NL63-CoV preference to infect nasal olfactory instead of respiratory epithelium might be due to another attachment factor [302, 303]. On the other hand, DPP4 is expressed in the lower respiratory tract, predominantly in type II alveolar epithelial cells. This distribution of DPP4 therefore corresponds with the tropism of MERS-CoV in the respiratory tract. Together these data suggest that receptor expression *in vivo* is an important determinant for these coronavirus infections.

In the lower respiratory tract, both MERS-CoV RNA and infectious virus were detected at day 1 pi. In some of the lung tissue samples that were MERS-CoV positive, IFN- β expression was also observed. The pSTAT1 staining in the lungs of MERS-CoV infected macaques at day 1 pi also supported this observation; pSTAT1 could be used as a surrogate marker of IFN expression [296]. We speculate that type I IFN plays a significant role in the rapid clearance of MERS-CoV from the lungs of the infected cynomolgus macaques. This is consistent with *in vitro* studies showing that MERS-CoV is highly sensitive to the antiviral action of type I IFNs [301]. Therefore, time-dependent sampling is important in the analysis of host responses to MERS-CoV in cynomolgus macaques. Only by analyzing very early time points after inoculation could the presence of infectious virus, interferon, and pSTAT1 be revealed. Experimental MERS-CoV infections have been previously performed in rhesus macaques. These macaques developed lower respiratory tract infection but the earliest time point after inoculation that animals were sacrificed was day 3 pi. Dependent on the inoculation route, MERS-CoV RNA was detected in the nasal and oropharyngeal swabs [64, 65]. In the lower respiratory tract, MERS-CoV mainly infected alveolar epithelial cells and induced mild-to-moderate interstitial pneumonia but infectious virus hardly could be detected [64, 65]. Thus, MERS-CoV replication and the ensuing host response in both rhesus and cynomolgus macaques seem to peak early in the infection. Additionally we provide evidence that although MERS-CoV RNA was shed in nasal and throat swabs up to day 11 pi, virus titration and immunohistochemistry staining showed that there is no evidence of upper respiratory tract infection, suggesting that the source of the excreted virus was the lower respiratory tract.

To further gain insight in the pathogenesis of MERS, historic samples from cynomolgus macaques inoculated with a similar dose of SARS-CoV through identical routes were used

for comparison. Unlike what we observed for MERS-CoV, SARS-CoV RNA is detected at much higher levels and infectious SARS-CoV is still present in the lungs at day 4 pi [300, 304]. SARS-CoV infectious virus is also continuously shed in the macaque upper respiratory tract for at least a week after virus inoculation [304, 305]. These *in vivo* observations are different from the growth characteristics of both viruses *in vitro*. Compared to SARS-CoV, MERS-CoV induces more severe cytopathology in both monkey and human cell lines [301], and is capable of infecting various cell lines, suggesting a broad tissue tropism [306]. MERS-CoV also replicates more efficiently in primary human airway epithelium cell culture compared to SARS-CoV [306, 307].

SARS-CoV most likely more efficiently circumvents the host immune response and therefore able to replicate and persist longer in the lungs of cynomolgus macaques. This is supported by observations showing partial resistance of SARS-CoV to IFN type I [301], and its capacity to block pSTAT1 translocation [296, 301]. Here we show that unlike SARS-CoV, MERS-CoV infection does not block pSTAT1 translocation *in vivo*, confirming our previous *in vitro* findings [301]. Together these data indicate that MERS-CoV is less pathogenic compared to SARS-CoV in macaques. Since MERS-CoV infection might be rapidly controlled by the host innate IFN response, healthy young adult macaques might not be the most appropriate animal to test therapeutic measures evaluating the therapeutic potential of IFN- α 2b [308].

Our study showed that MERS-CoV replication is limited in both upper and lower respiratory tract infection, associated with the distribution of DPP4 expression and type I IFN response. In comparison to SARS-CoV, MERS-CoV seems to be less pathogenic and possibly also less transmissible because of limited replication in the upper respiratory tract. This might be one reason why MERS-CoV has not spread as quickly and widely as SARS-CoV did in 2003 [282]. However, this does not exclude the possibility that some MERS infected patients transmit MERS-CoV efficiently. It is currently difficult to identify these individuals, since factors that could influence MERS-CoV transmission are still unknown. In our study, the only throat swab sample that was positive in virus culture came from a macaque that developed bacterial co-infection. This observation suggests that bacterial co-infection might increase the MERS-CoV infection. Age on the other hand is another important risk factor for fatal MERS infection in human [284]. We have previously reported that aged cynomolgus macaques developed much fatal SARS-CoV infection compared to the young ones, due to the incapacity of aged macaques to yield sufficient innate immune response post SARS-CoV inoculation [68]. Future studies dedicated to identify factors influencing MERS-CoV transmission would be important to pursue.

CHAPTER 7

SUMMARIZING DISCUSSION

OVERVIEW

The objective of the work presented in this thesis was to improve understanding of, and response to, emerging zoonotic respiratory viruses. To this end, various animal models were employed to represent respiratory viral infections in humans. In the normal situation, humans are vaccinated and/or infected with respiratory viruses multiple times throughout life, resulting in a complex infection history shaping an intricate immunological landscape. It is virtually impossible to adequately mimic this situation in animal models. Nonetheless, animal models can provide valuable insights into the interplay between viral characteristics and host responses. The viruses that were studied in most depth, influenza A/H7N9 and MERS-CoV, were selected rather opportunistically as they both emerged in real-time during the conception of this manuscript. As such, very little was known about them at the time, making them particularly pertinent subjects for further study.

In the introduction of this document, the relevance of the presented work was outlined; the high rate of emergence of novel human viruses and the relative lack of (timely) intervention strategies justify our continued efforts in this field. In addition, available animal models and intervention strategies were discussed to outline the tools we presently have at our disposal and to place our work in its current context.

Animal models were used in three rather different ways, underlining that the choice of animal model depends largely on the research question. In Chapter 2-4 a new model was developed that provides unique features compared to established influenza virus models. In Chapter 5, an established model was used to test a novel intervention strategy for an emerging influenza subtype. Finally in Chapter 6, a new model was explored to gain understanding of the pathogenesis of a recently emerged coronavirus.

Developing a new model that provides unique features

In Chapter 2, 3, 4 the groundwork was laid for a new model for influenza virus infection. Although numerous functional influenza virus models exist, studying particular aspects such as transmission and cellular immunity simultaneously has so far not been possible. Strain 2 guinea pigs provide unique features (isogenicity and the ability to transmit unadapted avian and human influenza viruses) that would make such studies achievable. However, before proceeding to more complex work, the baseline parameters of such a model must be explored to truly ascertain its suitability for the envisioned experiments. Firstly, in Chapter 2, viral replication and pathogenesis of infection with a pandemic influenza virus of zoonotic origin that now circulates seasonally (A/H1N1pdm09), was

described in this model after intranasal or intratracheal inoculation. It was concluded that viral replication peaked at 2 d.p.i and that virus continued to replicate only in the nose by day 7. When studying influenza in outbred guinea pigs, the intranasal route is used exclusively because intratracheal administration is technically more demanding. However our experiments showed that intratracheal inoculation is the preferable route when attempting to mimic human lower respiratory tract disease, as intranasal inoculation resulted in viral replication that appeared to be limited to the nasal cavity only.

Chapter 3 shows the replication kinetics of H7N9 virus after intratracheal inoculation, which was more severe and resulted in more protracted viral shedding than following H1N1pdm09 virus infection. In addition, infection with H7N9 caused more inflammation and necrosis particularly in the lower respiratory tract. This predilection for the lower respiratory tract may be explained by the receptor distribution as H7N9 is an avian virus that is thought to preferentially use the $\alpha 2,3$ receptor that is expressed to a greater extent in the lungs.

Chapter 4 shows that H1N1-primed animals showed decreased disease manifestation and viral shedding when challenged with H7N9 compared to unprimed animals, thus establishing the existence of heterosubtypic immunity in this model. The absence of cross-reactive neutralizing antibodies leads us to conclude that this observed protective effect is best explained by the induction of more broadly reactive (cellular) immune responses, but the exact correlates of protection remain to be identified.

The experiments described in Chapter 2, 3 and 4 pave the way for use of the guinea pig model in elucidating the role of cell mediated immunity on transmission dynamics. However to fully develop this model, further experiments are required. Although outbred guinea pigs are traditionally used for transmission studies and the high viral titres in nasal turbinates that were found in our experiments suggests that transmission would indeed be possible, the exact transmission dynamics of this particular model should be fully elucidated before proceeding. Transmission experiments should preferably be performed using the configuration that was developed by Herfst et al. to study airborne transmission in ferrets [19]. Some preliminary work (unpublished) that has been carried out shows that isolation and transfer of lymphocytes is indeed possible in strain 2 guinea pigs, but additional experiments are needed to optimize the methods. The final application of this model should include an experimental design in which infected recipient animals, either with or without transferred lymphocytes (ideally also assessing CD4⁺ and CD8⁺ subsets separately), are evaluated for their ability to transmit influenza to naive animals.

Information obtained from these experiments will help to better understand immune correlates of transmission, which can, in turn contribute to refining our approach in design of novel vaccines. If decreased transmission of heterologous subtypes can indeed be effectuated by adoptive transfer of CD4⁺ and/or CD8⁺ lymphocytes, this would provide further evidence to support the development of vaccines that induce both humoral *and* cellular immune responses.

Using an established model to test a novel intervention strategy

In Chapter 5, we showed how established animal models can be used in real-time to test novel vaccines in the face of the emergence of a novel zoonotic influenza subtype. During the 2009 H1N1 pandemic, the conventional production of (pre)pandemic vaccines fell short. Therefore when H7N9 emerged in 2013 and concerns arose regarding its pandemic potential, efforts focused on demonstrating the potential efficacy of alternatives to conventional production methods.

The ferret model is considered the gold standard for influenza research and the pathogenesis of many influenza subtypes (including H7N9) is well known in this species. The purpose of this paper was therefore not to use the model to characterize the disease, but rather to assess potential intervention strategies. A newly synthesized MVA-H7-Sh2 viral vector was used to immunize ferrets that were subsequently challenged with H7N9 virus via the intratracheal route. Unprotected animals that were mock-vaccinated or that received empty vector, developed interstitial pneumonia characterized by a marked alveolitis, accompanied by loss of appetite, weight loss and heavy breathing. In contrast, MVA-H7-Sh2 immunized animals were protected from severe disease, even after a single immunization.

As was discussed in more detail in the introduction, much progress has been made on the way to the development of universal influenza vaccines but many new, theoretically promising approaches still have to be verified in animal models and/or humans. In the development of the holy grail of influenza research, the universal influenza vaccine, candidates that induce both broad humoral and cell mediated responses show considerable promise. However until true universal vaccines become reality, attention must also be paid to pandemic preparedness and thus to increasing the speed of vaccine production. Platforms such as MVA are potentially very useful for inducing both arms of the adaptive immune system, as well as for decreasing response time in an outbreak situation. However clinical trials are needed as MVA-vectored vaccines are not yet

licensed for use in humans and at present their actual deployment in the face of a pandemic is still hampered by a number of logistical limitations [133].

A new model to gain understanding of pathogenesis

In Chapter 6, we explored the macaque as a model for (emerging) coronaviruses and elucidated some of the mechanisms responsible for its limited success. Since MERS-CoV emerged, much effort has focused on finding an appropriate animal model to study the disease and test interventions. Several groups have attempted to use the macaque model, but to little avail as it does not appear to faithfully reproduce the severe disease seen in humans. We delved deeper to better understand what may be responsible for the observed limited viral replication.

Young adult cynomolgus macaques were inoculated intranasally and intratracheally with MERS-CoV. Viral replication was limited to the lower respiratory tract and therefore corresponded to MERS-CoV receptor (DPP4) distribution. However, although the virus was able to replicate in the lower respiratory tract, it was cleared rapidly and appeared to cause only mild pathological changes. IFN- β and phosphorylated STAT1 expression levels were enhanced in the lungs of infected animals, indicating that virus infected cells respond normally to interferon signaling, in contrast to what is known for SARS-CoV.

According to our results, both receptor distribution and innate immunity have an important effect on restricting MERS-CoV replication. However, there are likely more than just these factors at play. Considering the relatively mild disease manifestation in young, immunocompetent individuals and the profile of severely affected patients, it is likely that the host response is the pivotal factor in the pathogenesis and the outcome of coronavirus infections. MERS-CoV affects predominantly middle-aged males with co-morbidities (WHO). Similarly, for the other human coronaviruses, host immunity appears to play a crucial role in disease manifestation [309-311]. To better understand host immunity to coronaviruses, some of the techniques that have been used in influenza research may prove interesting to extrapolate and explore, as will be further discussed below.

INFLUENZA AND CORONAVIRUSES, POTENTIAL PARALLELS AND FUTURE DIRECTIONS

Evidently, the field of influenza virology is significantly more advanced than the field of corona-virology, but we must consider that the first human coronavirus of (perceived) significant public health impact, SARS, emerged in 2003, whereas research on influenza has been ongoing since its discovery by veterinarian Richard Shope in 1931 [312]. Not only does influenza have a significant head start; it also has a far greater public health impact, which is reflected in the intensity of research and the allocated funding. Also, as discussed in this thesis, animal models for influenza viruses are more established, more representative of human disease and, as demonstrated by the isogenic guinea pig model, potentially more versatile. However in order not to re-invent the wheel for each different virus, we might ask if lessons learned from influenza can be of use to improving our understanding of coronaviruses.

Despite obvious differences in these pathogens, epidemiologically influenza and coronaviruses share some characteristics. Both comprise viruses or subtypes that circulate seasonally (coronaviruses NL63-CoV, 229E-CoV, OC43-CoV and HKU-1-CoV and, currently, Influenza A subtypes H3N2 and H1N1) affecting large numbers of people [313, 314]. Also, both are capable of causing pandemics when new viruses or subtypes emerge (for example SARS-CoV and MERS-CoV or Influenza A/H1N1pdm09). Hence in the face of a pandemic, the population is naive for the emerging virus but may have been exposed and developed immunity to the circulating viruses. In such situations, humoral immunity (in the form of neutralizing antibodies) provides little or no cross-protection between different subtypes or viruses. However this may not be the case for cell-mediated immunity (CMI). Following influenza virus infection, the induction of cross-reactive T cells by circulating subtypes has frequently been demonstrated and their protective role in CMI to (emerging) heterologous subtypes (including H7N9) is now well established [222]. Preliminary results obtained for α -coronaviruses 229E-CoV and NL63-CoV (unpublished) show that these viruses appear to be capable of inducing cross-reactive T cells. However, much remains to be answered about T cell responses to coronaviruses and equally, T cell responses to influenza viruses merit further attention, especially in the context of vaccination strategies and novel (universal) vaccines.

One of many fundamental questions that remain to be answered in the understanding of coronavirus infections regards the correlates of protection. It is as yet unclear whether pre-existing (cellular) immunity to homologous and heterologous coronaviruses is

protective or detrimental. Immune responses to coronaviruses are complicated and excessive or dysregulated reactions by pro-inflammatory cells appear to play a key role in their pathogenesis [315]. This information is not only important in understanding natural infection dynamics, it must also be taken into consideration when designing vaccines that may induce such responses.

Although we now have some evidence for the existence of α -coronavirus cross-reactive T cells, it would be of even more interest to establish whether cross-reactive T cells can also be demonstrated for β -coronaviruses (OC43-CoV, HKU-1-CoV, SARS-CoV and MERS-CoV). Influenza specific cross-reactive T cells have repeatedly been demonstrated using ELISPOT INF- γ assays [104, 111]. To ascertain whether these methods can be extrapolated and adapted for use with for β -coronaviruses, we performed pilot experiments. Unfortunately for such experiments, effective antigen presentation is required and SARS-CoV is known to interfere with such presentation [316, 317]. According to results of our pilot experiments, this may also be the case for MERS-CoV. Another important factor that hampers progress in this direction, is the lack of availability of PBMCs from known-exposed individuals and indeed the difficulty in even ascertaining such previous exposure. As with any well-designed experiment, results can only be interpreted in any meaningful way after the inclusion of appropriate controls. In this case, controls should ensure that the measured responses are indeed virus specific, and finding the ideal control has been another stumbling block in our efforts.

Further effort in optimizing such assays is justified as establishing the presence (or absence) of cross-reactive T cells would be useful not only to understand natural disease dynamics but is also essential information if diagnostic T cell assays for coronaviruses are to be developed. As for serological assays, a diagnostic T cell assay should be specific for the pathogen, and the existence of cross-reactivity would therefore interfere with the accuracy of such tests. Developing T cell assays for MERS-CoV could be of interest as it has been shown that in confirmed MERS-CoV infected individuals, a humoral immune response does not always develop. That is to say: several confirmed MERS-CoV infected (PCR-positive) individuals never seroconverted (personal communication) and therefore if surveillance is based on serology only, this would create an under-representation of the actual number of MERS-CoV cases.

The future experiments should ascertain the presence of MERS-CoV specific T cells in (recovered) patients and to further understand the exact epitopes targeted. For SARS-CoV, the presence of such cells has already been shown repeatedly and responses have been

mapped to epitopes on mostly the spike, nucleocapsid and membrane proteins [318] and the importance of CD8⁺ T cells has even been verified *in vivo* by adoptive transfer in the mouse model [319].

As for intervention strategies, MVA vaccines have shown effectiveness against influenza as demonstrated in Chapter 5 and there are indications that they may also be the key to control of emerging coronaviruses. For MERS-CoV, quite possibly vaccination of the intermediate host, the camel, is a more favorable approach than vaccinating humans. In the absence of an appropriate animal model as well as in the absence of financial incentive, a human vaccine is unlikely to be developed in the near future but fortunately recent experiments (in press) have shown that MVA-vectored MERS-CoV vaccines are safe and effective for use in camels. Another advantage of using such MVA vectored vaccines in this species is that they can potentially be deployed as dual efficacy MERS-CoV/Camelpox virus vaccines. Although MERS-CoV may not always be perceived as a problem in camel owners, camelpox is a known (zoonotic) threat and vaccines for this disease are already in use. A dual vaccine could thus face fewer barriers to being adopted. Although the presence of camelpox virus in the camel population also means that there may be pre-existing immunity to the vector, it has been shown for influenza that MVA vectored vaccines can be effective even in the face of such pre-existing immunity [135].

To conclude, the experiments suggested and the questions raised above represent only a tiny fraction of what remains to be answered, and will undoubtedly provide both fun and frustration for many generations of PhD candidates to come. Equally, work described in this thesis only constitutes a minute contribution to solving the colossal puzzle of emerging human respiratory viral infections, but as we all know; Rome wasn't built in a day.

COMMON ABBREVIATIONS

ACE2	Angiotensin-converting enzyme 2
ADE	Antibody dependent enhancement
AI	Avian influenza
APC	Antigen presenting cells
BSA	Bovine serum albumin
BSL-3	Biosafety level-3
CPE	Cytopathic effect
DEC	Dierexperimenten commissie
DNA	Deoxyribonucleic acid
dpi	Days post-inoculation
DPP4	Dipeptidyl peptidase-4
ELISPOT	Enzyme-Linked ImmunoSpot
FFPE	Formalin fixed paraffin embedded
HA	Haemagglutinin
HCoV	Human Coronavirus
HE	Haematoxylin and Eosin
IFN- γ	Interferon gamma
IHC	Immunohistochemistry
IMDM	Iscove's Modified Dulbecco's Medium
IN	Intra-nasal
ISH	In-situ hybridisation
IT	Intra-tracheal
MDCK	Madin- Darby Canine Kidney
MERS	Middle Eastern Respiratory Syndrome
mRNA	Messenger RNA
MVA	Modified Vaccinia Ankara
NA	Neuraminidase
NP	Nucleoprotein
PBMC	Peripheral blood monocyte
PBS	Phosphate buffered saline
PCR	Polymerase chain reaction
RNA	Ribonucleic acid
RT-PCR	Reverse transcriptase PCR
SA	sialic acid
SARS	Severe Acute Respiratory Syndrome
SD	Standard deviation
TCID ₅₀	Tissue Culture Infective Dose 50

REFERENCES

1. Wilcox, B.A. and D.J. Gubler, *Disease ecology and the global emergence of zoonotic pathogens*. Environ Health Prev Med, 2005. **10**(5): p. 263-72.
2. Kuiken, T., et al., *Emerging viral infections in a rapidly changing world*. Curr Opin Biotechnol, 2003. **14**(6): p. 641-6.
3. Jones, B.A., et al., *Zoonosis emergence linked to agricultural intensification and environmental change*. Proc Natl Acad Sci U S A, 2013. **110**(21): p. 8399-404.
4. Dykes, A.C., J.D. Cherry, and C.E. Nolan, *A clinical, epidemiologic, serologic, and virologic study of influenza C virus infection*. ARCH INTERN MED, 1980. **140**(10): p. 1295-8.
5. Matsuzaki, Y., et al., *Clinical features of influenza C virus infection in children*. J INFECT DIS, 2006. **193**(9): p. 1229-35.
6. Palese, P.S., M.L. , *Orthomyxoviridae: The viruses and their replication*, in *Fields Virology*2007, Lippincott Williams & Wilkins: Philadelphia, PA, USA. p. 1647-1689.
7. Vijaykrishna, D., et al., *The contrasting phylodynamics of human influenza B viruses*. eLife, 2015. **4**.
8. Molinari, N.A., et al., *The annual impact of seasonal influenza in the US: measuring disease burden and costs*. VACCINE, 2007. **25**(27): p. 5086-96.
9. Neumann, G., T. Noda, and Y. Kawaoka, *Emergence and pandemic potential of swine-origin H1N1 influenza virus*. Nature, 2009. **459**(7249): p. 931-9.
10. Van Kerkhove, M.D., et al., *Highly pathogenic avian influenza (H5N1): pathways of exposure at the animal-human interface, a systematic review*. PLoS ONE, 2011. **6**(1): p. e14582.
11. Imai, M., et al., *Transmission of influenza A/H5N1 viruses in mammals*. Virus Res, 2013. **178**(1): p. 15-20.
12. Liu, J., et al., *H7N9: a low pathogenic avian influenza A virus infecting humans*. Curr Opin Virol, 2014. **5**: p. 91-7.
13. Choi, Y.K., et al., *Continuing evolution of H9N2 influenza viruses in Southeastern China*. J VIROL, 2004. **78**(16): p. 8609-14.
14. Wei, S.H., et al., *Human infection with avian influenza A H6N1 virus: an epidemiological analysis*. Lancet Respir Med, 2013. **1**(10): p. 771-8.
15. Lopez-Martinez, I., et al., *Highly pathogenic avian influenza A(H7N3) virus in poultry workers, Mexico, 2012*. Emerg Infect Dis, 2013. **19**(9): p. 1531-4.
16. Tweed, S.A., et al., *Human illness from avian influenza H7N3, British Columbia*. Emerg Infect Dis, 2004. **10**(12): p. 2196-9.
17. Wiersma, L.C., et al., *Virus replication kinetics and pathogenesis of infection with H7N9 influenza virus in isogenic guinea pigs upon intratracheal inoculation*. Vaccine, 2015. **33**(49): p. 6983-7.
18. Richard, M., M. de Graaf, and S. Herfst, *Avian influenza A viruses: from zoonosis to pandemic*. Future Virol, 2014. **9**(5): p. 513-524.
19. Herfst, S., et al., *Airborne transmission of influenza A/H5N1 virus between ferrets*. SCIENCE, 2012. **336**(6088): p. 1534-41.
20. Linster, M., et al., *Identification, characterization, and natural selection of mutations driving airborne transmission of A/H5N1 virus*. Cell, 2014. **157**(2): p. 329-39.
21. Imai, M., et al., *Experimental adaptation of an influenza H5 HA confers respiratory droplet transmission to a reassortant H5 HA/H1N1 virus in ferrets*. Nature, 2012. **486**(7403): p. 420-8.
22. Russell, C.A., et al., *The potential for respiratory droplet-transmissible A/H5N1 influenza virus to evolve in a mammalian host*. SCIENCE, 2012. **336**(6088): p. 1541-7.
23. Herfst, S., et al., *Avian influenza virus transmission to mammals*. Curr Top Microbiol Immunol, 2014. **385**: p. 137-55.
24. Esper, F., Z. Ou, and Y.T. Huang, *Human coronaviruses are uncommon in patients with gastrointestinal illness*. J Clin Virol, 2010. **48**(2): p. 131-3.
25. Belouzard, S., et al., *Mechanisms of coronavirus cell entry mediated by the viral spike protein*. Viruses, 2012. **4**(6): p. 1011-33.
26. Masters, P.S., *The molecular biology of coronaviruses*. Adv Virus Res, 2006. **66**: p. 193-292.
27. van der Hoek, L., et al., *Identification of a new human coronavirus*. Nat Med, 2004. **10**(4): p. 368-73.

28. Hamre, D. and J.J. Procknow, *A new virus isolated from the human respiratory tract*. Proc Soc Exp Biol Med, 1966. **121**(1): p. 190-3.
29. Woo, P.C., et al., *Characterization and complete genome sequence of a novel coronavirus, coronavirus HKU1, from patients with pneumonia*. J Virol, 2005. **79**(2): p. 884-95.
30. McIntosh, K., et al., *Recovery in tracheal organ cultures of novel viruses from patients with respiratory disease*. Proc Natl Acad Sci U S A, 1967. **57**(4): p. 933-40.
31. Drosten, C., et al., *Identification of a novel coronavirus in patients with severe acute respiratory syndrome*. N Engl J Med, 2003. **348**(20): p. 1967-76.
32. Zaki, A.M., et al., *Isolation of a novel coronavirus from a man with pneumonia in Saudi Arabia*. N Engl J Med, 2012. **367**(19): p. 1814-20.
33. WHO, *Summary of probable SARS cases with onset of illness from 1 November 2002 to 31 July 2003*, 2004, WHO.
34. Knobler, S., et al., *Learning from SARS: Preparing for the Next Disease Outbreak: Workshop Summary, in Learning from SARS: Preparing for the Next Disease Outbreak: Workshop Summary*, S. Knobler, et al., Editors. 2004: Washington (DC).
35. van Boheemen, S., et al., *Genomic characterization of a newly discovered coronavirus associated with acute respiratory distress syndrome in humans*. MBio, 2012. **3**(6).
36. Tu, C., et al., *Antibodies to SARS coronavirus in civets*. Emerg Infect Dis, 2004. **10**(12): p. 2244-8.
37. Gossner, C., et al., *Human-Dromedary Camel Interactions and the Risk of Acquiring Zoonotic Middle East Respiratory Syndrome Coronavirus Infection*. Zoonoses Public Health, 2014.
38. Reusken, C.B., et al., *Middle East respiratory syndrome coronavirus neutralising serum antibodies in dromedary camels: a comparative serological study*. Lancet Infect Dis, 2013. **13**(10): p. 859-66.
39. Huynh, J., et al., *Evidence supporting a zoonotic origin of human coronavirus strain NL63*. J VIROL, 2012. **86**(23): p. 12816-25.
40. Graham, R.L. and R.S. Baric, *Recombination, reservoirs, and the modular spike: mechanisms of coronavirus cross-species transmission*. J VIROL, 2010. **84**(7): p. 3134-46.
41. Lai, M.M., *Coronavirus: organization, replication and expression of genome*. Annu Rev Microbiol, 1990. **44**: p. 303-33.
42. Lai, M.M. and D. Cavanagh, *The molecular biology of coronaviruses*. Adv Virus Res, 1997. **48**: p. 1-100.
43. Margine, I. and F. Krammer, *Animal models for influenza viruses: implications for universal vaccine development*. Pathogens, 2014. **3**(4): p. 845-74.
44. Thangavel, R.R. and N.M. Bouvier, *Animal models for influenza virus pathogenesis, transmission, and immunology*. J Immunol Methods, 2014. **410**: p. 60-79.
45. van den Brand, J.M., et al., *The pathology and pathogenesis of experimental severe acute respiratory syndrome and influenza in animal models*. J Comp Pathol, 2014. **151**(1): p. 83-112.
46. Bodewes, R., G.F. Rimmelzwaan, and A.D. Osterhaus, *Animal models for the preclinical evaluation of candidate influenza vaccines*. Expert Rev Vaccines, 2010. **9**(1): p. 59-72.
47. Leigh, M.W., et al., *Receptor specificity of influenza virus influences severity of illness in ferrets*. VACCINE, 1995. **13**(15): p. 1468-73.
48. Kim, H.M., et al., *The severe pathogenicity of alveolar macrophage-depleted ferrets infected with 2009 pandemic H1N1 influenza virus*. VIROLOGY, 2013. **444**(1-2): p. 394-403.
49. Bodewes, R., et al., *Infection of the upper respiratory tract with seasonal influenza A(H3N2) virus induces protective immunity in ferrets against infection with A(H1N1)pdm09 virus after intranasal, but not intratracheal, inoculation*. J VIROL, 2013. **87**(8): p. 4293-301.
50. Park, S.J., et al., *Evaluation of heterosubtypic cross-protection against highly pathogenic H5N1 by active infection with human seasonal influenza A virus or trivalent inactivated vaccine immunization in ferret models*. J GEN VIROL, 2014. **95**(Pt 4): p. 793-8.
51. Bouvier, N.M., *Animal models for influenza virus transmission studies: a historical perspective*. Curr Opin Virol, 2015. **13**: p. 101-8.
52. Ning, Z.Y., et al., *Detection of expression of influenza virus receptors in tissues of BALB/c mice by histochemistry*. Vet Res Commun, 2009. **33**(8): p. 895-903.
53. Ibricevic, A., et al., *Influenza virus receptor specificity and cell tropism in mouse and human airway epithelial cells*. J VIROL, 2006. **80**(15): p. 7469-80.
54. Kreijtz, J.H., R.A. Fouchier, and G.F. Rimmelzwaan, *Immune responses to influenza virus infection*. Virus Res, 2011. **162**(1-2): p. 19-30.

55. Bouvier, N.M. and A.C. Lowen, *Animal Models for Influenza Virus Pathogenesis and Transmission*. Viruses, 2010. **2**(8): p. 1530-1563.
56. Oshansky, C.M. and P.G. Thomas, *The human side of influenza*. J Leukoc Biol, 2012. **92**(1): p. 83-96.
57. Sun, Y., et al., *Guinea pig model for evaluating the potential public health risk of swine and avian influenza viruses*. PLoS One, 2010. **5**(11): p. e15537.
58. Thangavel, R.R. and N.M. Bouvier, *Animal models for influenza virus pathogenesis, transmission, and immunology*. J Immunol Methods, 2014.
59. Lassnig, C., et al., *Development of a transgenic mouse model susceptible to human coronavirus 229E*. Proc Natl Acad Sci U S A, 2005. **102**(23): p. 8275-80.
60. Jacomy, H., et al., *Human coronavirus OC43 infection induces chronic encephalitis leading to disabilities in BALB/C mice*. VIROLOGY, 2006. **349**(2): p. 335-46.
61. Jacomy, H. and P.J. Talbot, *Vacuolating encephalitis in mice infected by human coronavirus OC43*. VIROLOGY, 2003. **315**(1): p. 20-33.
62. Dijkman, R., et al., *Seroconversion to HCoV-NL63 in Rhesus Macaques*. Viruses, 2009. **1**(3): p. 647-56.
63. van Doremalen, N. and V.J. Munster, *Animal models of Middle East respiratory syndrome coronavirus infection*. Antiviral Res, 2015.
64. Yao, Y., et al., *An animal model of MERS produced by infection of rhesus macaques with MERS coronavirus*. J Infect Dis, 2014. **209**(2): p. 236-42.
65. de Wit, E., et al., *Middle East respiratory syndrome coronavirus (MERS-CoV) causes transient lower respiratory tract infection in rhesus macaques*. Proc Natl Acad Sci U S A, 2013. **110**(41): p. 16598-603.
66. Hamming, I., et al., *Tissue distribution of ACE2 protein, the functional receptor for SARS coronavirus. A first step in understanding SARS pathogenesis*. J Pathol, 2004. **203**(2): p. 631-7.
67. Vanhoof, G., et al., *Distribution of proline-specific aminopeptidases in human tissues and body fluids*. Eur J Clin Chem Clin Biochem, 1992. **30**(6): p. 333-8.
68. Smits, S.L., et al., *Exacerbated innate host response to SARS-CoV in aged non-human primates*. PLoS Pathog, 2010. **6**(2): p. e1000756.
69. Falzarano, D., et al., *Infection with MERS-CoV causes lethal pneumonia in the common marmoset*. PLoS Pathog, 2014. **10**(8): p. e1004250.
70. Johnson, R.F., et al., *Intratracheal exposure of common marmosets to MERS-CoV Jordan-n3/2012 or MERS-CoV EMC/2012 isolates does not result in lethal disease*. VIROLOGY, 2015. **485**: p. 422-30.
71. Agrawal, A.S., et al., *Generation of a transgenic mouse model of Middle East respiratory syndrome coronavirus infection and disease*. J VIROL, 2015. **89**(7): p. 3659-70.
72. Roberts, A., et al., *Animal models and vaccines for SARS-CoV infection*. Virus Res, 2008. **133**(1): p. 20-32.
73. Roberts, A., et al., *A mouse-adapted SARS-coronavirus causes disease and mortality in BALB/c mice*. PLoS Pathog, 2007. **3**(1): p. e5.
74. Chu, Y.K., et al., *The SARS-CoV ferret model in an infection-challenge study*. VIROLOGY, 2008. **374**(1): p. 151-63.
75. Darnell, M.E., et al., *Severe acute respiratory syndrome coronavirus infection in vaccinated ferrets*. J INFECT DIS, 2007. **196**(9): p. 1329-38.
76. van den Brand, J.M., et al., *Pathology of experimental SARS coronavirus infection in cats and ferrets*. Vet Pathol, 2008. **45**(4): p. 551-62.
77. Haagmans, B.L., et al., *Asymptomatic Middle East respiratory syndrome coronavirus infection in rabbits*. J VIROL, 2015. **89**(11): p. 6131-5.
78. Wiersma, L.C., G.F. Rimmelzwaan, and R.D. de Vries, *Developing Universal Influenza Vaccines: Hitting the Nail, Not Just on the Head*. Vaccines (Basel), 2015. **3**(2): p. 239-62.
79. Riedmann, E.M., *MERS vaccine is technically feasible, but is it commercially feasible?* Hum Vaccin Immunother, 2014. **10**(6): p. 1429-30.
80. Fiore, A.E., C.B. Bridges, and N.J. Cox, *Seasonal influenza vaccines*. Curr Top Microbiol Immunol, 2009. **333**: p. 43-82.
81. Smith, D.J., et al., *Mapping the antigenic and genetic evolution of influenza virus*. SCIENCE, 2004. **305**(5682): p. 371-6.
82. Ampofo, W.K., et al., *Improving influenza vaccine virus selection: report of a WHO informal consultation held at WHO headquarters, Geneva, Switzerland, 14-16 June 2010*. Influenza Other Respir Viruses, 2012. **6**(2): p. 142-52, e1-5.

83. Tricco, A.C., et al., *Comparing influenza vaccine efficacy against mismatched and matched strains: a systematic review and meta-analysis*. BMC Med, 2013. **11**: p. 153.
84. Laver, W.G. and R.G. Webster, *Preparation and immunogenicity of an influenza virus hemagglutinin and neuraminidase subunit vaccine*. VIROLOGY, 1976. **69**(2): p. 511-22.
85. Jefferson, T., et al., *Vaccines for preventing influenza in healthy children*. Cochrane Database Syst Rev, 2012. **8**: p. CD004879.
86. Osterholm, M.T., et al., *Efficacy and effectiveness of influenza vaccines: a systematic review and meta-analysis*. Lancet Infect Dis, 2012. **12**(1): p. 36-44.
87. Pfliegerer, M., et al., *Summary of knowledge gaps related to quality and efficacy of current influenza vaccines*. VACCINE, 2014. **32**(35): p. 4586-91.
88. Jefferson, T., et al., *Vaccines for preventing influenza in healthy adults*. Cochrane Database Syst Rev, 2014. **3**: p. CD001269.
89. Andersohn, F., et al., *Vaccination of children with a live-attenuated, intranasal influenza vaccine - analysis and evaluation through a Health Technology Assessment*. GMS Health Technol Assess, 2014. **10**: p. Doc03.
90. Mohn, K.G., et al., *Longevity of B-Cell and T-Cell Responses After Live Attenuated Influenza Vaccination in Children*. J INFECT DIS, 2014.
91. He, X.S., et al., *Cellular immune responses in children and adults receiving inactivated or live attenuated influenza vaccines*. J VIROL, 2006. **80**(23): p. 11756-66.
92. Bodewes, R., et al., *Pediatric influenza vaccination: understanding the T-cell response*. Expert Rev Vaccines, 2012. **11**(8): p. 963-71.
93. Bodewes, R., et al., *Vaccination against human influenza A/H3N2 virus prevents the induction of heterosubtypic immunity against lethal infection with avian influenza A/H5N1 virus*. PLoS ONE, 2009. **4**(5): p. e5538.
94. Carter, N.J. and M.P. Curran, *Live attenuated influenza vaccine (FluMist(R); Fluenz): a review of its use in the prevention of seasonal influenza in children and adults*. Drugs, 2011. **71**(12): p. 1591-622.
95. Zeng, H., et al., *Tropism and infectivity of influenza virus, including highly pathogenic avian H5N1 virus, in ferret tracheal differentiated primary epithelial cell cultures*. J VIROL, 2013. **87**(5): p. 2597-607.
96. Heiny, A.T., et al., *Evolutionarily conserved protein sequences of influenza A viruses, avian and human, as vaccine targets*. PLoS ONE, 2007. **2**(11): p. e1190.
97. Yassine, H.M., et al., *Hemagglutinin-stem nanoparticles generate heterosubtypic influenza protection*. Nat Med, 2015.
98. Impagliazzo, A., et al., *A stable trimeric influenza hemagglutinin stem as a broadly protective immunogen*. SCIENCE, 2015.
99. Laidlaw, B.J., et al., *Cooperativity between CD8+ T cells, non-neutralizing antibodies, and alveolar macrophages is important for heterosubtypic influenza virus immunity*. PLoS Pathog, 2013. **9**(3): p. e1003207.
100. Carragher, D.M., et al., *A novel role for non-neutralizing antibodies against nucleoprotein in facilitating resistance to influenza virus*. J IMMUNOL, 2008. **181**(6): p. 4168-76.
101. Thomas, P.G., et al., *Cell-mediated protection in influenza infection*. Emerg Infect Dis, 2006. **12**(1): p. 48-54.
102. Kreijtz, J.H., et al., *Primary influenza A virus infection induces cross-protective immunity against a lethal infection with a heterosubtypic virus strain in mice*. VACCINE, 2007. **25**(4): p. 612-20.
103. Kreijtz, J.H., et al., *Cross-recognition of avian H5N1 influenza virus by human cytotoxic T-lymphocyte populations directed to human influenza A virus*. J VIROL, 2008. **82**(11): p. 5161-6.
104. van de Sandt, C.E., et al., *Human cytotoxic T lymphocytes directed to seasonal influenza A viruses cross-react with the newly emerging H7N9 virus*. J VIROL, 2014. **88**(3): p. 1684-93.
105. Hillaire, M.L., et al., *Human T-cells directed to seasonal influenza A virus cross-react with 2009 pandemic influenza A (H1N1) and swine-origin triple-reassortant H3N2 influenza viruses*. J GEN VIROL, 2013. **94**(Pt 3): p. 583-92.
106. Grebe, K.M., J.W. Yewdell, and J.R. Bennink, *Heterosubtypic immunity to influenza A virus: where do we stand?* Microbes Infect, 2008. **10**(9): p. 1024-9.
107. Kreijtz, J.H., et al., *Infection of mice with a human influenza A/H3N2 virus induces protective immunity against lethal infection with influenza A/H5N1 virus*. VACCINE, 2009. **27**(36): p. 4983-9.

108. Bodewes, R., et al., *Vaccination against seasonal influenza A/H3N2 virus reduces the induction of heterosubtypic immunity against influenza A/H5N1 virus infection in ferrets*. J VIROL, 2011. **85**(6): p. 2695-702.
109. Florek, N.W., et al., *Modified vaccinia virus Ankara encoding influenza virus hemagglutinin induces heterosubtypic immunity in macaques*. J VIROL, 2014. **88**(22): p. 13418-28.
110. Nakayama, M., et al., *Protection against H5N1 highly pathogenic avian and pandemic (H1N1) 2009 influenza virus infection in cynomolgus monkeys by an inactivated H5N1 whole particle vaccine*. PLoS ONE, 2013. **8**(12): p. e82740.
111. Wilkinson, T.M., et al., *Preexisting influenza-specific CD4+ T cells correlate with disease protection against influenza challenge in humans*. Nat Med, 2012. **18**(2): p. 274-80.
112. McMichael, A.J., et al., *Cytotoxic T-cell immunity to influenza*. N Engl J Med, 1983. **309**(1): p. 13-7.
113. Sridhar, S., et al., *Cellular immune correlates of protection against symptomatic pandemic influenza*. Nat Med, 2013. **19**(10): p. 1305-12.
114. Wang, Z., et al., *Recovery from severe H7N9 disease is associated with diverse response mechanisms dominated by CD8(+) T cells*. Nat Commun, 2015. **6**: p. 6833.
115. Hayward, A.C., et al., *Natural T Cell-mediated Protection against Seasonal and Pandemic Influenza. Results of the Flu Watch Cohort Study*. Am J Respir Crit Care Med, 2015. **191**(12): p. 1422-31.
116. Hillaire, M.L., et al., *Cross-protective immunity against influenza pH1N1 2009 viruses induced by seasonal influenza A (H3N2) virus is mediated by virus-specific T-cells*. J GEN VIROL, 2011. **92**(Pt 10): p. 2339-49.
117. Khurana, S., et al., *MF59 adjuvant enhances diversity and affinity of antibody-mediated immune response to pandemic influenza vaccines*. Sci Transl Med, 2011. **3**(85): p. 85ra48.
118. Sun, H.X., Y. Xie, and Y.P. Ye, *ISCOMs and ISCOMATRIX*. VACCINE, 2009. **27**(33): p. 4388-401.
119. Rimmelzwaan, G.F., et al., *A randomized, double blind study in young healthy adults comparing cell mediated and humoral immune responses induced by influenza ISCOM vaccines and conventional vaccines*. VACCINE, 2000. **19**(9-10): p. 1180-7.
120. van de Sandt, C.E., et al., *Novel G3/DT adjuvant promotes the induction of protective T cells responses after vaccination with a seasonal trivalent inactivated split-virion influenza vaccine*. VACCINE, 2014. **32**(43): p. 5614-23.
121. Sambhara, S., et al., *Heterosubtypic immunity against human influenza A viruses, including recently emerged avian H5 and H9 viruses, induced by FLU-ISCOM vaccine in mice requires both cytotoxic T-lymphocyte and macrophage function*. Cell Immunol, 2001. **211**(2): p. 143-53.
122. Collins, P.L., A. Bukreyev, and B.R. Murphy, *What are the risks--hypothetical and observed--of recombination involving live vaccines and vaccine vectors based on nonsegmented negative-strain RNA viruses?* J VIROL, 2008. **82**(19): p. 9805-6.
123. Coughlan, L., C. Mullarkey, and S. Gilbert, *Adenoviral vectors as novel vaccines for influenza*. J Pharm Pharmacol, 2015.
124. Dudek, T. and D.M. Knipe, *Replication-defective viruses as vaccines and vaccine vectors*. VIROLOGY, 2006. **344**(1): p. 230-9.
125. He, F., S. Madhan, and J. Kwang, *Baculovirus vector as a delivery vehicle for influenza vaccines*. Expert Rev Vaccines, 2009. **8**(4): p. 455-67.
126. Draper, S.J., M.G. Cottingham, and S.C. Gilbert, *Utilizing poxviral vectored vaccines for antibody induction-progress and prospects*. VACCINE, 2013. **31**(39): p. 4223-30.
127. Robert-Guroff, M., *Replicating and non-replicating viral vectors for vaccine development*. Curr Opin Biotechnol, 2007. **18**(6): p. 546-56.
128. Lambe, T., *Novel viral vectored vaccines for the prevention of influenza*. Mol Med, 2012. **18**: p. 1153-60.
129. Mogler, M.A. and K.I. Kamrud, *RNA-based viral vectors*. Expert Rev Vaccines, 2015. **14**(2): p. 283-312.
130. Price, G.E., et al., *Single-dose mucosal immunization with a candidate universal influenza vaccine provides rapid protection from virulent H5N1, H3N2 and H1N1 viruses*. PLoS ONE, 2010. **5**(10): p. e13162.
131. Price, G.E., et al., *Mucosal immunization with a candidate universal influenza vaccine reduces virus transmission in a mouse model*. J VIROL, 2014. **88**(11): p. 6019-30.
132. Rimmelzwaan, G.F. and G. Sutter, *Candidate influenza vaccines based on recombinant modified vaccinia virus Ankara*. Expert Rev Vaccines, 2009. **8**(4): p. 447-54.

133. Altenburg, A.F., et al., *Modified vaccinia virus ankara (MVA) as production platform for vaccines against influenza and other viral respiratory diseases*. *Viruses*, 2014. **6**(7): p. 2735-61.
134. Sutter, G. and B. Moss, *Nonreplicating vaccinia vector efficiently expresses recombinant genes*. *Proc Natl Acad Sci U S A*, 1992. **89**(22): p. 10847-51.
135. Brewoo, J.N., et al., *Cross-protective immunity against multiple influenza virus subtypes by a novel modified vaccinia Ankara (MVA) vectored vaccine in mice*. *VACCINE*, 2013. **31**(14): p. 1848-55.
136. Kreijtz, J.H., et al., *Preclinical evaluation of a modified vaccinia virus Ankara (MVA)-based vaccine against influenza A/H5N1 viruses*. *VACCINE*, 2009. **27**(45): p. 6296-9.
137. Hessel, A., et al., *Vectors based on modified vaccinia Ankara expressing influenza H5N1 hemagglutinin induce substantial cross-clade protective immunity*. *PLoS ONE*, 2011. **6**(1): p. e16247.
138. Kreijtz, J.H., et al., *A Single Immunization With Modified Vaccinia Virus Ankara-Based Influenza Virus H7 Vaccine Affords Protection in the Influenza A(H7N9) Pneumonia Ferret Model*. *J INFECT DIS*, 2014.
139. Hessel, A., et al., *A pandemic influenza H1N1 live vaccine based on modified vaccinia Ankara is highly immunogenic and protects mice in active and passive immunizations*. *PLoS ONE*, 2010. **5**(8): p. e12217.
140. Kreijtz, J.H., et al., *Evaluation of a modified vaccinia virus Ankara (MVA)-based candidate pandemic influenza A/H1N1 vaccine in the ferret model*. *J GEN VIROL*, 2010. **91**(Pt 11): p. 2745-52.
141. Lillie, P.J., et al., *Preliminary assessment of the efficacy of a T-cell-based influenza vaccine, MVA-NP+M1, in humans*. *CLIN INFECT DIS*, 2012. **55**(1): p. 19-25.
142. Lambe, T., et al., *Immunity against heterosubtypic influenza virus induced by adenovirus and MVA expressing nucleoprotein and matrix protein-1*. *Sci Rep*, 2013. **3**: p. 1443.
143. Gilbert, S.C., *Clinical development of Modified Vaccinia virus Ankara vaccines*. *VACCINE*, 2013. **31**(39): p. 4241-6.
144. Kreijtz, J.H., et al., *Safety and immunogenicity of a modified-vaccinia-virus-Ankara-based influenza A H5N1 vaccine: a randomised, double-blind phase 1/2a clinical trial*. *Lancet Infect Dis*, 2014. **14**(12): p. 1196-207.
145. Cao, Z., et al., *Potent and persistent antibody responses against the receptor-binding domain of SARS-CoV spike protein in recovered patients*. *Virol J*, 2010. **7**: p. 299.
146. Du, L., et al., *The spike protein of SARS-CoV-a target for vaccine and therapeutic development*. *Nat Rev Microbiol*, 2009. **7**(3): p. 226-36.
147. Tang, F., et al., *Lack of peripheral memory B cell responses in recovered patients with severe acute respiratory syndrome: a six-year follow-up study*. *J Immunol*, 2011. **186**(12): p. 7264-8.
148. Czub, M., et al., *Evaluation of modified vaccinia virus Ankara based recombinant SARS vaccine in ferrets*. *VACCINE*, 2005. **23**(17-18): p. 2273-9.
149. Yip, M.S., et al., *Antibody-dependent infection of human macrophages by severe acute respiratory syndrome coronavirus*. *Virol J*, 2014. **11**: p. 82.
150. Mou, H., et al., *The receptor binding domain of the new Middle East respiratory syndrome coronavirus maps to a 231-residue region in the spike protein that efficiently elicits neutralizing antibodies*. *J VIROL*, 2013. **87**(16): p. 9379-83.
151. Du, L., et al., *Identification of a receptor-binding domain in the S protein of the novel human coronavirus Middle East respiratory syndrome coronavirus as an essential target for vaccine development*. *J VIROL*, 2013. **87**(17): p. 9939-42.
152. Du, L., et al., *A truncated receptor-binding domain of MERS-CoV spike protein potently inhibits MERS-CoV infection and induces strong neutralizing antibody responses: implication for developing therapeutics and vaccines*. *PLoS ONE*, 2013. **8**(12): p. e81587.
153. Song, F., et al., *Middle East respiratory syndrome coronavirus spike protein delivered by modified vaccinia virus Ankara efficiently induces virus-neutralizing antibodies*. *J VIROL*, 2013. **87**(21): p. 11950-4.
154. Channappanavar, R., J. Zhao, and S. Perlman, *T cell-mediated immune response to respiratory coronaviruses*. *Immunol Res*, 2014. **59**(1-3): p. 118-28.
155. Martin, J.E., et al., *A SARS DNA vaccine induces neutralizing antibody and cellular immune responses in healthy adults in a Phase I clinical trial*. *VACCINE*, 2008. **26**(50): p. 6338-43.
156. Cameron, M.J., et al., *Human immunopathogenesis of severe acute respiratory syndrome (SARS)*. *Virus Res*, 2008. **133**(1): p. 13-9.
157. Xu, X. and X. Gao, *Immunological responses against SARS-coronavirus infection in humans*. *Cell Mol Immunol*, 2004. **1**(2): p. 119-22.

158. Wang, Y.D., et al., *T-cell epitopes in severe acute respiratory syndrome (SARS) coronavirus spike protein elicit a specific T-cell immune response in patients who recover from SARS*. J VIROL, 2004. **78**(11): p. 5612-8.
159. Zhao, J., J. Zhao, and S. Perlman, *T cell responses are required for protection from clinical disease and for virus clearance in severe acute respiratory syndrome coronavirus-infected mice*. J VIROL, 2010. **84**(18): p. 9318-25.
160. Regla-Nava, J.A., et al., *Severe acute respiratory syndrome coronaviruses with mutations in the E protein are attenuated and promising vaccine candidates*. J VIROL, 2015. **89**(7): p. 3870-87.
161. See, R.H., et al., *Comparative evaluation of two severe acute respiratory syndrome (SARS) vaccine candidates in mice challenged with SARS coronavirus*. J GEN VIROL, 2006. **87**(Pt 3): p. 641-50.
162. Zhou, J., et al., *Immunogenicity, safety, and protective efficacy of an inactivated SARS-associated coronavirus vaccine in rhesus monkeys*. VACCINE, 2005. **23**(24): p. 3202-9.
163. Lamirande, E.W., et al., *A live attenuated severe acute respiratory syndrome coronavirus is immunogenic and efficacious in golden Syrian hamsters*. J VIROL, 2008. **82**(15): p. 7721-4.
164. Graham, R.L., et al., *A live, impaired-fidelity coronavirus vaccine protects in an aged, immunocompromised mouse model of lethal disease*. Nat Med, 2012. **18**(12): p. 1820-6.
165. Qu, D., et al., *Intranasal immunization with inactivated SARS-CoV (SARS-associated coronavirus) induced local and serum antibodies in mice*. VACCINE, 2005. **23**(7): p. 924-31.
166. Fett, C., et al., *Complete protection against severe acute respiratory syndrome coronavirus-mediated lethal respiratory disease in aged mice by immunization with a mouse-adapted virus lacking E protein*. J VIROL, 2013. **87**(12): p. 6551-9.
167. Tseng, C.T., et al., *Immunization with SARS coronavirus vaccines leads to pulmonary immunopathology on challenge with the SARS virus*. PLoS ONE, 2012. **7**(4): p. e35421.
168. Honda-Okubo, Y., et al., *Severe acute respiratory syndrome-associated coronavirus vaccines formulated with delta inulin adjuvants provide enhanced protection while ameliorating lung eosinophilic immunopathology*. J VIROL, 2015. **89**(6): p. 2995-3007.
169. Zhang, N., S. Jiang, and L. Du, *Current advancements and potential strategies in the development of MERS-CoV vaccines*. Expert Rev Vaccines, 2014. **13**(6): p. 761-74.
170. Tang, J., et al., *Optimization of antigen dose for a receptor-binding domain-based subunit vaccine against MERS coronavirus*. Hum Vaccin Immunother, 2015. **11**(5): p. 1244-50.
171. Ma, C., et al., *Searching for an ideal vaccine candidate among different MERS coronavirus receptor-binding fragments--the importance of immunofocusing in subunit vaccine design*. VACCINE, 2014. **32**(46): p. 6170-6.
172. Yang, Z.Y., et al., *A DNA vaccine induces SARS coronavirus neutralization and protective immunity in mice*. Nature, 2004. **428**(6982): p. 561-4.
173. Lokugamage, K.G., et al., *Chimeric coronavirus-like particles carrying severe acute respiratory syndrome coronavirus (SCoV) S protein protect mice against challenge with SCoV*. VACCINE, 2008. **26**(6): p. 797-808.
174. Pichla-Gollon, S.L., et al., *Effect of preexisting immunity on an adenovirus vaccine vector: in vitro neutralization assays fail to predict inhibition by antiviral antibody in vivo*. J VIROL, 2009. **83**(11): p. 5567-73.
175. Volz, A., et al., *Protective Efficacy of Recombinant Modified Vaccinia Virus Ankara Delivering Middle East Respiratory Syndrome Coronavirus Spike Glycoprotein*. J VIROL, 2015. **89**(16): p. 8651-6.
176. Guo, X., et al., *Systemic and mucosal immunity in mice elicited by a single immunization with human adenovirus type 5 or 41 vector-based vaccines carrying the spike protein of Middle East respiratory syndrome coronavirus*. Immunology, 2015. **145**(4): p. 476-84.
177. Kim, E., et al., *Immunogenicity of an adenoviral-based Middle East Respiratory Syndrome coronavirus vaccine in BALB/c mice*. VACCINE, 2014. **32**(45): p. 5975-82.
178. WHO, *Influenza (seasonal) fact sheet number 211 in access date 6-6-2014*2014.
179. Garten, R.J., et al., *Antigenic and genetic characteristics of swine-origin 2009 A(H1N1) influenza viruses circulating in humans*. Science, 2009. **325**(5937): p. 197-201.
180. Dawood, F.S., et al., *Emergence of a novel swine-origin influenza A (H1N1) virus in humans*. N Engl J Med, 2009. **360**(25): p. 2605-15.
181. Neumann, G., et al., *H5N1 influenza viruses: outbreaks and biological properties*. Cell Res, 2010. **20**(1): p. 51-61.

182. Gong, Z., et al., *Epidemiology of the avian influenza A (H7N9) outbreak in Zhejiang Province, China*. BMC Infect Dis, 2014. **14**(1): p. 244.
183. Kroeze, E.J., T. Kuiken, and A.D. Osterhaus, *Animal models*. Methods Mol Biol, 2012. **865**: p. 127-46.
184. van den Brand, J.M., et al., *The Pathology and Pathogenesis of Experimental Severe Acute Respiratory Syndrome and Influenza in Animal Models*. J Comp Pathol, 2014.
185. Jayaraman, A., et al., *Decoding the distribution of glycan receptors for human-adapted influenza A viruses in ferret respiratory tract*. PLoS One, 2012. **7**(2): p. e27517.
186. Bodewes, R., et al., *Pathogenesis of Influenza A/H5N1 virus infection in ferrets differs between intranasal and intratracheal routes of inoculation*. Am J Pathol, 2011. **179**(1): p. 30-6.
187. Lowen, A.C., et al., *The guinea pig as a transmission model for human influenza viruses*. Proc Natl Acad Sci U S A, 2006. **103**(26): p. 9988-92.
188. Moncla, L.H., et al., *A novel nonhuman primate model for influenza transmission*. PLoS One, 2013. **8**(11): p. e78750.
189. Lipscomb, M.F., et al., *The antigen-induced selective recruitment of specific T lymphocytes to the lung*. J Immunol, 1982. **128**(1): p. 111-5.
190. Phair, J.P., et al., *Influenza virus infection of the guinea pig: immune response and resistance*. Med Microbiol Immunol, 1979. **165**(4): p. 241-54.
191. Schafer, H. and R. Burger, *Tools for cellular immunology and vaccine research the in the guinea pig: monoclonal antibodies to cell surface antigens and cell lines*. Vaccine, 2012. **30**(40): p. 5804-11.
192. Mizutani, N., et al., *Intratracheal sensitization/challenge-induced biphasic asthmatic response and airway hyperresponsiveness in guinea pigs*. Biol Pharm Bull, 2010. **33**(12): p. 1949-52.
193. Lipscomb, M.F., et al., *Persistence of influenza as an immunogen in pulmonary antigen-presenting cells*. Infect Immun, 1983. **42**(3): p. 965-72.
194. Edelman, P.H., *The Guinea pig model of legionnaires' disease*. Methods Mol Biol, 2013. **954**: p. 521-40.
195. Steel, J., et al., *Transmission of pandemic H1N1 influenza virus and impact of prior exposure to seasonal strains or interferon treatment*. J Virol, 2010. **84**(1): p. 21-6.
196. Azoulay-Dupuis, E., et al., *Lung alterations in guinea-pigs infected with influenza virus*. J Comp Pathol, 1984. **94**(2): p. 273-83.
197. WHO, *WHO Manual on Animal Influenza Diagnosis and Surveillance*, in access date 6-6-20142002.
198. Rimmelzwaan, G.F., et al., *Comparison of RNA hybridization, hemagglutination assay, titration of infectious virus and immunofluorescence as methods for monitoring influenza virus replication in vitro*. J Virol Methods, 1998. **74**(1): p. 57-66.
199. van den Brand, J.M., et al., *Comparison of temporal and spatial dynamics of seasonal H3N2, pandemic H1N1 and highly pathogenic avian influenza H5N1 virus infections in ferrets*. PLoS One, 2012. **7**(8): p. e42343.
200. Van Hoeven, N., et al., *Pathogenesis of 1918 pandemic and H5N1 influenza virus infections in a guinea pig model: antiviral potential of exogenous alpha interferon to reduce virus shedding*. J Virol, 2009. **83**(7): p. 2851-61.
201. Tang, X. and K.T. Chong, *Histopathology and growth kinetics of influenza viruses (H1N1 and H3N2) in the upper and lower airways of guinea pigs*. J Gen Virol, 2009. **90**(Pt 2): p. 386-91.
202. Kwon, Y.K., A.S. Lipatov, and D.E. Swayne, *Bronchointerstitial pneumonia in guinea pigs following inoculation with H5N1 high pathogenicity avian influenza virus*. Vet Pathol, 2009. **46**(1): p. 138-41.
203. van den Brand, J.M., et al., *Severity of pneumonia due to new H1N1 influenza virus in ferrets is intermediate between that due to seasonal H1N1 virus and highly pathogenic avian influenza H5N1 virus*. J Infect Dis, 2010. **201**(7): p. 993-9.
204. Brederoo, P. and W.T. Daems, *The ultrastructure of guinea pig heterophil granulocytes and the heterogeneity of the granules*. Cell Tissue Res, 1978. **194**(2): p. 183-205.
205. Gleich, G.J., D.A. Loegering, and J.E. Maldonado, *Identification of a major basic protein in guinea pig eosinophil granules*. J Exp Med, 1973. **137**(6): p. 1459-71.
206. Wetherbee, R.E., *Induction of systemic delayed hypersensitivity during experimental viral infection of the respiratory tract with a myxovirus or paramyxovirus*. J Immunol, 1973. **111**(1): p. 157-63.
207. WHO. *WHO Risk Assessment of human infection with avian influenza A(H7N9) virus*. 2015 [cited 2015 03-05-2015].
208. Qi, X., et al., *Probable person to person transmission of novel avian influenza A (H7N9) virus in Eastern China, 2013: epidemiological investigation*. BMJ, 2013. **347**: p. f4752.

209. Shi, J., et al., *A detailed epidemiological and clinical description of 6 human cases of avian-origin influenza A (H7N9) virus infection in Shanghai*. PLoS One, 2013. **8**(10): p. e77651.
210. Hu, J., et al., *Limited human-to-human transmission of avian influenza A(H7N9) virus, Shanghai, China, March to April 2013*. Euro Surveill, 2014. **19**(25).
211. Zaraket, H., et al., *Mammalian adaptation of influenza A(H7N9) virus is limited by a narrow genetic bottleneck*. Nat Commun, 2015. **6**: p. 6553.
212. Kreijtz, J.H., et al., *A Single Immunization With Modified Vaccinia Virus Ankara-Based Influenza Virus H7 Vaccine Affords Protection in the Influenza A(H7N9) Pneumonia Ferret Model*. J Infect Dis, 2015. **211**(5): p. 791-800.
213. Kreijtz, J.H., et al., *Low pathogenic avian influenza A(H7N9) virus causes high mortality in ferrets upon intratracheal challenge: a model to study intervention strategies*. Vaccine, 2013. **31**(43): p. 4995-9.
214. Belsler, J.A., et al., *Pathogenesis and transmission of avian influenza A (H7N9) virus in ferrets and mice*. Nature, 2013. **501**(7468): p. 556-9.
215. Wiersma, L.C., et al., *Pathogenesis of Infection with 2009 Pandemic H1N1 Influenza Virus in Isogenic Guinea Pigs after Intranasal or Intratracheal Inoculation*. Am J Pathol, 2015. **185**(3): p. 643-50.
216. Gabbard, J.D., et al., *Novel H7N9 influenza virus shows low infectious dose, high growth rate, and efficient contact transmission in the guinea pig model*. J Virol, 2014. **88**(3): p. 1502-12.
217. de Graaf, M. and R.A. Fouchier, *Role of receptor binding specificity in influenza A virus transmission and pathogenesis*. EMBO J, 2014. **33**(8): p. 823-41.
218. Nicholls, J.M., et al., *Sialic acid receptor detection in the human respiratory tract: evidence for widespread distribution of potential binding sites for human and avian influenza viruses*. Respir Res, 2007. **8**: p. 73.
219. Siegers, J.Y., et al., *Novel avian-origin influenza A (H7N9) virus attachment to the respiratory tract of five animal models*. J Virol, 2014. **88**(8): p. 4595-9.
220. York, I. and R.O. Donis, *The 2009 pandemic influenza virus: where did it come from, where is it now, and where is it going?* Curr Top Microbiol Immunol, 2013. **370**: p. 241-57.
221. Schulman, J.L. and E.D. Kilbourne, *Induction of Partial Specific Heterotypic Immunity in Mice by a Single Infection with Influenza A Virus*. J Bacteriol, 1965. **89**: p. 170-4.
222. Altenburg, A.F., G.F. Rimmelzwaan, and R.D. de Vries, *Virus-specific T cells as correlate of (cross-)protective immunity against influenza*. VACCINE, 2015. **33**(4): p. 500-6.
223. Heinen, P.P., E.A. de Boer-Luijtzte, and A.T. Bianchi, *Respiratory and systemic humoral and cellular immune responses of pigs to a heterosubtypic influenza A virus infection*. J Gen Virol, 2001. **82**(Pt 11): p. 2697-707.
224. Reeth, K.V., et al., *Genetic relationships, serological cross-reaction and cross-protection between H1N2 and other influenza A virus subtypes endemic in European pigs*. Virus Res, 2004. **103**(1-2): p. 115-24.
225. Latorre-Margalef, N., et al., *Heterosubtypic immunity to influenza A virus infections in mallards may explain existence of multiple virus subtypes*. PLoS Pathog, 2013. **9**(6): p. e1003443.
226. Fereidouni, S.R., et al., *Highly pathogenic avian influenza virus infection of mallards with homo- and heterosubtypic immunity induced by low pathogenic avian influenza viruses*. PLoS One, 2009. **4**(8): p. e6706.
227. Seo, S.H. and R.G. Webster, *Cross-reactive, cell-mediated immunity and protection of chickens from lethal H5N1 influenza virus infection in Hong Kong poultry markets*. J Virol, 2001. **75**(6): p. 2516-25.
228. Seo, S.H., M. Peiris, and R.G. Webster, *Protective cross-reactive cellular immunity to lethal A/Goose/Guangdong/1/96-like H5N1 influenza virus is correlated with the proportion of pulmonary CD8(+) T cells expressing gamma interferon*. J Virol, 2002. **76**(10): p. 4886-90.
229. Straight, T.M., et al., *Evidence of a cross-protective immune response to influenza A in the cotton rat model*. Vaccine, 2006. **24**(37-39): p. 6264-71.
230. Rimmelzwaan, G.F., R.A. Fouchier, and A.D. Osterhaus, *Age distribution of cases caused by different influenza viruses*. Lancet Infect Dis, 2013. **13**(8): p. 646-7.
231. Yap, K.L., G.L. Ada, and I.F. McKenzie, *Transfer of specific cytotoxic T lymphocytes protects mice inoculated with influenza virus*. Nature, 1978. **273**(5659): p. 238-9.
232. Tan, B.T., et al., *Production of monoclonal antibodies defining guinea pig T-cell surface markers and a strain 13 Ia-like antigen: the value of immunohistological screening*. Hybridoma, 1985. **4**(2): p. 115-24.
233. Epstein, S.L., *Prior H1N1 influenza infection and susceptibility of Cleveland Family Study participants during the H2N2 pandemic of 1957: an experiment of nature*. J Infect Dis, 2006. **193**(1): p. 49-53.

234. Krammer, F. and P. Palese, *Influenza virus hemagglutinin stalk-based antibodies and vaccines*. *Curr Opin Virol*, 2013. **3**(5): p. 521-30.
235. Bodewes, R., et al., *Vaccination with whole inactivated virus vaccine affects the induction of heterosubtypic immunity against influenza virus A/H5N1 and immunodominance of virus-specific CD8+ T-cell responses in mice*. *J Gen Virol*, 2010. **91**(Pt 7): p. 1743-53.
236. Weinfurter, J.T., et al., *Cross-reactive T cells are involved in rapid clearance of 2009 pandemic H1N1 influenza virus in nonhuman primates*. *PLoS Pathog*, 2011. **7**(11): p. e1002381.
237. Jameson, J., et al., *Human CD8+ and CD4+ T lymphocyte memory to influenza A viruses of swine and avian species*. *J Immunol*, 1999. **162**(12): p. 7578-83.
238. Gao, R., et al., *Human Infection with a Novel Avian-Origin Influenza A (H7N9) Virus*. *N Engl J Med*, 2013.
239. Li, Q., et al., *Preliminary Report: Epidemiology of the Avian Influenza A (H7N9) Outbreak in China*. *N Engl J Med*, 2013.
240. Chen, E., et al., *Human infection with avian influenza A(H7N9) virus re-emerges in China in winter 2013*. *Euro Surveill*, 2013. **18**(43).
241. *Cases of H7N9 Influenza in China by Week of Onset (May 16, 2014)*. 2014 16-5-2014 [cited 2014 23-5-2014]
242. van Riel, D., et al., *Novel avian-origin influenza A (H7N9) virus attaches to epithelium in both upper and lower respiratory tract of humans*. *Am J Pathol*, 2013. **183**(4): p. 1137-43.
243. Collin, N., X. de Radigues, and H.N.V.T.F. World Health Organization, *Vaccine production capacity for seasonal and pandemic (H1N1) 2009 influenza*. *Vaccine*, 2009. **27**(38): p. 5184-6.
244. IFPMA, *Authoritative New Study Reveals Global Pandemic Influenza Vaccine Capacity in accessed May 20, 2010*.
245. Couch, R.B., et al., *Evaluations for in vitro correlates of immunogenicity of inactivated influenza a H5, H7 and H9 vaccines in humans*. *PLoS One*, 2012. **7**(12): p. e50830.
246. De Groot, A.S., et al., *Low immunogenicity predicted for emerging avian-origin H7N9: implication for influenza vaccine design*. *Hum Vaccin Immunother*, 2013. **9**(5): p. 950-6.
247. Miller, E., et al., *Risk of narcolepsy in children and young people receiving AS03 adjuvanted pandemic A/H1N1 2009 influenza vaccine: retrospective analysis*. *BMJ*, 2013. **346**: p. f794.
248. Kreijtz, J.H., A.D. Osterhaus, and G.F. Rimmelzwaan, *Vaccination strategies and vaccine formulations for epidemic and pandemic influenza control*. *Hum Vaccin*, 2009. **5**(3): p. 126-35.
249. Zhang, L., et al., *Optimal designs of an HA-based DNA vaccine against H7 subtype influenza viruses*. *Hum Vaccin Immunother*, 2014. **10**(7).
250. Chu, D.H., et al., *Potency of an inactivated influenza vaccine prepared from A/duck/Mongolia/119/2008 (H7N9) against the challenge with A/Anhui/1/2013 (H7N9)*. *Vaccine*, 2014.
251. Yan, J., et al., *Protective immunity to H7N9 influenza viruses elicited by synthetic DNA vaccine*. *Vaccine*, 2014. **32**(24): p. 2833-42.
252. Bart, S.A., et al., *A Cell Culture-Derived MF59-Adjuvanted Pandemic A/H7N9 Vaccine Is Immunogenic in Adults*. *Sci Transl Med*, 2014. **6**(234): p. 234ra55.
253. Goff, P.H., et al., *Induction of cross-reactive antibodies to novel H7N9 influenza virus by recombinant Newcastle disease virus expressing a North American lineage H7 subtype hemagglutinin*. *J Virol*, 2013. **87**(14): p. 8235-40.
254. Krammer, F., et al., *Divergent H7 immunogens offer protection from H7N9 virus challenge*. *J Virol*, 2014. **88**(8): p. 3976-85.
255. Klausberger, M., et al., *One-shot vaccination with an insect cell-derived low-dose influenza A H7 virus-like particle preparation protects mice against H7N9 challenge*. *Vaccine*, 2014. **32**(3): p. 355-62.
256. Margine, I., P. Palese, and F. Krammer, *Expression of functional recombinant hemagglutinin and neuraminidase proteins from the novel H7N9 influenza virus using the baculovirus expression system*. *J Vis Exp*, 2013(81): p. e51112.
257. Fries, L.F., G.E. Smith, and G.M. Glenn, *A recombinant viruslike particle influenza A (H7N9) vaccine*. *N Engl J Med*, 2013. **369**(26): p. 2564-6.
258. Hahn, T., et al., *Rapid Manufacture and Release of a GMP Batch of Avian Influenza A(H7N9) Virus-Like Particle Vaccine Made Using Recombinant Baculovirus-Sf9 Insect Cell Culture Technology*. *Bioprocessing Journal*, 2013. **12**(2): p. 4-17.
259. Kreijtz, J.H., S.C. Gilbert, and G. Sutter, *Poxvirus vectors*. *Vaccine*, 2013. **31**(39): p. 4217-9.

260. Moss, B., *Reflections on the early development of poxvirus vectors*. *Vaccine*, 2013. **31**(39): p. 4220-2.
261. Kreijtz, J.H., et al., *Recombinant modified vaccinia virus Ankara expressing the hemagglutinin gene confers protection against homologous and heterologous H5N1 influenza virus infections in macaques*. *J Infect Dis*, 2009. **199**(3): p. 405-13.
262. Kreijtz, J.H., et al., *MVA-based H5N1 vaccine affords cross-clade protection in mice against influenza A/H5N1 viruses at low doses and after single immunization*. *PLoS One*, 2009. **4**(11): p. e7790.
263. Kreijtz, J.H., et al., *Recombinant modified vaccinia virus Ankara-based vaccine induces protective immunity in mice against infection with influenza virus H5N1*. *J Infect Dis*, 2007. **195**(11): p. 1598-606.
264. Veits, J., et al., *Protective efficacy of several vaccines against highly pathogenic H5N1 avian influenza virus under experimental conditions*. *Vaccine*, 2008.
265. Sutter, G., et al., *A recombinant vector derived from the host range-restricted and highly attenuated MVA strain of vaccinia virus stimulates protective immunity in mice to influenza virus*. *Vaccine*, 1994. **12**(11): p. 1032-40.
266. Berthoud, T.K., et al., *Potent CD8+ T-cell immunogenicity in humans of a novel heterosubtypic influenza A vaccine, MVA-NP+M1*. *Clin Infect Dis*, 2011. **52**(1): p. 1-7.
267. Hessel, A., et al., *MVA vectors expressing conserved influenza proteins protect mice against lethal challenge with H5N1, H9N2 and H7N1 viruses*. *PLoS One*, 2014. **9**(2): p. e88340.
268. Kremer, M., et al., *Easy and efficient protocols for working with recombinant vaccinia virus MVA*. *Methods Mol Biol*, 2012. **890**: p. 59-92.
269. Wyatt, L.S., et al., *Multiprotein HIV type 1 clade B DNA and MVA vaccines: construction, expression, and immunogenicity in rodents of the MVA component*. *AIDS Res Hum Retroviruses*, 2004. **20**(6): p. 645-53.
270. Palmer, D., Dowle, W., Coleman M., Schild G., *Haemagglutination inhibition test*, in *Advanced laboratory techniques for influenza diagnosis. Procedural Guide*1975, US Dept. Hlth. ED.: Atlanta. p. 25-62.
271. McCullers, J.A., et al., *Recipients of vaccine against the 1976 "swine flu" have enhanced neutralization responses to the 2009 novel H1N1 influenza virus*. *Clin Infect Dis*, 2010. **50**(11): p. 1487-92.
272. van den Brand, J.M., et al., *Efficacy of vaccination with different combinations of MF59-adjuvanted and nonadjuvanted seasonal and pandemic influenza vaccines against pandemic H1N1 (2009) influenza virus infection in ferrets*. *J Virol*, 2011. **85**(6): p. 2851-8.
273. Schrauwen, E.J., et al., *The multibasic cleavage site in H5N1 virus is critical for systemic spread along the olfactory and hematogenous routes in ferrets*. *J Virol*, 2012. **86**(7): p. 3975-84.
274. Richard, M., et al., *Limited airborne transmission of H7N9 influenza A virus between ferrets*. *Nature*, 2013. **501**(7468): p. 560-3.
275. Xu, L., et al., *Novel avian-origin human influenza A(H7N9) can be transmitted between ferrets via respiratory droplets*. *J Infect Dis*, 2014. **209**(4): p. 551-6.
276. Chen, Z., et al., *Development of a High-Yield Live Attenuated H7N9 Influenza Virus Vaccine That Provides Protection against Homologous and Heterologous H7 Wild-Type Viruses in Ferrets*. *J Virol*, 2014. **88**(12): p. 7016-7023.
277. Xu, Q., et al., *Evaluation of live attenuated H7N3 and H7N7 vaccine viruses for their receptor binding preferences, immunogenicity in ferrets and cross reactivity to the novel H7N9 virus*. *PLoS One*, 2013. **8**(10): p. e76884.
278. Keawcharoen, J., et al., *Repository of Eurasian influenza A virus hemagglutinin and neuraminidase reverse genetics vectors and recombinant viruses*. *Vaccine*, 2010. **28**(36): p. 5803-9.
279. Prill, M.M., et al., *Human coronavirus in young children hospitalized for acute respiratory illness and asymptomatic controls*. *Pediatr Infect Dis J*, 2012. **31**(3): p. 235-40.
280. Lu, R., et al., *Characterization of human coronavirus etiology in Chinese adults with acute upper respiratory tract infection by real-time RT-PCR assays*. *PLoS One*, 2012. **7**(6): p. e38638.
281. Zumla, A., D.S. Hui, and S. Perlman, *Middle East respiratory syndrome*. *Lancet*, 2015. **386**(9997): p. 995-1007.
282. Peiris, J.S., Y. Guan, and K.Y. Yuen, *Severe acute respiratory syndrome*. *Nat Med*, 2004. **10**(12 Suppl): p. S88-97.
283. World Health Organization, *Disease outbreak news: Middle East respiratory syndrome coronavirus (MERS-CoV) per 13 November 2015*, 2015, Global Alert and Response (GAR) - World Health Organization (WHO).

284. The WHO MERS-CoV Research Group, *State of Knowledge and Data Gaps of Middle East Respiratory Syndrome Coronavirus (MERS-CoV) in Humans*. PLoS Curr, 2013. **5**.
285. Drosten, C., et al., *Transmission of MERS-coronavirus in household contacts*. N Engl J Med, 2014. **371**(9): p. 828-35.
286. Memish, Z.A., et al., *Screening for Middle East respiratory syndrome coronavirus infection in hospital patients and their healthcare worker and family contacts: a prospective descriptive study*. Clin Microbiol Infect, 2014. **20**(5): p. 469-74.
287. Raj, V.S., et al., *Dipeptidyl peptidase 4 is a functional receptor for the emerging human coronavirus-EMC*. Nature, 2013. **495**(7440): p. 251-4.
288. Li, W., et al., *Angiotensin-converting enzyme 2 is a functional receptor for the SARS coronavirus*. Nature, 2003. **426**(6965): p. 450-4.
289. Hofmann, H., et al., *Human coronavirus NL63 employs the severe acute respiratory syndrome coronavirus receptor for cellular entry*. Proc Natl Acad Sci U S A, 2005. **102**(22): p. 7988-93.
290. Nguyen, D.T., et al., *Paramyxovirus infections in ex vivo lung slice cultures of different host species*. J Virol Methods, 2013. **193**(1): p. 159-65.
291. Corman, V.M., et al., *Detection of a novel human coronavirus by real-time reverse-transcription polymerase chain reaction*. Euro Surveill, 2012. **17**(39).
292. Wu, P.S., et al., *Clinical manifestations of human coronavirus NL63 infection in children in Taiwan*. Eur J Pediatr, 2008. **167**(1): p. 75-80.
293. Ksiazek, T.G., et al., *A novel coronavirus associated with severe acute respiratory syndrome*. N Engl J Med, 2003. **348**(20): p. 1953-66.
294. Finney, D.J., *The Spearman-Kärber method*, in *Statistical Methods in Biological Assays* D.J. Finney, Editor 1964, Charles Griffin London, UK.
295. Kotewicz, M.L., et al., *Optical mapping and 454 sequencing of Escherichia coli O157 : H7 isolates linked to the US 2006 spinach-associated outbreak*. Microbiology, 2008. **154**(Pt 11): p. 3518-28.
296. de Lang, A., et al., *Functional genomics highlights differential induction of antiviral pathways in the lungs of SARS-CoV-infected macaques*. PLoS Pathog, 2007. **3**(8): p. e112.
297. Kint, J., et al., *Infectious Bronchitis Coronavirus Inhibits STAT1 Signaling and Requires Accessory Proteins for Resistance to Type I Interferon Activity*. J Virol, 2015. **89**(23): p. 12047-57.
298. Wang, F., et al., *RNAscope: a novel in situ RNA analysis platform for formalin-fixed, paraffin-embedded tissues*. J Mol Diagn, 2012. **14**(1): p. 22-9.
299. Morgenstern, B., et al., *Ribavirin and interferon-beta synergistically inhibit SARS-associated coronavirus replication in animal and human cell lines*. Biochem Biophys Res Commun, 2005. **326**(4): p. 905-8.
300. Smits, S.L., et al., *Distinct severe acute respiratory syndrome coronavirus-induced acute lung injury pathways in two different nonhuman primate species*. J Virol, 2011. **85**(9): p. 4234-45.
301. de Wilde, A.H., et al., *MERS-coronavirus replication induces severe in vitro cytopathology and is strongly inhibited by cyclosporin A or interferon-alpha treatment*. J Gen Virol, 2013. **94**(Pt 8): p. 1749-60.
302. Milewska, A., et al., *Human coronavirus NL63 utilizes heparan sulfate proteoglycans for attachment to target cells*. J Virol, 2014. **88**(22): p. 13221-30.
303. Milho, R., et al., *A heparan-dependent herpesvirus targets the olfactory neuroepithelium for host entry*. PLoS Pathog, 2012. **8**(11): p. e1002986.
304. Rockx, B., et al., *Comparative pathogenesis of three human and zoonotic SARS-CoV strains in cynomolgus macaques*. PLoS One, 2011. **6**(4): p. e18558.
305. McAuliffe, J., et al., *Replication of SARS coronavirus administered into the respiratory tract of African Green, rhesus and cynomolgus monkeys*. Virology, 2004. **330**(1): p. 8-15.
306. Chan, J.F., et al., *Differential cell line susceptibility to the emerging novel human betacoronavirus 2c EMC/2012: implications for disease pathogenesis and clinical manifestation*. J Infect Dis, 2013. **207**(11): p. 1743-52.
307. Kindler, E., et al., *Efficient replication of the novel human betacoronavirus EMC on primary human epithelium highlights its zoonotic potential*. MBio, 2013. **4**(1): p. e00611-12.
308. Falzarano, D., et al., *Treatment with interferon-alpha2b and ribavirin improves outcome in MERS-CoV-infected rhesus macaques*. Nat Med, 2013. **19**(10): p. 1313-7.
309. Totura, A.L. and R.S. Baric, *SARS coronavirus pathogenesis: host innate immune responses and viral antagonism of interferon*. Curr Opin Virol, 2012. **2**(3): p. 264-75.

310. Cabeça, T.K., C. Granato, and N. Bellei, *Epidemiological and clinical features of human coronavirus infections among different subsets of patients*. *Influenza Other Respir Viruses*, 2013. **7**(6): p. 1040-7.
311. Kuypers, J., et al., *Clinical disease in children associated with newly described coronavirus subtypes*. *Pediatrics*, 2007. **119**(1): p. e70-6.
312. Taubenberger, J.K., J.V. Hultin, and D.M. Morens, *Discovery and characterization of the 1918 pandemic influenza virus in historical context*. *Antivir Ther*, 2007. **12**(4 Pt B): p. 581-91.
313. Bedford, T., et al., *Global circulation patterns of seasonal influenza viruses vary with antigenic drift*. *Nature*, 2015. **523**(7559): p. 217-20.
314. Gaunt, E.R., et al., *Epidemiology and clinical presentations of the four human coronaviruses 229E, HKU1, NL63, and OC43 detected over 3 years using a novel multiplex real-time PCR method*. *J Clin Microbiol*, 2010. **48**(8): p. 2940-7.
315. Perlman, S. and A.A. Dandekar, *Immunopathogenesis of coronavirus infections: implications for SARS*. *Nat Rev Immunol*, 2005. **5**(12): p. 917-27.
316. Zhao, J., et al., *Evasion by stealth: inefficient immune activation underlies poor T cell response and severe disease in SARS-CoV-infected mice*. *PLoS Pathog*, 2009. **5**(10): p. e1000636.
317. Yoshikawa, T., et al., *Severe acute respiratory syndrome (SARS) coronavirus-induced lung epithelial cytokines exacerbate SARS pathogenesis by modulating intrinsic functions of monocyte-derived macrophages and dendritic cells*. *J VIROL*, 2009. **83**(7): p. 3039-48.
318. Janice Oh, H.L., et al., *Understanding the T cell immune response in SARS coronavirus infection*. *Emerg Microbes Infect*, 2012. **1**(9): p. e23.
319. Channappanavar, R., et al., *Virus-specific memory CD8 T cells provide substantial protection from lethal severe acute respiratory syndrome coronavirus infection*. *J VIROL*, 2014. **88**(19): p. 11034-44.

NEDERLANDSE SAMENVATTING

INLEIDING

Nieuwe virale luchtweginfecties bij de mens worden de laatste jaren steeds vaker gerapporteerd. Tijdens de totstandkoming van dit proefschrift zijn twee belangrijke, nieuwe, opkomende pathogenen beschreven: het Influenza A H7N9-virus uit pluimvee in China en het *Middle East Respiratory Syndrome* (MERS) -coronavirus uit dromedarissen in Saoedi-Arabië. De opkomst van deze pathogenen is voor een groot deel te wijten aan veranderingen in menselijk gedrag, waaronder toenemende landbouw en veehouderij, groeiende populaties en stijgende globale mobiliteit.

Om deze zoönotische ziekteverwekkers zo goed mogelijk te bestuderen, zijn diermodellen die de ziekte in mensen zo nauwkeurig mogelijk nabootsen vooralsnog onmisbaar. Het uiteindelijke doel hiervan is het ontwikkelen van effectieve interventiestrategieën, in dit geval vooral vaccins. Diermodellen en de toepassing daarvan voor het bestuderen van Influenza A en coronavirussen, zijn dan ook het onderwerp van dit proefschrift.

Influenza A-virussen, beter bekend als griepvirussen, zijn negatiefstrengs RNA-virussen met een gesegmenteerd genoom dat uit acht (PB2, PB1, PA, HA, NP, NA, M en NS) delen bestaat die meerdere eiwitten coderen. De virussen worden onderverdeeld in subtypes op basis van hun oppervlakte-eiwitten HA en NA. Er zijn achttien HA subtypes en 11 NA subtypes bekend, waarvan H1N1 en H3N2 momenteel verantwoordelijk zijn voor jaarlijkse griep epidemieën bij de mens. Om deze griep epidemieën te beperken, bestaan verschillende soorten vaccins. Dode vaccins induceren humorale immuniteit, oftewel antilichamen, die voornamelijk gericht zijn tegen de kop van de HA, en in mindere mate de NA, eiwitten van de op dat moment circulerende subtypes. Aangezien het huidige proces van vaccinvervaardiging zeer traag is, moet reeds zes maanden voor het griepseizoen de keuze gemaakt worden welke virussen als vaccinstammen gebruikt zullen worden. Doordat de polymerase van influenza niet erg nauwkeurig is, kunnen mutaties echter zodanig snel optreden dat de bescherming die geboden wordt door deze vaccins, tegen de tijd dat de griep epidemie begint, soms niet meer van toepassing is op het inmiddels veranderde virus. In deze gevallen is de bevolking niet beschermd en zal er in dat seizoen een verhoogde morbiditeit en mortaliteit optreden. Naast het feit dat de huidige dode

vaccins dus niet voldoen voor seizoensgebonden griep, gaat de productie van vaccins ook te traag wanneer een geheel nieuw subtype opkomt. Het virus kan niet alleen overspringen vanuit een dierlijk reservoir maar kan tevens recombineren door gensegmenten van verschillende virussen uit verschillende gastheren (bijvoorbeeld vogels en varkens) uit te wisselen. Bestaande levende vaccins bieden enig voordeel ten opzichte van dode vaccins, omdat ze naast humorale ook cellulaire immuniteit kunnen induceren. Een zeer wenselijke eigenschap, aangezien cellulaire immuniteit een bredere bescherming biedt, omdat het tevens tegen geconserveerde eiwitten gericht is. Levende vaccins zijn echter onderhevig aan dezelfde beperkingen als de reeds beschreven dode varianten en bieden daarom geen goed alternatief.

De focus van de influenzawetenschap richt zich al enige tijd op het ontwikkelen van nieuwe vaccins die idealiter een dusdanig brede bescherming bieden dat jaarlijkse vaccinatie overbodig wordt en de bevolking beschermd is tegen alle mogelijke (opkomende) subtypes; een universeel vaccin. Er zijn talloze manieren getest die immuniteit zouden kunnen verbreden en/of gebruik maken van nieuwe formuleringen om dit te bereiken. Een voorbeeld daarvan is het *Modified Vaccinia Ankara (MVA)* vaccin dat gebruik maakt van een vaccinia virus vector om de gekozen influenza eiwitten te vervaardigen in de gastheer. Deze vaccins zijn effectief, veilig en relatief snel te maken en zijn dus, in combinatie met de juiste eiwitten, een veelbelovende combinatie.

Diermodellen zijn van groot belang, zowel om meer te weten te komen over het samenspel tussen het influenzavirus en de gastheer, als voor het testen van nieuwe vaccins. De meest gebruikte diermodellen voor influenza zijn muizen, fretten en cavia's. Al deze diersoorten hebben voor- en nadelen maar tot op heden wordt de fret beschouwd als de *gold standard* voor influenzaonderzoek. In hoofdstuk 5 van dit proefschrift hebben wij dan ook gebruik gemaakt van dit diermodel om een nieuw MVA-vaccin tegen het recent opgekomen influenza A/H7N9-virus te testen. Isogene fretten zijn echter niet verkrijgbaar en daarom is dit diermodel niet optimaal voor het bestuderen van cellulaire immuniteit, waarvoor voornamelijk muizen gebruikt worden. In tegenstelling tot fretten zijn muizen echter geen goed model voor het bestuderen van transmissie van influenzavirussen. In hoofdstuk 2, 3 en 4 worden de eerste stappen voor het ontwikkelen van een nieuw diermodel beschreven. Het betreft de isogene stam-2-cavia, die uitzonderlijk geschikt zou zijn voor gelijktijdig onderzoek naar transmissie en naar cellulaire immuniteit. Coronavirussen (CoV) zijn positiefstrengs RNA-virussen die bedekt zijn met conisch gevormde oppervlakte-eiwitten (het S-eiwit) die rondom het viruspartikel de kroon vormen waaraan het virus zijn naam verleend. Deze S-eiwitten zijn belangrijk voor het

binden van het virus aan de receptoren op de gastheercel en deze eiwitten zijn dan ook bepalend voor welke diersoorten door het virus geïnfecteerd kunnen worden. Er zijn momenteel zes humane coronavirussen bekend, twee α -coronavirussen (229E- en NL63-CoV) en vier β -coronavirussen (OC43-, HKU-1-, SARS- en MERS-CoV), die alle voornamelijk respiratoire klachten veroorzaken.

Het eerste humane coronavirus dat beschouwd werd als belangrijk voor de volksgezondheid, het *Severe Acute Respiratory Syndrome* (SARS)-CoV, sprong rond 2002 over van de civetkat naar de mens en veroorzaakte een uitbraak in meer dan 8000 mensen waarvan er ongeveer 800 stierven. Voor het opkomen van SARS-CoV, waren alleen OC43-CoV en 229E-CoV bekend als veroorzakers van overwegend milde bovenste luchtweginfecties bij de mens. Na de SARS-CoV-uitbraak werden nog twee virussen ontdekt, NL63-CoV en HKU-1-CoV, die eveneens voornamelijk milde bovenste luchtweg-infecties veroorzaken. Het was enige tijd stil rondom coronavirussen tot in 2012 MERS-CoV werd geïdentificeerd als de veroorzaker van ernstige lagere luchtweginfectie bij mensen in het Midden-Oosten. Na uitvoerig onderzoek werd de dromedaris als tussengastheer voor dit virus aangewezen. Door de genetische verwantschap met coronavirussen die in vleermuizen gevonden zijn, wordt aangenomen dat zowel SARS- als MERS-CoV oorspronkelijk voort zijn gekomen uit deze diersoort.

Gezien de relatief recente ontdekking van coronavirussen als pathogenen bij de mens, is veel minder bekend over de pathogenese vergeleken met influenza. Ondanks meerdere veelbelovende kandidaten (waaronder wederom MVA-vaccins, ditmaal op basis van het S-eiwit) is er op dit moment dan ook nog geen vaccin op de markt. Dit komt deels door het feit dat het zeer uitdagend is gebleken om representatieve diermodellen te ontwikkelen voor deze virussen. Diermodellen voor SARS-CoV zijn wel ontwikkeld, onder andere fretten en (na aanpassing van het virus) muizen kunnen geïnfecteerd worden, maar geen van deze modellen bootst het ziektebeeld in mensen goed na. Ziekteverschijnselen in oudere makaken leken tot nu toe het best overeen te komen met de ziekte in mensen, maar om ethische en praktische redenen is dit model van weinig nut voor algemeen onderzoek. In Hoofdstuk 6 worden diermodellen voor MERS-CoV en NL63-CoV onderzocht en vergeleken met historische informatie over SARS-CoV. Naast een transgene muis, en mogelijk het penseelaapje, zijn diermodellen voor MERS-CoV tot nu toe helaas weinig representatief.

DIERMODELLEN VOOR INFLUENZAVIRUSSEN

Isogene stam-2-cavia's lijken een veelbelovend diermodel om transmissie en cellulaire immuniteit gelijktijdig te bestuderen, iets wat niet mogelijk is in fretten of muizen. Om een diermodel te ontwikkelen, moeten echter eerst de basisprincipes vastgesteld worden. Zoals beschreven in hoofdstuk 2, zijn ten eerste cavia's intra-nasale of intra-tracheaal geïnoculeerd met de pandemische stam van influenza A H1N1 (H1N1pdm09). Hieruit bleek dat intra-tracheale inoculatie meer longontsteking veroorzaakt en dat het virus na intra-nasale inoculatie vrijwel uitsluitend in de neus te vinden is. Omdat het model toegepast zal worden om de immunreactie op ernstige longontsteking te onderzoeken, is intra-tracheale inoculatie dus een betere methode. Uit dit experiment bleek ook dat de piek van virusreproductie reeds op dag 2 plaatsvond en deze informatie is eveneens belangrijk voor toekomstige experimenten.

In hoofdstuk 3 zijn de lessen die geleerd zijn uit hoofdstuk 2 toegepast om een soortgelijk experiment uit te voeren in isogene cavia's, ditmaal met het Influenza A H7N9-virus. Dit virus bleek ernstiger laesies te veroorzaken, met name in de longen. Dit komt overeen met de verwachtingen, aangezien dit virus van aviaire herkomst is, dus aan α -2,3-sialzuur gekoppelde receptoren bindt, die zowel bij de cavia als bij de mens in hogere mate aanwezig zijn in de lagere luchtwegen. Het H7N9-virus bleek eveneens langer via de neus uitgescheiden te worden dan H1N1pdm09.

Nadat gegevens over het gedrag van deze twee virussen (H1N1 en H7N9) in dit model verzameld waren, was de volgende stap om de basisprincipes van de immuniteit tegen influenza in isogene cavia's vast te stellen door het aantonen van heterosubtypische immuniteit. Heterosubtypische immuniteit treedt op wanneer een infectie met een influenza -subtype (gedeeltelijke) bescherming biedt tegen infectie met een ander subtype. Zoals in hoofdstuk 4 wordt beschreven, werden cavia's hiervoor eerst geïnoculeerd met H1N1pdm09 of met een zoutoplossing (controledieren). Vier weken later werden de dieren wederom geïnoculeerd maar ditmaal met H7N9- virus. De virale kinetiek en de laesies werden vergeleken en het bleek dat dieren die eerder een H1N1 virusinfectie doorgemaakt hadden deels beschermd waren tegen H7N9- virus. Er werd aangetoond dat antilichamen niet verantwoordelijk waren voor de geobserveerde bescherming en dus is het aannemelijk gemaakt dat dit een manifestatie van cel gemedieerde heterosubtypische immuniteit is.

In hoofdstuk 5 werd het belang aangetoond van het gebruik van bestaande diermodellen om nieuwe interventiemethoden preklinisch te testen. Het vaccin werd samengesteld uit MVA in combinatie met het HA-eiwit van het H7N9-virus. Fretten werden op verschillende wijze gevaccineerd, meerdere malen en/of met verschillende dosis, en hieruit bleek dat een enkele vaccinatie met een hoge dosis al genoeg is voor bescherming. Tweemaal vaccineren met een lage dosis bleek daarentegen minder effectief. MVA vaccins lijken interessante vaccinkandidaten, aangezien ze effectief en veilig zijn en daarnaast in relatief korte tijd in grote hoeveelheden geproduceerd kunnen worden.

DIERMODELLEN VOOR CORONAVIRUSSEN

Voor de humane coronavirussen die voornamelijk milde symptomen in de bovenste luchtwegen veroorzaken, is vooralsnog niet veel bekend over mogelijke diermodellen, mede omdat er weinig stimulans is om deze virussen in meer detail te onderzoeken. Terwijl er voor SARS-CoV aanzienlijk meer inspanning is geleverd, heeft dat relatief weinig opgeleverd. In hoofdstuk 6 wordt het makaakmodel gebruikt om beter te begrijpen waarom MERS-CoV-replicatie in dit diermodel zo beperkt is en worden de verkregen resultaten vergeleken met andere coronavirussen NL63-CoV en SARS-CoV. De receptor voor MERS-CoV, DPP4, wordt vrijwel uitsluitend in de lagere luchtwegen gevonden wat zou kunnen verklaren waarom dit virus vooralsnog niet eenvoudig overspringt van mens naar mens. ACE-2, de receptor voor SARS- en NL63-CoV, is aanwezig in zowel de bovenste als de lagere luchtwegen en longen, maar waar SARS-CoV in het gehele respiratoire systeem lijkt te repliceren, wordt NL63-CoV voornamelijk in de bovenste luchtwegen gevonden. Ook wordt aangetoond dat, in tegenstelling tot wat bekend is voor SARS-CoV, MERS-CoV geïnfecteerde cellen wél vatbaar zijn voor de antivirale werking van IFN- β en dat het aangeboren (innate) immuunsysteem op die manier de infectie beperkt.

DISCUSSIE

De tot nu vergaarde kennis over coronavirussen loopt achter op het influenza onderzoeksveld, maar in beide disciplines zijn nog vele vragen onbeantwoord. Het is van belang dat onderzoek voortgezet wordt omdat het risico dat nieuwe virussen uit deze families in de toekomst op zullen komen zodanig is dat het eerder een kwestie van *wanneer* dan *of* het zal gebeuren.

Een universeel vaccin blijft het hoogste doel van influenzaonderzoek, maar voordat dit vaccin daadwerkelijk ontwikkeld en klaar voor gebruik is, zullen nog vele jaren verstrijken. Gedurende deze periode is het belangrijk, mede door middel van diermodellen, aandacht te besteden aan zowel het virus als de gastheerrespons. Daarnaast kunnen bestaande interventiestrategieën zoals MVA geoptimaliseerd worden om zo beter en sneller voorbereid te zijn mocht een nieuwe influenzapandemie zich voordoen.

Voor het bestuderen van coronavirussen liggen nog veel meer vragen open, niet in het minst hoe de ziektes adequaat bestudeerd kunnen worden in de afwezigheid van goede diermodellen. Mogelijk kunnen experimenten met humane witte bloedcellen, zoals die uitgevoerd zijn voor influenza, uitkomst bieden voor in vitro studies naar immuniteit. Het is vooral van groot belang om meer informatie te vergaren over de exacte rol van het immuunsysteem, want tot dusver is het niet altijd duidelijk wanneer en hoe het bijdraagt aan bescherming en wanneer het juist ziekteverschijnselen bevordert. Deze informatie is van groot belang voor vaccinontwikkeling.

Dit proefschrift omvat slechts een minuscuul deel van een kolossale globale puzzel, maar alle beetjes helpen; Rome is immers ook niet op een dag gebouwd.

ABOUT THE AUTHOR

CURRICULUM VITAE



The author of this thesis was born on the 7th of July 1982 in Gouda, the Netherlands. She attended high school in Addis Ababa, Ethiopia, Bangkok, Thailand and briefly, Oegstgeest, the Netherlands after which, thanks to the Dutch lottery system for veterinary medicine admission, she spent a year travelling and working in South America. She then applied to university in the United Kingdom, as well as the Netherlands, and ended up having an unforgettable time studying veterinary medicine at

Bristol University. In her third year of veterinary medicine, she realized she should have studied medicine. However instead of completely changing track, she decided to dedicate herself to the interface between veterinary and human medicine. She subsequently briefly interrupted her studies in 2004 to complete an intercalated Bachelor degree in Immunology and Virology at the medical faculty of the University of Bristol. In 2005, she negotiated vehemently with the veterinary faculty to be the first Bristol veterinary student to be permitted to partake in the Erasmus exchange programme, for which she spent a year at the Ecole Nationale Vétérinaire d'Alfort, Paris, France. After graduating and a short stint in companion animal emergency care in clinics in Paris, she was accepted for a residency in veterinary pathology at the University of Utrecht. She spent just over three years, partook in many interesting projects at the human/domestic animal/wildlife interface and obtained her European College of Veterinary Pathology diploma in 2012. After three years in Holland, she felt claustrophobic and ready for new adventures, which she found by working for the emerging zoonoses group of the Robert Koch Institute in Berlin, Germany. She did some very adventurous fieldwork indeed in the Democratic Republic of the Congo but after falling seriously ill, she resigned herself to return to the safety/predictability of the Netherlands when she was offered the wonderful opportunity of becoming a PhD candidate at the Viroscience Lab of the Erasmus Medical Centre in Rotterdam, where she spent 3 great years. In the end all these convoluted roads did, as the saying promises, lead to Rome and therefore that is where she now resides.

PHD PORFOLIO

EDUCATION

2008 - 2011

Resident in Veterinary pathology at the department of pathobiology, faculty of veterinary medicine, University of Utrecht (the Netherlands). Diploma of the European College of Veterinary Pathologists (ECVP) Subspecialty Wildlife and Exotics obtained in 2012.

2001 - 2007

Bachelor of Veterinary Science (BVSc) at the faculty of veterinary medicine, University of Bristol, United Kingdom, including Erasmus year at the Ecole Nationale Vétérinaire d'Alfort, Paris, France from 2005-2006.

2004 - 2005

Bachelor of Science with Honours (BSc Hons) in Immunology and Virology at the Faculty of Medicine, University of Bristol, United Kingdom.

CONFERENCES/SEMINARS/MEETINGS/WORKSHOPS

European Wildlife Disease Association

Chair of the EWDA Student Chapter (2012-2015) Member of the organizing committee of the 2013 and 2015 EWDA student workshops in France . Participant at the 2012 conference in EWDA/WDA in Lyon and speaker at the 2014 EWDA conference, Edinburgh, United Kingdom.

Comparative Pathology Meetings

Participant and, from 2013 onwards, member of the organizing committee. Initially monthly meetings, now biennial meetings, at the Erasmus Medical Centre.

MolMed days

Erasmus Medical Center day for PhD students. Participant and poster presentation in 2013 and 2014.

3rd International One Health Conference

Amsterdam 15-18 March 2015. Participant.

Options for the Control of Influenza VIII

Cape Town 5-10 September, 2013. Participant and poster presentation.

COURSES

FP7 ANTIGONE One Health Courses

Participant in 2014 (Bonn, Germany), 2013 (Ciudad Real, Spain) and 2012 (Rotterdam, The Netherlands), 3 weeks full-time each.

Artikel 9 Course

Compulsory qualification for working with laboratory animals. Completed in November 2012 at the UMC in Leiden.

Erasmus Medical Centre School of Molecular Medicine courses

Excel course 2013, Presenting skills 2014, Virology course 2014.

Masterclasses School of Entrepreneurship, University of Utrecht

Series of evening lectures on the interface between entrepreneurship and academia.

Health to Market (FP7) Innovation and Entrepreneurship in Health Sciences

Courses organized by SKEMA business school (France) in Rome, Italy.

TEACHING

Viruskennner coach

2013 - 2015, education on infectious diseases for high school students.

Master Infection and Immunity

Teaching for lab rotations and co-supervisor for master student.

PUBLICATIONS

Wiersma L , Widagdo W, Smits S, de Vries R, Getu S, Schipper D, Raj S, Kuiken T, Osterhaus A, van den Brand J, Haagmans B, Confined DPP4 expression and interferon signaling in the respiratory tract of non-human primates are associated with restricted MERS coronavirus replication (manuscript in preparation).

Wiersma LC, Rimmelzwaan GF, de Vries RD. Developing Universal Influenza Vaccines: Hitting the Nail, Not Just on the Head. *Vaccines*. 2015;3(2):239-62.

Wiersma LC, Kreijtz JH, Vogelzang-van Trierum SE, van Amerongen G, van Run P, Ladwig M, et al. Virus replication kinetics and pathogenesis of infection with H7N9 influenza virus in isogenic guinea pigs upon intratracheal inoculation. *Vaccine*. 2015 Dec 8;33(49):6983-7.

Wiersma LC, Vogelzang-van Trierum SE, Kreijtz JH, van Amerongen G, van Run P, Ladwig M, et al. Heterosubtypic immunity to H7N9 influenza virus in isogenic guinea pigs after infection with pandemic H1N1 virus. *Vaccine*. 2015 Dec 8;33(49):6977-82.

Bexton S, Wiersma LC, Getu S, van Run PR, Verjans GM, Schipper D, et al. Detection of Circovirus in Foxes with Meningoencephalitis, United Kingdom, 2009-2013. *Emerging infectious diseases*. 2015 Jul;21(7):1205-8.

Wiersma LC, Vogelzang-van Trierum SE, van Amerongen G, van Run P, Nieuwkoop NJ, Ladwig M, et al. Pathogenesis of Infection with 2009 Pandemic H1N1 Influenza Virus in Isogenic Guinea Pigs after Intranasal or Intratracheal Inoculation. *The American journal of pathology*. 2015 Mar;185(3):643-50.

Kreijtz JH, Wiersma LC, De Gruyter HL, Vogelzang-van Trierum SE, van Amerongen G, Stittelaar KJ, et al. A Single Immunization With Modified Vaccinia Virus Ankara-Based Influenza Virus H7 Vaccine Affords Protection in the Influenza A(H7N9) Pneumonia Ferret Model. *The Journal of infectious diseases*. 2015 Mar 1;211(5):791-800.

Pauly M, Hoppe E, Mugisha L, Petrzalkova K, Akoua-Koffi C, Couacy-Hymann E, et al. High prevalence and diversity of species D adenoviruses (HAdV-D) in human populations of four Sub-Saharan countries. *Virology journal*. 2014;11:25.

Hiemstra S, Harkema L, Wiersma LC, Keesler RI. Beyond Parasitism: Hepatic Lesions in Stranded Harbor Porpoises (*Phocoena phocoena*) Without Trematode (*Campyla oblonga*) Infections. *Veterinary pathology*. 2014 Dec 8.

Schaumburg F, Pauly M, Anoh E, Mossoun A, Wiersma L, Schubert G, et al. *Staphylococcus aureus* complex from animals and humans in three remote African regions. *Clinical microbiology and infection : the official publication of the European Society of Clinical Microbiology and Infectious Diseases*. 2014 Dec 11.

Raj VS, Smits SL, Provacia LB, van den Brand JM, Wiersma L, Ouwendijk WJ, et al. Adenosine deaminase acts as a natural antagonist for dipeptidyl peptidase 4-mediated entry of the Middle East respiratory syndrome coronavirus. *Journal of virology*. 2014 Feb;88(3):1834-8.

Maio E, Begeman L, Bisselink Y, van Tulden P, Wiersma L, Hiemstra S, et al. Identification and typing of *Brucella* spp. in stranded harbour porpoises (*Phocoena phocoena*) on the Dutch coast. *Veterinary microbiology*. 2014 Sep 17;173(1-2):118-24.

Hoogduijn MJ, van den Beukel JC, Wiersma LC, Ijzer J. Morphology and size of stem cells from mouse and whale: observational study. *BMJ*. 2013;347:f6833.

Bodewes R, Rubio Garcia A, Wiersma LC, Getu S, Beukers M, Schapendonk CM, et al. Novel B19-like parvovirus in the brain of a harbor seal. *PloS one*. 2013;8(11):e79259.

Wiersma L, Reubsaet FA, Wolfe AG, de Jong PA, Grone A. Unilateral granulomatous orchitis in a harbour porpoise (*Phocoena phocoena*): a case report. *Tijdschrift voor diergeneeskunde*. 2011 Feb 1;136(2):94-8.

Wiersma L, Kuiper RV, Grone A. Hepatic extraskeletal chondroblastic osteosarcoma with unusual angioinvasion of the caudal vena cava in a dog. *Tijdschrift voor diergeneeskunde*. 2010 Dec 15;135(24):940-3.

ACKNOWLEDGEMENTS

The acknowledgements are widely known to be the (only) part of a thesis that is really read. So the pressure is on, especially because it's hard to express the immense gratitude I feel for everyone who's helped me both start and finish this. It has been quite a ride, interesting and intense and I am happy to have shared it with everyone on the 17th floor and beyond. There are so many people without whom it would never ever have been possible.

Een persoon steekt daar natuurlijk met kop en schouders bovenuit, en niet alleen omdat ie zo lang is. Guus, dankzij jouw drive en je pragmatische aanpak heb ik veel kunnen bereiken in korte tijd. Ik heb veel van je geleerd, zoals hoe een Amsterdams accent in het Engels klinkt en alle mogelijke controles die je in een experiment kan verwerken. Ook erg belangrijk: ik weet nu wie Cruijff is en zelfs wat hij allemaal gezegd heeft. Zoals: "Vaak moet er iets gebeuren voordat er iets gebeurt". Maar wat ik vooral heb geleerd is hoe je serieus in je werk kunt zijn, zonder ooit kans voorbij te laten gaan om te lachen of een feestje te vieren. Je bent altijd op de eerste plaats mens, en dan pas professor, promotor of baas. Ik heb respect voor hoe jij veel kunt bereiken terwijl je buiten je werk om ook nog een heel rijk leven leidt (waarom zijn we nou nooit gaan golfen?!). Ik ben me er volledig van bewust dat het zonder jouw steun nooit was gelukt om alles voor elkaar te krijgen en daar ben ik je diep dankbaar voor.

Bart, uiteindelijk hebben we minder samengewerkt dan gepland was, maar zoals het er nu uitziet gaat het leukste deel van onze samenwerking misschien nog komen! Jij en Guus hebben een volledig tegenovergestelde aanpak en het was een grote verrijking voor mij om beide mee te maken. Wat jullie wel delen is dat jullie allebei op de eerste plaats ontzettend fijne mensen zijn. Dank je wel voor de tijd die je in me gestoken hebt en wees een beetje mild voor Do ;).

Thijs, niet mijn officiële promotor maar wel al vele jaren mijn mentor. Zonder jou en Ab was ik überhaupt nooit bij het EMC terechtgekomen. De comparative pathology meetings, de EWDA, de ANTIGONE One Health courses en natuurlijk vooral jijzelf hebben een enorm belangrijke rol gespeeld in mijn professionele vorming en daar pluk ik nu dagelijks de vruchten van. Ik heb enorm respect voor je precisie en de passie waarmee je te werk gaat. Er zijn weinig keren dat ik niet uit jouw kantoor kwam met een nieuw inzicht of een beetje nieuwe energie om toch verder te gaan. Dank je wel voor je geduld en je begeleiding, ook al was ik niet jouw promovenda, je hebt me wel als zodanig ondersteund.

Ab, zoals gezegd, zonder jouw visie was ik nooit in het EMC terecht gekomen. Je bent een master manipulator maar gelukkig gebruik je die superpower alleen voor goede doeleinden (dat hoop ik tenminste!). Ik ben blij dat ik levend genoeg uit Congo terug ben gekomen om deel uit te maken van de fantastische afdeling die jij gecreëerd hebt. Een perfecte combinatie van work hard, play hard waar tegen ik alle toekomstige werkplekken zal afmeten. Ik weet dat je me vooral Truusje-met-de-grote-bek vindt maar zolang je genoeg moppert weet ik dat het nog goed zit. Het was jammer dat je halverwege mijn PhD weg was, maar net zoals het verrijkend was om zowel Bart als Guus mee te maken, was het ook leerzaam om onder twee verschillende afdelingshoofden te werken.

Marion, bedankt vooral voor de laatste paar maanden, het werk voor COMPARE heeft me precies op het juiste spoor gezet om aan de slag te kunnen bij de FAO. Ik ben erg benieuwd wat de toekomst allemaal zal brengen. En natuurlijk ook bedankt voor een beetje girlpower bij Viroscience; dat was nooit Ab's sterkste punt ;)

Dan de andere persoon naast Guus zonder wie dit allemaal nooit gelukt was: m'n (lab) mattie Stella SuperStar (Ziekrikzeese zinderende zwoele zuipheks). Wat ben toch een onwijze lieverd! Super fijn om in het lab lekker te kunnen knallen zonder te klagen, integendeel; wat hebben wij een lol gehad! Met onze X-rated BSL3 conversaties die gelukkig, net als alle pathogenen veilig daar op het lab blijven (toch??). We hebben allebei moeilijke momenten gehad in de laatste paar maanden/jaren maar gelukkig konden we bij elkaar uithuilen en lachen. Dank je wel voor alles wat je voor gedaan hebt en wat je voor me betekend hebt; jij maakte de dagelijkse dingen dragelijk en zelfs leuk. En vergeet niet: everything will be all right in the end, and if it's not all right, it's not the end...

Lieve Josanne, ik weet nog de eerste keer dat wij elkaar ontmoeten. In 2009, een nacht lange roadtrip in een gammel autootje naar Annecy en jij woest mooi met je dreadlocks. Wisten wij veel dat we zoveel gingen delen in de daaropvolgende jaren? Je bent een wervelwind van ideeën, inspiratie en energie. Het was fijn om te weten dat ik niet de enige was die altijd met een been in een hele andere wereld stond, dat maakte het minder eenzaam. Je bent een bijzonder mens; warm, lief, creatief en vooral nooit voorspelbaar.

Judith, al vanaf voor het ECVP examen heb je me altijd geholpen, zelfs als je zelf overliep. Je hebt de weg gebaad voor een generatie EMC pathologen/PhDs! Ik heb zo veel van je geleerd, het was super fijn om met je samen te werken; precies, betrouwbaar, didactisch en vooral heel lief. Dank je voor de zorg voor Koen de Karma Koevia, ik hoop dat ie voor ons beiden een goed woordje doet in de proefdierhemel...

Ben, mister man, what would I have done without you... and dinosaurs ... and COFFEE?? I think we perfected the art of procaffeinating. The comfy chairs, coffee and a lot of bullsh*t to brighten the rainy Rotterdam days, thanks for keeping me (in)sane.

Lineke, heb ik eindelijk ook eens een jonger zusje! Het is een eer dat je in mijn voetsporen treedt en ik heb geen twijfel dat je het vele malen beter gaat doen dan ik! Jammer dat we in Rotterdam niet langer samen hebben kunnen werken, maar dat komt vast wel weer... Zal ik alvast in Rome op zoek gaan naar een leuk huis voor wanneer je hier aan de slag gaat? ;)

Geert, de eindeloze uren gebogen over isolatoren, al je lelijke grapjes (voor wiens carrière moet deze dood?) en onze mooie conversaties, je bent uniek, bruuut en toch perfectionistisch en zonder jou waren mijn experimenten heel anders gelopen. Je bent onbetaalbaar :D

Team Koevia, you know who you are, ja toch? Word up?? Serieus, Dennis M en Vincent V het was mij een eer om met jullie te werken, weer of geen weer (toch geen last van in het EDC), weekend of geen weekend, altijd gezelligheid en vage dubbelzinnige gesprekken ;) En natuurlijk ook veel dank en excuses aan de koevia's en andere onfortuinlijke proefdieren zelf, naast alle mensen die dit werk mogelijk hebben gemaakt mogen zij niet ontbreken...

Kamer Ee 1771... wat kan ik zeggen... het is als een wereld op zich, waar het licht niet van de zon komt maar van Opa's lamp en waar je altijd op je hoede moet zijn voor het geval je iets naar je kop krijgt (verbaal of fysiek). Waar het (bijna) altijd vrijdag is en (bijna) nooit rustig. Soms een wespennest, soms een beestenboel maar meestal de allerbeste plek van het EMC. Wie weet was ik ergens anders productiever geweest, maar bij jullie had ik sowieso meer lol. Zonder volgorde (wil geen ruzie!): Dr. Herfst, jonguh, dank je voor je smerige humor en de moral support. Rory, altijd relaxed en even koffie/sport verslaafd als ik, dank je voor je hulp en je geduld en vergeet niet soms een 1 aprilgrap voor Guus te maken, houdt hem scherp. Eefje, rooie tornado, heerlijke collega met altijd een optimistische insteek, dank voor alle conversaties. Carolien, dankt voor de hulp met experimenten, je kennis en je geduldige antwoord op al mijn stomme vragen. Miranda, toen je eenmaal ontdooid was bleek je eigenlijk een gewoon lieverdje (daar gaat je reputatie als b*tch). Nella, dank voor al je hulp en de mooie momenten, ben blij dat het zo goed met je gaat! Arwen, heel veel succes, het is over voor je het weet. Mark, overleef tussen de dames! Joost, zonder jou geen hoofdstuk 5 en zonder hoofdstuk 5 geen proefschrift dus ik ben je dankbaar en vond het super relaxed werken met je :) Rogier, gast, wij komen elkaar vast nog wel tegen; jij gaat volgens mij hele gave dingen doen, of anders ga je op 40ste met pensioen maar wat het ook is, altijd met een big smile.

De andere (ex-)leden van FLU-II: Gerrie, Tiny, Heidi, Marine en Ruud, dank jullie voor het delen van al jullie kennis en voor de hulp, het was een plezier om met jullie te werken.

De wildlife groep, mijn tweede thuis :) Peter, wat heb jij ontzettend veel voor me gedaan en je was nooit gestrest en altijd vrolijk, maakt het leven een heel stuk prettiger! Lonneke en Marco, ook jullie bedankt voor alle hulp. Jurre, life's a trip, have a good one! Debby, superwoman, dank voor de gezelligheid, de steun en het optimisme, ben benieuwd wat jij allemaal nog gaat doen. Edwin, ik ben geloof ik langer collega's met jou geweest dan wie dan ook, en gelukkig maar want ik vond het super fijn om met je samen te werken.

Bart's group, Do, dude, you're a unique combination of the grumpiest and the most cheerful person I know. Thank you for the life-saving shoulder massages, the unsolicited and often unflattering appraisals of how I looked and everything you did for the MERS paper. Just hang in there, there is light at the end of the tunnel I promise! Stalin, Saskia, Debby S., en Lisette dank jullie voor de fijne samenwerking!

Mathilde ma belle, thanks for being there, even if we never managed to meet up as much as we intended, it was great having you around for chats, dinners and moral support. Kirsty and Keng, thanks for all the delicious dinners and the wonderful evenings of randomness, hope to make it to Australia one day to see you. Ramona thanks for the fun dinners and chats.

Leslie, thank you for pancakes, barbeques, EWDA meetings, dog walks, visits to Anney and philosophical chats. I look forward to working with you in the future, not sure how or when but I sense it will happen.

Dear Stefanie and Mechtild, thank you and your lovely team at the BfR so much for all you help and wonderful coordination. I enjoyed our meetings and although I am happy not to do any animal experiments anymore, I will miss my visits. I hope our paths will cross in the future and I wish you the very best. Dear Hubert, thank you for the support of the guinea pig project, I

sincerely hope that my work will help justify the maintenance of the colony, in Berlin or elsewhere.

Theo, dank je voor alles wat ik van je geleerd hebt, voor alle keren dat je me (uit de brand) geholpen hebt en er voor me was. David, bedankt voor hulp met cijfertjes. Rik bedankt voor het lenen van proefdier gadgets. Ron bedankt voor je scherpe oog. Sarah bedankt voor ISH. Oanh, bedankt voor virus transport medium. Marco bedankt voor Viruskenner, wat heb je dat gaaf gedaan, ik hoop dat het blijft groeien!

Exotics groep, Byron, Penelope, Petra, Jeroen, Stephanie, bedankt voor de goeie borrels. Andere fijne collegas, ook bedankt, Brooke, Bri, Monique, Mart, Gijs, Hans, Robert, Stefan x2, Pascal x2, Jonneke, Bjorn, Bernadette, Kim, Kleine Sander, Martin, Chantal, Cox, Sumeyra, Lennert, Wesley, Colin, Judy en de mensen van ViroClinics.

Dames van het secretariaat: Loubna, Maria, Anouk, Simone, dank jullie voor alle moeite en alle gezelligheid. Ik hoop dat ik niet te vervelend ben geweest, ik ben jullie in ieder geval erg dankbaar!

Everyone from the EWDA student chapter, the EWDA board and the one health/wildlife community; it has been great working with you. Christian and Marianna, gracias por todo, espero que nos veamos a Roma. Bienneke en Aniek, jullie zijn mooie dames en ik hoop in de toekomst nog vaak met jullie te werken.

Fellow pathologists / marine mammal buddies Mark, Andrew, Lonneke, Tilen and Thierry and of course my honorary older sister Johanna, thanks for all the fun, parties and support. Ex-collegas uit Utrecht, dank voor de mooie tijden.

And then friends, you all know what you mean to me but I have to keep saying it, you guys kept me afloat over the years even if we are in different countries. Ainhoa, Amaia, Liza, Diane, Line, Pablo, Dimi and Sergio, you guys are the best!

All my acro buddies from around the globe, acrobatics is what kept me going while writing this and so you guys were indispensable. Gemma y Diana, guapas, espero que coincidimos en algún lugar del mundo para entrenar, y espero que os vaya muy bien con la tesis. Paul, Hans en Fedde dank jullie wel, ik mis de dinsdagavond vreselijk en ik mis jullie als maatjes, samen spelen was precies wat ik nodig had voor balans, jullie zijn me zo dierbaar! Sabine ik denk niet dat een vliegende proefschrift verdediging er nog in zit, maar alle lol die wij in de lucht hebben gehad heeft ook dit boekje mogelijk gemaakt.

Tango friends, Cherif, Dragan and Derek, thank you so much for teaching me how to lose control and be led.

Extended family, Tobias&Lisette en Fons&Jorijn dank voor jullie steun en onvoorwaardelijke vriendschap.

Cat, thank you for being being you. You make me feel less weird :) You were part of making this thesis in many ways. My trips to Berlin to pick up a new load of unfortunate experimental animals were made so much better by knowing that I got to hang out with you. You always

took such great care of me. You helped me so much both in real support with the layout and in moral support. Just knowing you're there makes everything better :)

Carlo and Gilda, I'm so glad you guys came back home to Rome, you have no idea how happy I am that you're here. You've been amazing, I hope there are more many barbeques and bullsh*t to come. Thank you most of all for introducing me to my Prince in the White Fiat Panda aka il Pangolino Gigante, the only man who is both tall enough and weird enough for me. By doing this, you have changed my life forever and I am so grateful for that.

Soph, I was so hoping to share this with you. I know you would have been my only friend who would have actually read it and then asked me a million questions about it. Words fail me to describe how empty it feels now you are gone... Your beautiful girls will always be safe with me. I love you.

En dan mijn Marius, DIT PROEFSCHRIFT WERD MEDE MOGELIJK GEMAAKT DOOR MARIUS VAN DER PLOEG ;) Je bent m'n enige grote broer en je hebt me altijd en op iedere manier ondersteund, je hebt achter me gestaan en me een veilige plek gegeven. Je bent zo lief en genereus, zorg alsjeblieft goed voor jezelf.

Dan mijn familie. Hier kom ik echt woorden tekort. Ik krijg niet zo vaak de kans om op papier te zetten hoe ontzettend veel ik van jullie allemaal hou. Ik heb zo'n geluk dat ik uit zo'n veilig warm nest kom, dat heeft me alle kansen gegeven om ver uit te vliegen. Ik heb altijd een vangnet en ik weet dat wat er ook gebeurt en waar ik ook ben, jullie stuk voor stuk altijd allemaal achter me staan en als het nodig is, in het eerste vliegtuig stappen om bij me te zijn. Mijn paranimf, zusje en beste vriendinnetje Rienke, ik hou zo ontzettend veel van je en ben je zo dankbaar voor alles. Ik ben blij dat je nu ook Eelco hebt voor alle mooie en moeilijke tijden, maar ik blijf ook voor je klaar staan. Marijn en Tos en jullie ontzettend mooie lieve Sacha, Tijmen, Mila en Ytsa, ik weet dat jullie trouwen belangrijker vinden dan promoveren en ik ga zorgen dat ik in al jullie wensen voorzie ;) Fem en Jan, ik heb zo vaak bij Fem aangeklopt voor praktische dingen en je staat altijd klaar, ik weet niet of ik je daar wel vaak genoeg voor bedankt heb? En dan Pap en Mam, ze zeggen dat je je eigen dromen aan je kinderen doorgeeft, en dus misschien dat ik daarom nu promoveer en met een Italiaan ga trouwen? Gelukkig maar dat jullie zulke mooie dromen hadden....

Pango mio, I know you hate PDA (oh my gosh) but I have to say, thank Carlo we met! You are the man I thought didn't exist, the last surviving unicorn. You have changed everything, and I am so happy with you. Your family is like my family and that is the biggest compliment I can give; grazie per tutto Vitti e Paolo!) Pangolone, thank you for your infinite patience and understanding while I was doing this. It helps that you know what it feels like. I love you so much and I am so happy that we will be Dr. Pango and Dr. Panga aka da Pangooooooooo (whistle the song).

